AD-A089 072 NOVA UNIV OCEAN SCIENCE CENTER DANIA FL F/G 8/5
EXTENDED APPLICABILITY OF THE SPHERICAL-HARMONIC AND POINT-MASS--ETC(U)
FEB 80 G BLAHA F19628-78-C-0013
UNCLASSIFIED SCIENTIFIC-2 AFGL-TR-80-0180 NL

1 OF 2

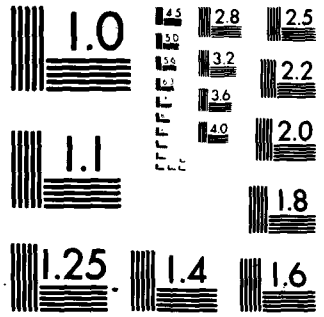

MICROCOPY RESOLUTION TEST CHART

LEVEL III

(12)

AFGL-TR-80-0180

EXTENDED APPLICABILITY OF THE SPHERICAL-HARMONIC AND POINT-MASS MODELING OF THE GRAVITY FIELD

Georges Blaha

Nova University Ocean Sciences Center
8000 North Ocean Drive
Dania, Florida 33004

AD A089072

DTIC
ELECTE
SEP 11 1980
S D
C

Scientific Report No. 2

February 1980

Approved for public release; distribution unlimited

AIR FORCE GEOPHYSICS LABORATORY
AIR FORCE SYSTEMS COMMAND
UNITED STATES AIR FORCE
HANSCOM AFB, MASSACHUSETTS 01731

DDC FILE COPY

80 9 11 002

Qualified requestors may obtain additional copies from the Defense Documentation Center. All others should apply to the National Technical Information Service.

Unclassified

SECURITY CLASSIFICATION OF THIS PAGE (When Data Entered)

19 REPORT DOCUMENTATION PAGE

READ INSTRUCTIONS BEFORE COMPLETING FORM

1. REPORT NUMBER: 18 AFGL-TR-80-0180

2. GOVT ACCESSION NO.: AD-A089 072

3. RECIPIENT'S CATALOG NUMBER

4. TITLE (and Subtitle): 6 EXTENDED APPLICABILITY OF THE SPHERICAL-HARMONIC AND POINT-MASS MODELING OF THE GRAVITY FIELD

5. TYPE OF REPORT & PERIOD COVERED: 14 Scientic ~~Report No.~~ 2

6. PERFORMING ORG. REPORT NUMBER

7. AUTHOR(s): 10 Georges Blaha

8. CONTRACT OR GRANT NUMBER(s): 15 F19628-78-C-0013

9. PERFORMING ORGANIZATION NAME AND ADDRESS:
Nova University Ocean Sciences Center
8000 North Ocean Drive
Dania, Florida 33004

10. PROGRAM ELEMENT, PROJECT, TASK AREA & WORK UNIT NUMBERS:
61102F
16 2309G1AP
17 G1

11. CONTROLLING OFFICE NAME AND ADDRESS:
Air Force Geophysics Laboratory
Hanscom AFB, Massachusetts 01731
Contract Monitor: George Hadgigeorge/LWG

12. REPORT DATE: 11 February 1980

13. NUMBER OF PAGES: 132

14. MONITORING AGENCY NAME & ADDRESS (if different from Controlling Office): 12 131

15. SECURITY CLASS. (of this report): Unclassified

15a. DECLASSIFICATION/DOWNGRADING SCHEDULE

16. DISTRIBUTION STATEMENT (of this Report)

Approved for public release; distribution unlimited.

17. DISTRIBUTION STATEMENT (of the abstract entered in Block 20, if different from Report)

18. SUPPLEMENTARY NOTES

19. KEY WORDS (Continue on reverse side if necessary and identify by block number)

Disturbing potential	Spherical harmonics	Gravity anomalies
Gravity disturbance	Point masses	Deflections of the vertical
Second-order derivatives	Satellite altimetry	Horizontal gradients of gravity
Tensor analysis	Geoid undulations	Vertical gradients of gravity

20. ABSTRACT (Continue on reverse side if necessary and identify by block number)

Recent research aimed at improving the knowledge of the earth's gravity field and its fundamental surface, the geoid, has been based to a large extent on a short-arc mode of satellite altimetry. The global geoidal parameters have consisted of spherical harmonic potential coefficients, and the local parameters have consisted of point mass magnitudes. It is shown that an adjustment solely in terms of the point masses is not desirable due to the spherical approximation

(Continued)

DD FORM 1 JAN 73 1473 EDITION OF 1 NOV 65 IS OBSOLETE

Unclassified

SECURITY CLASSIFICATION OF THIS PAGE (When Data Entered)

393 866

in the point-mass algorithm which would compromise the accuracy in the determination of the oceanic geoid, attainable with the SEASAT altimetry or with a similar high-precision observational system.

A mathematical framework is provided in order to model observations such as the horizontal (north and east) and vertical gradients of gravity or gravity disturbance. This development is based on the tensor approach to theoretical geodesy and is mostly concerned with the second-order derivatives, along local Cartesian axes, of a general scalar function of position; the derivatives are expressed in spheroidal and, for a variety of practical applications, in spherical coordinates. The scalar function of position is specialized to represent the (total) earth's potential, the standard (or normal) potential and, especially, the disturbing potential.

This specialization allows, among other things, to model the gradients of gravity disturbance directly by a suitable set of parameters, such as spherical harmonic potential coefficients and point mass magnitudes. The pertinent adjustment algorithms developed in terms of both these kinds of model parameters are presented in detail. In addition, similar algorithms are recapitulated for geoid undulations and gravity anomalies, and developed for the deflections (north and east) of the vertical. The adjustment algorithms in terms of the potential coefficients contain minimal approximations, while those in terms of the point masses contain the familiar spherical approximation.

Two further topics discussed in this report are related to the sea surface topography. The first deals with the average influence of the astronomical tidal forces on the flattening of an idealized mean sea level, and the second is concerned with the development of a model in which the presence of sea surface slopes with respect to an equipotential surface is taken into account. In a separate development, a comparative analysis is carried out for the node-point approach and the point-mass approach, focusing on the deterministic partial derivatives entering the observation equations.

Accession For
NTIS GRA&I
DDC TAB
Unannounced
Justification
By
Distribution/
Availability
Dist. Avail and/or special
A

TABLE OF CONTENTS

CHAPTER	SECTION	DESCRIPTION	PAGE NO.
		ABSTRACT	i
1		OUTLINE OF THE RESEARCH TOPICS	1
2		SPHERICAL APPROXIMATION AS A LIMITING FACTOR TO USING POINT MASSES IN A GLOBAL GEOIDAL REPRESENTATION	6
3		SECOND-ORDER DERIVATIVES IN A LOCAL FRAME DEVELOPED IN SPHEROIDAL AND SPHERICAL COORDINATES	12
	3.1	Introduction	12
	3.2	Derivations in Spheroidal Coordinates	20
	3.3	Transformation of the Results from Spheroidal to Spherical Coordinates	33
	3.4	Separate Derivations in Spherical Coordinates	41
	3.5	Practical Applicability of the Results	48
	3.6	Summary and Conclusion	60
4		ADJUSTMENT MODELS FOR FIVE INVESTIGATED OBSERVATIONAL MODES	64
	4.1	Mathematical Background	64
	4.2	Geoid Undulations	72
	4.3	Gravity Anomalies	77
	4.4	Deflections of the Vertical	79
	4.5	Horizontal Gradients of Gravity Disturbance	84
	4.6	Vertical Gradients of Gravity Disturbance	87

TABLE OF CONTENTS (CONTINUED)

CHAPTER	SECTION	DESCRIPTION	PAGE NO.
5		SPECIFIC CONSIDERATIONS RELATED TO SEA SURFACE TOPOGRAPHY	89
	5.1	Outline	89
	5.2	Considerations Related to Static Geoid	93
	5.3	Considerations Related to Sea Surface Slopes	103
APPENDIX		COMPARISON OF THE NODE-POINT APPROACH AND THE POINT-MASS APPROACH	112
		REFERENCES	123

LIST OF FIGURES

FIGURE NO.	DESCRIPTION	PAGE NO.
3.1	Schematic representation of four kinds of right-handed orthonormal triads, i, i', i" and $\bar{i}$	16
3.2	A few elements of the geometry pertinent to the spheroidal coordinate system	22
5.1	Schematic representation of the static geoid and equilibrium tide	96
5.2	Illustration of two basic areas (1 and 2) and a bent zero line; the area 1 is delimited by the points 1, 2, 3, 4, Q	106
5.3	Spherical triangles depicting the zero line and an observation point (A)	109
A.1	Scaled covariance functions for N in the node-point approach and comparable functions in the point-mass approach	119
A.2	Scaled cross-covariance functions for Δg,N in the node-point approach and comparable functions in the point-mass approach	120

1. OUTLINE OF THE RESEARCH TOPICS

In the recent past, research has been conducted aimed at improving the knowledge of the earth's gravity field and its fundamental surface, the geoid. The most extensively treated observational mode has been satellite altimetry. The adjustment model utilized in this task has been the short-arc model, described and refined in several reports and papers, e.g. in [Brown, 1973] and [Blaha, 1975,1977,1979]. The body of altimeter data has been initially obtained via the GEOS-3 satellite. However, several aspects of the SEASAT observational system have been investigated along with the GEOS-3 system in view of improved determinations of the oceanic geoid. For example, the SEASAT altimeter has been considered in conjunction with the so-called precise ephemeris (having the standard error in position of approximately 2 m) and the recommendation has been reached that the time interval for each satellite arc should not significantly exceed 7 minutes, in order to eliminate aliasing effects that could become noticeable at points far from the mid-arc epoch.

The geoidal surface or its parts have been adjusted in two steps. The first adjustment has proceeded in terms of a truncated set of spherical harmonic potential coefficients involving global data sets and resulting in a fairly smooth global geoid. The second adjustment, based on regional altimetry residuals from the first adjustment, has had point mass magnitudes as parameters and its main purpose has been a more detailed (but localized) determination of the oceanic geoid. The location of the point masses, including their depth underneath the earth's surface considered as a sphere,

has been stipulated beforehand. A question has arisen whether the point mass parameters could serve for both the global and local geoid determinations. However, the discussion in Chapter 2 shows that due to accuracy considerations such an approach is not desirable. In particular, the geoid determination could be affected by errors of several decimeters due to the spherical approximation in the point mass algorithm alone. On the other hand, if the point mass adjustment is based on a higher-order surface as obtained through a global spherical harmonic adjustment this approximation will not compromise the accuracy of the results.

Originally, the satellite altimetry has been complemented by mean gravity anomalies which have prevented the system of normal equations from being ill-conditioned due to the gaps in altimeter data (especially over the continents). Eventually, however, need has been felt for the modeling of additional kinds of observations. In order to satisfy such requirements, Chapter 3 provides the mathematical framework for several observational modes, notably for horizontal and vertical gradients of gravity or gravity disturbance. It is mostly concerned with the development and application of second-order derivatives, along local Cartesian axes, of a scalar function of position, expressed in spherical coordinates. This development is based on the tensor approach to theoretical geodesy, introduced by Marussi [1951] and further elaborated by Hotine [1969], which can lead to significantly shorter demonstrations when compared to conventional approaches.

The second-order derivatives of Chapter 3 are formulated in quite general terms and are applicable to any scalar function of position (denoted F). If F becomes W (the earth's potential) the six distinct second-order

derivatives -- which include one vertical and two horizontal gradients of gravity -- relate the symmetric Marussi tensor to the curvature parameters of the field. The second-order derivatives are developed also in spheroidal coordinates. This serves, besides its own theoretical interest, for a verificiation of the desired formulas in spherical coordinates by confirming them indirectly, through a coordinate transformation involving differential quantities and relationships.

The general formulas for the second-order derivatives of F are specialized to yield the second-order derivatives of U (standard potential, often called normal potential) and of T (disturbing potential), which allows the latter to be modeled by a suitable set of parameters, for example, by spherical harmonic potential coefficients, chosen localized parameters such as point mass magnitudes, etc. The second-order derivatives of T where the property $\Delta T = 0$ is explicitly incorporated are also given. According to the required precision, the spherical approximation may or may not be desirable; both kinds of results are presented. The derived formulas can be used for the modeling of the second-order derivatives of W or T at ground level as well as at moderate or high altitudes. They can be further applied in a rotating or a nonrotating field.

In Chapter 4, adjustment algorithms are developed for five observational modes including: geoid undulations, gravity anomalies, deflections (north and east) of the vertical, horizontal gradients (north and east) of gravity disturbance and vertical gradients of gravity disturbance. Each model is presented in the spherical harmonic (S.H.) formulation and in the point mass (P.M.) formulation. The former does not contain the familiar

spherical approximation of the earth, while the latter does. The procedure for computing predicted values of the above observation modes, as well as their variances, is a part of this development. Also included is the practical discussion regarding the cut-off distance in the P.M. adjustment, i.e., the size of a spherical cap centered at an observation point beyond which the P.M. parameters are ignored during the formation of an observation equation.

Of the above five models, the first two (i.e., for geoid undulations and gravity anomalies) have been developed earlier. However, they are recapitulated in a concise manner, with the cut-off considerations added on, and their format conforms to that of the other three models. Most of the new development is based on the formulas of Chapter 3. In this respect Chapter 4 is the only chapter built upon another. Most of the chapters in this report as well as the appendix are presented essentially in a self-contained manner and can be read independently. A good example of this format is Chapter 3 whose shortened version is being presented separately as [Blaha,1980].

Chapter 5 contains two topics related to the sea surface topography. The first deals with the average influence of the astronomical tidal forces on the flattening of an idealized mean sea level, and the second is concerned with the development of a model in which the presence of sea surface slopes with respect to an equipotential surface is taken into account. Such slopes are known to exist in different parts of the world where they can reach a few decimeters. Considering the precision of the SEASAT observational system or other such high-precision systems, these features are detectable. They can

be modeled and eventually incorporated into the adjustment process. By repeating this process at different time epochs, the time history of sea surface slopes in an area such as the Equatorial Pacific Ocean can be studied.

The appendix of this report is mostly concerned with comparing the node-point approach and the point-mass approach. The bulk of such a comparison -- which could include a multi-quadric model or other models used to describe the local geoid -- is the study of the "covariance" function giving rise to the deterministic partial derivatives forming the matrix of observation equations. The analysis indicates that the main difference between the above two approaches consists in the somewhat different shapes of their respective "covariance" functions. If the depth of the point masses corresponds to the complexity of the reference surface forming the basis of the node-point approach, the similarity between the deterministic partial derivatives in the two approaches can be remarkably good.

2. SPHERICAL APPROXIMATION AS A LIMITING FACTOR TO USING POINT MASSES IN A GLOBAL GEOIDAL REPRESENTATION

A point mass model, in which the adjustable parameters have been the point mass magnitudes while the location of the point masses has been stipulated beforehand, lends itself to an efficient treatment only if the spherical approximation is part of the model. This has been, in fact, the approach followed in previous applications which have led to a detailed geoidal representation over a limited area. In such applications, altimeter data collected by GEOS-3 satellite have been utilized, together with the so-called broadcast ephemeris (having a positional standard error of about 20 meters). A question emerges when a global geoidal resolution -- as opposed to a localized resolution -- is contemplated in terms of the point mass parameters alone: Would the potential accuracy of such a model be acceptable in view of the SEASAT (or a similar) observational system which is far superior to the GEOS-3 system (in both altimeter and ephemeris accuracy)?

We shall first consider a few aspects in the formulation of a global point mass model and then discuss the applicability of the model in terms of future accuracy requirements approaching one decimeter in geoidal determination. At the outset, such a model should be subject to the global constraints defining the coordinate system. In spherical harmonic applications, the coordinate system has been usually defined by stipulating the values of the following spherical harmonic potential coefficients:

$$C_{10}=0, \quad C_{11}=0, \quad S_{11}=0, \quad C_{21}=0, \quad S_{21}=0, \quad S_{22}=\text{constant}. \tag{2.1}$$

The first five relations correspond to the "forbidden harmonics" and the value of the last one depends on the orientation of the x,y axes with respect to the principle axes of inertia.

The following expressions are given, in a similar form, on page 61 of [Heiskanen and Moritz, 1967]:

$$A_{00} = \int d(kM) = kM \; ; \tag{2.2a}$$

$$\left.\begin{aligned} &A_{10} = \int z d(kM), \quad A_{11} = \int x d(kM), \quad B_{11} = \int y d(kM) \; , \\ &A_{21} = \int xz \, d(kM), \; B_{21} = \int yz \, d(kM), \quad B_{22} = \tfrac{1}{2} \int xy \, d(kM) \; ; \end{aligned}\right\} \tag{2.2b}$$

$$A_{20} = \tfrac{1}{2} \int (2z^2 - x^2 - y^2) \, d(kM) \; ; \tag{2.2c}$$

$$A_{22} = \tfrac{1}{4} \int (x^2 - y^2) \, d(kM) \; . \tag{2.2d}$$

Here the integral extends over the whole earth, k is the gravitational constant and M is the earth's mass. Further we have (see Section 2-5 of the same reference):

$$A_{nm} = (kM) \, a^n \, C_{nm} \; ,$$

$$B_{nm} = (kM) \, a^n \, S_{nm} \; ,$$

where a is the earth's equatorial radius.

Considering a discrete distribution of mass, the formulas (2.2b) - (2.2d) yield

$$\left.\begin{aligned}
A_{10} &\equiv (kM)\, a\, C_{10} = \sum_j z_j (kM)_j\,, \\
A_{11} &\equiv (kM)\, a\, C_{11} = \sum_j x_j (kM)_j\,, \\
B_{11} &\equiv (kM)\, a\, S_{11} = \sum_j y_j (kM)_j\,, \\
A_{21} &\equiv (kM)\, a^2\, C_{21} = \sum_j x_j z_j (kM)_j\,, \\
B_{21} &\equiv (kM)\, a^2\, S_{21} = \sum_j y_j z_j (kM)_j\,, \\
B_{22} &\equiv (kM)\, a^2\, S_{22} = \tfrac{1}{2}\sum_j x_j y_j (kM)_j\,;
\end{aligned}\right\} \qquad (2.2b')$$

$$A_{20} \equiv (kM)\, a^2\, C_{20} = \tfrac{1}{2}\sum_j (2z_j^2 - x_j^2 - y_j^2)\,(kM)_j\,; \qquad (2.2c')$$

$$A_{22} \equiv (kM)\, a^2\, C_{22} = \tfrac{1}{4}\sum_j (x_j^2 - y_j^2)\,(kM)_j\,. \qquad (2.2d')$$

From (2.2b'), the relations (2.1) now read

$$\left.\begin{aligned}
&\sum_j z_j (kM)_j = 0\,, \quad \sum_j x_j (kM)_j = 0\,, \quad \sum_j y_j (kM)_j = 0\,, \\
&\sum_j x_j z_j (kM)_j = 0\,, \quad \sum_j y_j z_j (kM)_j = 0\,, \quad \sum_j x_j y_j (kM)_j = 2(kM)\, a^2\, S_{22}.
\end{aligned}\right\} \qquad (2.3)$$

Further,

$$\sum_j (2z_j^2 - x_j^2 - y_j^2)\ (kM)_j = 2(kM)\ a^2\ C_{20}\ ; \tag{2.4}$$

$$\sum_j (x_j^2 - y_j^2)\ (kM)_j = 4(kM)\ a^2\ C_{22}\ . \tag{2.5}$$

However, it is more advantageous to deal with the disturbing potential (T) than with the actual, "full" potential and the related quantities, since by far the largest point mass magnitudes would be "wasted" in reproducing the known normal field. Since all the potential coefficients except C_{20} , C_{40} , etc., are zero in the normal field, the equations (2.3) defining the coordinate system apply exactly as they stand also in this new situation. In the adjustment terminology, they represent constraints. If, in a point mass adjustment, an equivalent of the ellipsoidal coefficient C_{20} should be enforced, the relation (2.4) would represent another constraint whose right-hand side, however, should be set to zero (it would now represent the departure from the value corresponding to the ellipsoidal C_{20}). If an equivalent of C_{22} should be held at a predetermined value, the relation (2.5) would become a constraint exactly as it stands.

Besides the six constraints presented in (2.3) -- and perhaps two or more optional constraints similar to (2.4), (2.5), etc. -- two additional constraints could be utilized in order to match the constraints often encountered in adjustments of spherical harmonic potential coefficients. In particular, the mass of the reference ellipsoid, taken as the mean earth ellipsoid, and its potential are usually preserved throughout the adjustment.

This corresponds to preserving the following relationship:

$$\int d(kM) = 0 ,$$

$$\int T \, d\sigma = 0 ,$$

where the first integral extends over all of the "anomalous masses" and the second integral extends over the whole unit sphere. In terms of the point mass parameters, these two equations represent the constraints of the following form:

$$\sum_j (kM)_j = 0 ,$$

$$\sum_i \sum_j (1/\ell_{ij})(kM)_j \, d\sigma_i = 0 ,$$

where ℓ_{ij} is the distance between the j-th point mass and the i-th surface element ($d\sigma_i$).

One disadvantage of the point mass model based on the ellipsoidal surface as opposed to a higher order surface would be noticed if geoid undulations (N) should be the predicted quantities in an adjustment of only gravity anomalies. It has been indicated (see [Blaha, 1977], pages 166 - 168, on which the results presented by Needham [1970] are recapitulated) that large errors could be expected in N if the locations of point masses were limited only to one area. However, much smaller errors are believed to occur in the predictions of geoid undulations or gravity anomalies if the adjusted and the predicted quantities are of the same kind.

Another disadvantage of the approach considered emerges upon scrutinizing the basis of the point mass algorithm. If no initial adjustment in terms of spherical harmonics takes place, the "residuals" describing the discrepancy between the observed and the ellipsoidal surfaces will be relatively large (they may reach 100 m or more in some areas). The role of the point mass adjustment is to model these discrepancies. However, since the point mass model contains the spherical approximation and thus produces results reliable to no more than 2 or 3 significant digits, this approach would be unable to yield results even approaching a decimeter accuracy. In fact, the geoid determination could be affected by errors of several decimeters, due to the spherical approximation alone.

On the other hand, a global adjustment of satellite altimetry in terms of fairly high degree and order spherical harmonic coefficients produces residuals of only a few meters. If entered into a subsequent adjustment in terms of point mass parameters, these residuals will yield results which will be essentially unaffected by the spherical approximation.

In summary, upon considering the effect of the spherical approximation in the point mass model, it becomes clear that the accuracy requirements are a limiting factor in adjustments of point mass parameters alone. Indeed, instead of referring a point mass adjustment to the figure of an ellipsoid, an introduction of a higher-order surface as obtained through a global spherical harmonic adjustment is recommended. Based on the altimetry residuals in a region of high-density altimeter data, a point mass adjustment can then follow in order to produce a detailed representation of the local geoid.

3. SECOND ORDER DERIVATIVES IN A LOCAL FRAME DEVELOPED IN SPHEROIDAL AND SPHERICAL COORDINATES

3.1 Introduction

In some geodetic applications use is made of a 3 x 3 symmetric matrix of second-order derivatives of the geopotential (W) with respect to the length elements along local Cartesian coordinate axes. This matrix relates the symmetric Marussi tensor to the five curvature parameters of the field and to the vertical gradient of gravity as can be gathered e.g. from the formulas (12.162) of [Hotine, 1969]. One of the Cartesian axes points east, one points north and one points toward the local zenith. Such an orientation of Cartesian axes at a given point in space (P) is linked to the equipotential surface W = constant passing through P. The directions of these local Cartesian axes are revealed by various sensors and are thus physically meaningful.

However, it is sometimes expedient to work with orthogonal triads whose orientation varies slightly from that of the triad just mentioned. The orientation may correspond to the surface U = constant where U is the standard potential, to the surface α = constant, a spheroid, where α is the third coordinate in the $\{\omega,u,\alpha\}$ spheroidal coordinate system described in Chapter 22 of [Hotine, 1969], or to the surface r = constant, a sphere, where r is the third coordinate in the $\{\lambda,\bar{\phi},r\}$ spherical coordinate system, λ and $\bar{\phi}$ being the geocentric longitude and latitude, respectively. Furthermore, the function of position whose second-order derivatives are sought may be not only W but also U, T (disturbing potential, T = W-U), a generalized coordinate α, r, etc. Before a specialization is made, such a function will be assigned the general notation F.

The unit vectors along the local Cartesian axes x^1, x^2, and x^3, corresponding respectively to general east, north and "up" directions, are denoted as $\ell^r_{(1)}$, $\ell^r_{(2)}$ and $\ell^r_{(3)}$ where the superscript "r" indicates the vector's contravariant components (in Cartesian coordinates, covariant and contravariant components are identical). In [Hotine, 1969], abbreviated henceforth as [H], the above right-handed orthonormal triad is denoted as λ^r, μ^r, ν^r, but for our purpose it is advantageous to associate the i-th unit vector with the subscript "(i)". In the local Cartesian coordinates the triad is depicted as

$$\ell^r_{(1)} = \{1,0,0\} \text{ ... pointing in general east,}$$

$$\ell^r_{(2)} = \{0,1,0\} \text{ ... pointing in general north,}$$

$$\ell^r_{(3)} = \{0,0,1\} \text{ ... pointing in general "up".}$$

The desired second-order derivatives of F with respect to the length elements along the local Cartesian axes x^1, x^2, x^3 can themselves be viewed as scalar functions of position; any of them can be expressed as

$$\partial^2 F/\partial x^i \partial x^j = (\partial^2 F/\partial x^r \partial x^s)\ell^r_{(i)}\ell^s_{(j)}, \tag{3.1}$$

where use is made of the summation convention for repeating indices and where the symmetric matrix composed of $\partial^2 F/\partial x^r \partial x^s$ for $r,s = 1,2,3$ is

$$\{\partial^2 F/\partial x^r \partial x^s\} = \begin{bmatrix} \partial^2 F/\partial x^1 \partial x^1 & \partial^2 F/\partial x^1 \partial x^2 & \partial^2 F/\partial x^1 \partial x^3 \\ \partial^2 F/\partial x^1 \partial x^2 & \partial^2 F/\partial x^2 \partial x^2 & \partial^2 F/\partial x^2 \partial x^3 \\ \partial^2 F/\partial x^1 \partial x^3 & \partial^2 F\ \partial x^2 \partial x^3 & \partial^2 F/\partial x^3 \partial x^3 \end{bmatrix}.$$

As in this example, { } will indicate a matrix where either of the indices assumes the values 1,2,3. Another notation convention which will be adhered to is the replacement of dx^i by $ds_{(i)}$ as a length element along the axis x^i. Since in Cartesian coordinates $\partial^2F/\partial x^r\partial x^s$ are identical to the second covariant derivatives F_{rs}, (3.1) can be rewritten as

$$\partial^2F/\partial s_{(i)}\partial s_{(j)} = F_{rs}\ell^r_{(i)}\ell^s_{(j)}. \tag{3.2}$$

But this is a tensor invariant which, as its name indicates, has the same value regardless of the coordinate system in which the given vectors $\ell^r_{(k)}$ and the covariant derivatives F_{rs} are expressed. The six distinct values obtained from (3.2) with (i),(j) = 1,2,3 correspond to the left-hand sides of the six equations in (12.162) of [H], provided our notations F, $\ell_{(1)}$, $\ell_{(2)}$, $\ell_{(3)}$ are made to coincide with the notations N, λ, μ, ν of [H], respectively.

Later on when the final results are listed, the more usual geodetic conventions will be adopted where the first axis (x) corresponds to the northerly direction, the second axis (y) corresponds to the easterly direction and the third axis (z) corresponds to the "up" direction. Thus, the following transliterations will take place:

$$\left.\begin{aligned}
\partial^2F/\partial s_{(1)}\partial s_{(1)} &\equiv \partial^2F/\partial y^2 \equiv F_{yy}, \\
\partial^2F/\partial s_{(1)}\partial s_{(2)} &\equiv \partial^2F/\partial y\partial x \equiv \partial^2F/\partial x\partial y \equiv F_{xy}, \\
\partial^2F/\partial s_{(1)}\partial s_{(3)} &\equiv \partial^2F/\partial y\partial z \equiv F_{yz},
\end{aligned}\right\} \tag{3.3}$$

$$\left.\begin{aligned} \partial^2F/\partial s_{(2)}\partial s_{(2)} &\equiv \partial^2F/\partial x^2 \equiv F_{xx}, \\ \partial^2F/\partial s_{(2)}\partial s_{(3)} &\equiv \partial^2F/\partial x\partial z \equiv F_{xz}, \\ \partial^2F/\partial s_{(3)}\partial s_{(3)} &\equiv \partial^2F/\partial z^2 \equiv F_{zz}. \end{aligned}\right\}$$

As indicated at the outset, more than one orthonormal triad emanating from P will be considered. In fact, four right-handed orthonormal triads will be utilized where the index in parentheses identifies not only the particular unit vector of a triad but also the triad itself. Upon denoting the geocenter by O, the following description applies with regard to the third vector of each triad:

$\ell^r_{(3)}$ ... vector orthogonal to a sphere centered at O,

$\ell^r_{(3')}$ ... vector orthogonal to a spheroid centered at O,

$\ell^r_{(3'')}$ ... vector orthogonal to an equipotential surface (spherop) in the standard gravity field, centered at O,

$\ell^r_{(\bar{3})}$ ... a general vector coplanar with the other three vectors above.

This situation is illustrated in Figure 3.1 with some additional notations; for example, $\hat{\phi}$ indicates the direction of the line of force at P in the standard gravity field (in agreement with [H], the word "standard" is used in lieu of "normal"). From the figure one reads

$$\phi = \bar{\phi} + \delta_1 , \tag{3.4a}$$

$$\hat{\phi} = \phi + \delta_2 = \bar{\phi} + \delta_1 + \delta_2; \tag{3.4b}$$

sometimes the notation

$$\delta = \delta_1 + \delta_2 \tag{3.4c}$$

will be utilized. Figure 3.1 depicts also $\ell^r_{(\bar{2})}$, while $\ell^r_{(\bar{1})} = \ell^r_{(1)} = \ell^r_{(1')} = \ell^r_{(1'')}$ go into the plane of the paper at P.

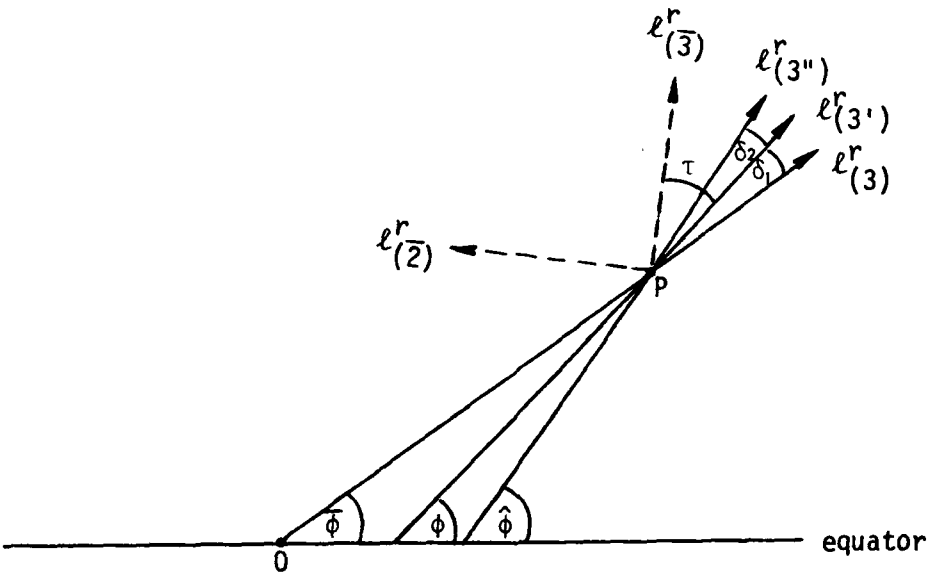

Figure 3.1

Schematic representation of four kinds of right-handed orthonormal triads, i, i', i" and $\bar{i}$

The triad $\bar{i}$ is obtained from the triad i' by means of the rotation $R_1(-\tau)$, giving rise to the following vector equations valid in any coordinates:

$$\left.\begin{aligned} \ell^r_{(\bar{1})} &= \ell^r_{(1')} , \\ \ell^r_{(\bar{2})} &= \cos\tau\, \ell^r_{(2')} - \sin\tau\, \ell^r_{(3')} , \\ \ell^r_{(\bar{3})} &= \sin\tau\, \ell^r_{(2')} + \cos\tau\, \ell^r_{(3')} ; \end{aligned}\right\} \tag{3.5}$$

in the matrix notations, these equations are represented by

$$\{\ell^r_{(\bar{i})}\} = R_1(-\tau)\ \{\ell^r_{(i')}\}. \tag{3.5'}$$

The special cases of interest are the following:

$$\left.\begin{array}{ll} \tau = \delta_2 & \ldots \text{ triad } \bar{i} \text{ becomes triad } i'' , \\ \tau = 0 & \ldots \text{ triad } \bar{i} \text{ becomes triad } i' , \\ \tau = -\delta_1 & \ldots \text{ triad } \bar{i} \text{ becomes triad } i . \end{array}\right\} \tag{3.6}$$

Starting with equation (3.2), we keep in mind that tensor or vector equations are valid in any coordinates, such as local Cartesian, earth-fixed Cartesian (which need not be mentioned again), spheroidal, spherical, etc. Only two kinds of coordinate systems will be utilized here in order to develop expressions such as (3.2): the spheroidal coordinate system and the spherical coordinate system. The former is identified by primes; we thus consider $\{x'^1, x'^2, x'^3\} \equiv \{\omega,u,\alpha\}$, ℓ'^r, ℓ'_r, F'_{rs}, etc. In the latter the primes are absent and the corresponding notations are $\{x^1, x^2, x^3\} \equiv \{\lambda,\bar{\phi},r\}$, ℓ^r, ℓ_r, F_{rs}, etc. That all the expressions so far have been written without primes does not mean that they will be considered only in spherical coordinates. For example, (3.2) can equally well be written as

$$\partial^2 F'/\partial s_{(i)}\partial s_{(j)} = F'_{rs}\ell'^r_{(i)}\ell'^s_{(j)} ; \tag{3.7}$$

since $F' \equiv F$, the prime on the left-hand side serves only to indicate in which coordinate system the computation is being made. Similarly, (3.5) can be written in spheroidal coordinates, i.e., every ℓ^r can be replaced by ℓ'^r.

The desired second-order derivatives of F will first be developed in spheroidal coordinates. The form of the results will correspond to (3.7) in which, however, use will be made of a more general triad $\bar{i}$, i.e.,

$$\partial^2 F'/\partial s_{(\bar{i})}\partial s_{(\bar{j})} = F'_{rs}\ell'^{r}_{(\bar{i})}\ell'^{s}_{(\bar{j})} . \tag{3.8}$$

The other cases, including (3.7), can be deduced from this result upon specializing τ as in (3.6).

Subsequently, the corresponding expressions will be obtained in spherical coordinates. However, this will not be done directly using the matrix tensor, the associated metric tensor and the Christoffel symbols in these coordinates, but indirectly using the already known Christoffel symbols in spheroidal coordinates and several differential relations obtained from the geometric properties of the two systems. On one hand, this could be considered merely an academic exercise since the results can be obtained much faster in spherical coordinates by direct means. On the other hand, such an approach could prove useful if one wanted to proceed from the spheroidal (or some other) coordinate system to a more complicated system without utilizing the metric, the Christoffel symbols, etc., in this new system. (Although the associated metric tensor in this new system can be derived through the same differential relations as mentioned above and although the metric tensor as well as the Christoffel symbols can be derived subsequently, such a process might not be always shorter than the one discussed.) Be that as it may, the link between the two approaches can also serve as an independent verification of the results obtained separately in one and the other coordinate system.

In the next step, the development will be carried out directly in the spherical coordinate system, leading to the results of type (3.2) but with a more general triad $\bar{i}$, i.e.,

$$\partial^2 F/\partial s_{(\bar{i})}\partial s_{(\bar{j})} = F_{rs}\ell^r_{(\bar{i})}\ell^s_{(\bar{j})}. \tag{3.9}$$

The specializations indicated in (3.6) will again encompass the other cases considered, including (3.2). The approach of [H] adopted in this study will be seen to lead to the desired results much faster than more conventional approaches in which advantage is not taken of tensors and their properties.

In the closing part of this chapter, the practical applicability of the results obtained in spherical coordinates will be discussed. As an example, three of the six distinct second-order derivatives of W can routinely be measured as one vertical and two horizontal gradients of gravity. Upon using the derived results, formulas for the second-order derivatives of T will be established making it possible to model, among other things, the "anomalous gradients of gravity". Advantage will be taken of the Laplace equation $\Delta T = 0$ which will eliminate the need for the second derivatives of the associated Legendre functions with respect to $\bar{\phi}$, should these be a part of the explicit model. The desired second-order derivatives of T will be expressed for a general point in space, whether on the earth's surface or above it (e.g. at aircraft or satellite altitudes). The results will be further generalized by being made applicable to a rotating field as well as a nonrotating field.

3.2 Derivations in Spheroidal Coordinates

In order to evaluate various quantities in spheroidal coordinates $\{\omega,u,\alpha\}$ the values of these coordinates should be known. If, for example, the earth-fixed coordinates are given, the spherical coordinates $\{\lambda,\bar{\phi},r\}$ can be computed immediately from

$$\left.\begin{aligned} tg\lambda &= Y/X, \\ tg\bar{\phi} &= Z/(X^2+Y^2)^{\frac{1}{2}} \quad , \\ r &= (X^2+Y^2+Z^2)^{\frac{1}{2}} \ . \end{aligned}\right\} \tag{3.10}$$

When working with spheroidal coordinates the situation is more complicated. The bulk of the pertinent geometry is presented on pages 187 - 190 of [H]. We shall now review some of the basic geometric relationships with the aid of Figure 3.2. The absolute space constant (ae), considered known, gives rise to a family of spheroids (rotational ellipsoids) one of which passes through P. The eccentricity (e), the semi-major axis (a) and the semi-minor axis (b) of the spheroid α = constant passing through P are related as follows:

$$e \equiv \sin\alpha \ , \tag{3.11a}$$

$$b = a(1-e^2)^{\frac{1}{2}} \equiv a\cos\alpha \ . \tag{3.11b}$$

Except for the (well-known) last equality in (3.12a) below, all the relations in (3.12) can be read directly from Figure 3.2:

$$PR = r \sin\bar{\phi} = b \sin u = \nu \cos^2\alpha \sin\phi \ , \tag{3.12a}$$

$$OR = r \cos\bar{\phi} = a \cos u = \nu \cos\phi \ ; \tag{3.12b}$$

it thus follows that

$$\mathrm{tg}\bar{\phi} = \cos\alpha \ \mathrm{tg}\ u = \cos^2\alpha \ \mathrm{tg}\phi \ . \tag{3.13}$$

From the same figure and from the definition of an ellipse we have

$$d_1^2 = [r \cos\bar{\phi} + (ae)]^2 + (r \sin\bar{\phi})^2 \ ,$$

$$d_2^2 = [r \cos\bar{\phi} - (ae)]^2 + (r \sin\bar{\phi})^2 \ ,$$

$$a = \tfrac{1}{2}(d_1 + d_2).$$

The spheroidal coordinates are thus computed from

$$\left.\begin{aligned} \omega &= \lambda \ , \\ \sin\alpha &= (ae)/a, \\ \mathrm{tg}\, u &= \mathrm{tg}\bar{\phi}/\cos\alpha \ , \end{aligned}\right\} \tag{3.14}$$

where, in addition to (ae), also λ and $\bar{\phi}$ are known beforehand (see e.g. equations 3.10). Upon consulting (3.13) and (3.4a) or Figure 3.2, one can write

$$\mathrm{tg}\phi = \mathrm{tg}\ u/\cos\alpha = \mathrm{tg}\bar{\phi}/\cos^2\alpha \ , \tag{3.15}$$

$$\delta_1 = \phi - \bar{\phi} \ . \tag{3.16}$$

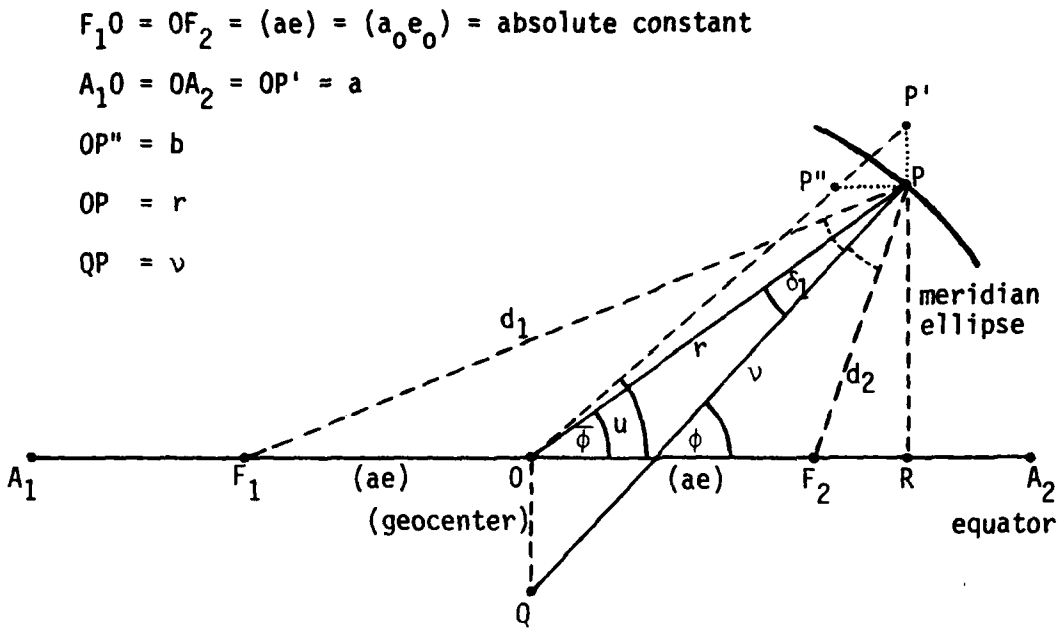

Figure 3.2

A few elements of the geometry pertinent to the spheroidal coordinate system

From (22.25) of [H], the metric in spheroidal coordinates is

$$ds^2 = (a^2\cos^2 u)d\omega^2 + (\nu^2\cos^2\alpha)du^2 + (\nu^2\mathrm{cotg}^2\alpha)d\alpha^2 .$$

This results in the following metric and associated metric tensors:

$$\{g'_{rs}\} = \text{diag. } \{a^2\cos^2 u,\ \nu^2\cos^2\alpha,\ \nu^2\mathrm{cotg}^2\alpha\} , \tag{3.17a}$$

$$\{g'^{rs}\} = \text{diag. } \{1/(a^2\cos^2 u),\ 1/(\nu^2\cos^2\alpha),\ 1/(\nu^2\mathrm{cotg}^2\alpha)\}. \tag{3.17b}$$

In a triply orthogonal coordinate system we have along the coordinate lines: $ds_{(1)} = (g_{11})^{\frac{1}{2}}dx^1$, etc. When introduced in the general formula $\ell^r = dx^r/ds$, this yields $\ell^r_{(1)} = \{(g^{11})^{\frac{1}{2}}, 0 , 0 \}$, etc. Applying this outcome to the

(triply orthogonal) spheroidal coordinate system and adhering to the earlier conventions, we deduce

$$\left.\begin{aligned} \ell'^{r}_{(1')} &= \{1/(a\cos u),\ 0\ ,\ 0\ \}\ , \\ \ell'^{r}_{(2')} &= \{0\ ,\ 1/(\nu\cos\alpha)\ \ ,\ 0\ \}\ , \\ \ell'^{r}_{(3')} &= \{0\ ,\ 0\ ,\ -1/(\nu\cot g\alpha)\}\ . \end{aligned}\right\} \tag{3.18}$$

The minus sign in the last relation above is due to α increasing inward; by contrast, the third vector of our orthonormal triad is an outward-drawn normal. To reconcile this difference we have adopted $-d\alpha/ds_{(3')}$ as the vector's third component. Taking (3.12b) into consideration, in agreement with (3.5) we write

$$\left.\begin{aligned} \ell'^{r}_{(\bar{1})} &= \{1/(\nu\cos\phi)\ ,\ 0\ ,\ 0\ \}\ , \\ \ell'^{r}_{(\bar{2})} &= \{0\ ,\ \cos\tau/(\nu\cos\alpha)\ ,\ \sin\tau/(\nu\cot g\alpha)\}\ , \\ \ell'^{r}_{(\bar{3})} &= \{0\ ,\ \sin\tau/(\nu\cos\alpha)\ ,-\cos\tau/(\nu\cot g\alpha)\}\ . \end{aligned}\right\} \tag{3.19}$$

The Christoffel symbols of the second kind, needed in forming second covariant derivatives of F, are defined in any coordinates as

$$\Gamma^{t}_{rs} = g^{tk}[rs,\ k]\ , \tag{3.20a}$$

$$[rs,\ k] = \tfrac{1}{2}(\partial g_{rk}/\partial x^{s} + \partial g_{sk}/\partial x^{r} - \partial g_{rs}/\partial x^{t}). \tag{3.20b}$$

The symbols Γ^t_{rs} are symmetric in the lower indices and as such, are often denoted by the symbol $\{{}^t_{rs}\}$ in tensor calculus. However, in the present context the symbolism of [H] will be utilized. The above formulas are applied to our system in a straightforward fashion. In the process, the following differential relations are utilized:

$$\partial a/\partial\omega = 0, \quad \partial a/\partial u = 0, \quad \partial a/\partial\alpha = -a \operatorname{cotg}\alpha ,$$

$$\partial\nu/\partial\omega = 0, \quad \partial\nu/\partial u = (a^2/\nu)\operatorname{tg}^2\alpha \sin u \cos u, \quad \partial\nu/\partial\alpha = \nu(-\operatorname{cotg}\alpha + \operatorname{tg}\alpha \sin^2\phi).$$

After some manipulation we obtain essentially (22.38) and (22.39) of [H] which, in this reference, were derived somewhat differently. The nonzero Christoffel symbols (symmetric in the lower indices) are listed as

$$\left.\begin{aligned}
\Gamma'^{1}_{12} &= -\operatorname{tg} u = -\cos\alpha \operatorname{tg}\phi , \\
\Gamma'^{1}_{13} &= -\operatorname{cotg}\alpha ; \\
\Gamma'^{2}_{11} &= \sin\phi \cos\phi/\cos\alpha , \\
\Gamma'^{2}_{22} &= \sin\alpha \operatorname{tg}\alpha \sin\phi \cos\phi , \\
\Gamma'^{2}_{23} &= -a^2/(\nu^2 \sin\alpha \cos\alpha) , \\
\Gamma'^{2}_{33} &= -\sin\phi \cos\phi/\cos\alpha ;
\end{aligned}\right\} \tag{3.21}$$

$$\left.\begin{aligned}
\Gamma'^{3}_{11} &= \mathrm{tg}\alpha \cos^2\phi \ , \\
\Gamma'^{3}_{22} &= (a^2/\nu^2)\mathrm{tg}\alpha \ , \\
\Gamma'^{3}_{23} &= \sin\alpha \ \mathrm{tg}\alpha \ \sin\phi \ \cos\phi \ , \\
\Gamma'^{3}_{33} &= -\mathrm{cotg}\alpha - a^2/(\nu^2 \sin\alpha \cos\alpha) \ .
\end{aligned}\right|$$

The general formula giving the second covariant derivatives (symmetric) of F reads

$$F_{rs} = \partial^2 F/\partial x^r \partial x^s - \Gamma^t_{rs} F_t \ , \qquad F_t \equiv \partial F/\partial x^t \ . \tag{3.22}$$

In spheroidal coordinates this results in

$$\left.\begin{aligned}
F'_{11} &= \partial^2 F/\partial\omega^2 - (\sin\phi \ \cos\phi/\cos\alpha)\partial F/\partial u - \mathrm{tg}\alpha \ \cos^2\phi \ \partial F/\partial\alpha \ , \\
F'_{12} &= \partial^2 F/\partial\omega\partial u + \cos\alpha \ \mathrm{tg}\phi \ \partial F/\partial\omega \ , \\
F'_{13} &= \partial^2 F/\partial\omega\partial\alpha + \mathrm{cotg}\alpha \ \partial F/\partial\omega \ , \\
F'_{22} &= \partial^2 F/\partial u^2 - \sin\alpha \ \mathrm{tg}\alpha \ \sin\phi \ \cos\phi \ \partial F/\partial u - (a^2/\nu^2)\mathrm{tg}\alpha \ \partial F/\partial\alpha \ , \\
F'_{23} &= \partial^2 F/\partial u\partial\alpha + [a^2/(\nu^2 \sin\alpha \ \cos\alpha)] \ \partial F/\partial u - \sin\alpha \ \mathrm{tg}\alpha \ \sin\phi \ \cos\phi \ \partial F/\partial\alpha \ , \\
F'_{33} &= \partial^2 F/\partial\alpha^2 + (\sin\phi \ \cos\phi/\cos\alpha)\partial F/\partial u + [\mathrm{cotg}\alpha + a^2/(\nu^2 \sin\alpha \ \cos\alpha)] \ \partial F/\partial\alpha \ .
\end{aligned}\right\} \tag{3.23}$$

We can proceed according to the formula (3.8), symmetric in $(\bar{i})$, $(\bar{j})$, in which the values (3.19) and (3.23) are utilized. The results are

$$
\left.
\begin{aligned}
\partial^2F'/\partial s_{(\bar{1})}\partial s_{(\bar{1})} &= (1/\nu^2\cos^2\phi)\partial^2F/\partial\omega^2 - [\mathrm{tg}\phi/(\nu^2\cos\alpha)]\ \partial F/\partial u \\
&\qquad - [1/(\nu^2\mathrm{cotg}\alpha)]\ \partial F/\partial\alpha, \\
\partial^2F'/\partial s_{(\bar{1})}\partial s_{(\bar{2})} &= [\cos\tau/(\nu^2\cos\alpha\cos\phi)]\,\partial^2F/\partial\omega\partial u \\
&\quad + [\sin\tau/(\nu^2\mathrm{cotg}\alpha\cos\phi)]\,\partial^2F/\partial\omega\partial\alpha \\
&\quad + [\sin(\phi+\tau)/(\nu^2\cos^2\phi)]\,\partial F/\partial\omega, \\
\partial^2F'/\partial s_{(\bar{1})}\partial s_{(\bar{3})} &= [\sin\tau/(\nu^2\cos\alpha\cos\phi)]\,\partial^2F/\partial\omega\partial u \\
&\quad - [\cos\tau/(\nu^2\mathrm{cotg}\alpha\cos\phi)]\,\partial^2F/\partial\omega\partial\alpha \\
&\quad - [\cos(\phi+\tau)/(\nu^2\cos^2\phi)]\,\partial F/\partial\omega, \\
\partial^2F'/\partial s_{(\bar{2})}\partial s_{(\bar{2})} &= [\cos^2\tau/(\nu^2\cos^2\alpha)]\,\partial^2F/\partial u^2 \\
&\quad + [\sin 2\tau/(\nu^2\cos\alpha\mathrm{cotg}\alpha)]\,\partial^2F/\partial u\partial\alpha \\
&\quad + [\sin^2\tau/(\nu^2\mathrm{cotg}^2\alpha)]\,\partial^2F/\partial\alpha^2 \\
&\quad - [1/(\nu^2\cos\alpha\mathrm{cotg}^2\alpha)]\,[\cos 2\tau * \sin\phi\cos\phi \\
&\quad - \sin 2\tau * a^2/(\nu^2\sin^2\alpha)]\,\partial F/\partial u \\
&\quad - [1/(\nu^2\mathrm{cotg}^3\alpha)]\,[\cos 2\tau * a^2/(\nu^2\sin^2\alpha) \\
&\quad + \sin 2\tau * \sin\phi\cos\phi - \sin^2\tau\mathrm{cotg}^2\alpha]\,\partial F/\partial\alpha, \\
\partial^2F'/\partial s_{(\bar{2})}\partial s_{(\bar{3})} &= \tfrac{1}{2}[\sin 2\tau/(\nu^2\cos^2\alpha)]\,\partial^2F/\partial u^2 \\
&\quad - [\cos 2\tau/(\nu^2\cos\alpha\mathrm{cotg}\alpha)]\,\partial^2F/\partial u\partial\alpha \\
&\quad - \tfrac{1}{2}[\sin 2\tau/(\nu^2\mathrm{cotg}^2\alpha)]\,\partial^2F/\partial\alpha^2 \\
&\quad - [1/(\nu^2\cos\alpha\mathrm{cotg}^2\alpha)]\,[\cos 2\tau * a^2/(\nu^2\sin^2\alpha) \\
&\quad + \sin 2\tau * \sin\phi\cos\phi]\,\partial F/\partial u \\
&\quad + [1/(\nu^2\mathrm{cotg}^3\alpha)]\,[\cos 2\tau * \sin\phi\cos\phi \\
&\quad - \sin 2\tau * a^2/(\nu^2\sin^2\alpha) \\
&\quad - \tfrac{1}{2}\sin 2\tau * \mathrm{cotg}^2\alpha]\,\partial F/\partial\alpha,
\end{aligned}
\right\} \qquad (3.24)
$$

$$
\begin{aligned}
\partial^2 F'/\partial s_{(\overline{3})}\partial s_{(\overline{3})} = {} & [\sin^2\tau/(\nu^2\cos^2\alpha)]\,\partial^2 F/\partial u^2 \\
& - [\sin 2\tau/(\nu^2\cos\alpha\,\mathrm{cotg}\,\alpha)]\,\partial^2 F/\partial u\partial\alpha \\
& + [\cos^2\tau/(\nu^2\mathrm{cotg}^2\alpha)]\,\partial^2 F/\partial\alpha^2 \\
& + [1/(\nu^2\cos\alpha\,\mathrm{cotg}^2\alpha)]\,[\cos 2\tau * \sin\phi\cos\phi \\
& - \sin 2\tau * a^2/(\nu^2\sin^2\alpha)]\,\partial F/\partial u \\
& + [1/(\nu^2\mathrm{cotg}^3\alpha)]\,[\cos 2\tau * a^2/(\nu^2\sin^2\alpha) \\
& + \cos^2\tau\,\mathrm{cotg}^2\alpha + \sin 2\tau * \sin\phi\cos\phi]\,\partial F/\partial\alpha.
\end{aligned}
$$

By setting τ to δ_2 , 0 , or $-\delta_1$ we obtain the desired second-order derivatives of F for the triads i" , i' , or i , respectively, as indicated in (3.6). The choice $\tau = 0$ results in particularly simple formulas; they can be, of course, obtained also more directly upon replacing in (3.8) the triad (3.19) by the triad (3.18). The expression for the Laplacian of F in spheroidal coordinates ($\Delta F'$) is obtained as the trace of the symmetric matrix composed of the elements in (3.24) regardless of the choice of τ, i.e.,

$$
\Delta F' = [1/(\nu^2\cos^2\phi)]\,\partial^2 F/\partial\omega^2 + [1/(\nu^2\cos^2\alpha)]\,\partial^2 F/\partial u^2 + [1/(\nu^2\mathrm{cotg}^2\alpha)]\,\partial^2 F/\partial\alpha^2 - [\mathrm{tg}\phi/(\nu^2\cos\alpha)]\,\partial F/\partial u;
$$

a similar form appeared in (22.41) of [H]. Since the Laplacian is a tensor invariant the same value must be obtained in any coordinates (spheroidal, spherical, Cartesian, etc.).

The computation of δ_1 is an easy matter as was already shown in (3.16). On the other hand, the computation of δ_2 involves a formula expressing U (standard potential, in Chapter 23 of [H] denoted as -W) at P. The main task consists in projecting the vector U'_r ($\equiv \partial U/\partial x'^r$) onto the triad (3.18), the projections being respectively

$$\left.\begin{aligned} \partial U'/\partial s_{(1')} &\equiv U'_r \ell'^r_{(1')} = 0 \,, \\ \partial U'/\partial s_{(2')} &\equiv U'_r \ell'^r_{(2')} = [1/(\nu\cos\alpha)]\,\partial U/\partial u \,, \\ \partial U'/\partial s_{(3')} &\equiv U'_r \ell'^r_{(3')} = -[1/(\nu\,\mathrm{cotg}\,\alpha)]\,\partial U/\partial \alpha \,. \end{aligned}\right\} \tag{3.25}$$

The expression for U is given in (23.13) of [H] essentially as

$$U = GM\alpha/(ae) + GA_{20}Q_2(i\,\mathrm{cotg}\,\alpha)\,P_2(\sin u) + [\tilde{\omega}^2a^2/3 - \tilde{\omega}^2a^2P_2(\sin u)/3], \tag{3.26}$$

where GM is the product of the gravitational constant and the earth's mass, $\tilde{\omega}$ is the angular velocity of the earth's rotation, $P_2(\sin u)$ is the Legendre function in argument sin u and, according to (22.52) and (23.12) of [H],

$$Q_2(i\,\mathrm{cotg}\,\alpha) = \tfrac{1}{2}i(\alpha + 3\alpha\,\mathrm{cotg}^2\alpha - 3\,\mathrm{cotg}\,\alpha) \,, \tag{3.27a}$$

$$iGA_{20} = -(2/3)\tilde{\omega}^2a_0^2/[3\,\mathrm{cotg}\,\alpha_0 - \alpha_0(1 + 3\,\mathrm{cotg}^2\alpha_0)] \,, \tag{3.27b}$$

where a_0, α_0 correspond to a given base equipotential spheroid. Outside this particular spheroid the equipotential surfaces U = constant are not spheroids. It is to be noted that if the standard field should be nonrotating, such as considered in some satellite applications, the terms in (3.26) containing $\tilde{\omega}^2$ explicitly would disappear (the numerical value of

the constant iGA_{20} in 3.27b would remain unchanged). In this case, none of the modified surfaces U = constant would ever coincide with a spheroid. The angle δ_2 would be computed exactly as in the present approach except that the explicit symbols $\tilde{\omega}^2$ in the pertinent expressions would be replaced by zeros.

Carr ing out the indicated operations, from (3.25) we obtain

$$\partial U'/\partial s_{(2')} = \left[3 \sin u \cos u/ (\nu \cos\alpha)\right]\left[GA_{20}Q_2(i \operatorname{cotg}\alpha) - \tilde{\omega}^2 a^2/3\right] ; \qquad (3.28a)$$

on the base spheroid the expression in the second brackets becomes zero (in the rotating field). Further we have

$$\partial U'/\partial s_{(3')} = -\left[1/(\nu \operatorname{cotg}\alpha)\right]\left[J + LP_2(\sin u)\right] , \qquad (3.28b)$$

where, similar to (23.31) of [H],

$$J = GM/(ae) - (2/3)\tilde{\omega}^2 a^2 \operatorname{cotg}\alpha ,$$

$$L = -iGA_{20}(-2 - 3\operatorname{cotg}^2\alpha + 3\alpha \operatorname{cotg}\alpha + 3\alpha \operatorname{cotg}^3\alpha) + (2/3)\tilde{\omega}^2 a^2 \operatorname{cotg}\alpha .$$

Since both (3.28a), (3.28b) are in general negative outside the equipotential spheroid (rotating field), the desired angle δ_2 is obtained from

$$\operatorname{tg}\delta_2 = (-\partial U'/\partial s_{(2')})/(-\partial U'/\partial s_{(3')}) , \qquad (3.29)$$

and it is in general positive (at the poles or on the equator it is zero).

In the nonrotating field the value of δ_2 would be usually negative; it can be shown that this sign would start changing at high altitudes, approximately at $a_o/3$ (about 2.1×10^6m) above the base spheroid.

Denoting the standard gravity at P by γ , its normal component (positive inward along $-ds_{(3')}$) by γ_n and its meridian component (positive north along $ds_{(2')}$) by γ_m, we have

$$\gamma_n = -\partial U'/\partial s_{(3')} , \tag{3.30a}$$

$$\gamma_m = \partial U'/\partial s_{(2')} , \tag{3.30b}$$

$$\gamma = (\gamma_n^2 + \gamma_m^2)^{\frac{1}{2}} , \tag{3.30c}$$

and from (3.29),

$$\mathrm{tg}\ \delta_2 = -\gamma_m/\gamma_n . \tag{3.31}$$

We notice that the Somigliana formula appearing in (23.24) of [H] gives γ_n at any point in space (on the base spheroid it follows from 3.28a that $\gamma_m=0$ and $\gamma=\gamma_n$). However, γ_n given by that formula is computed from γ_e and γ_p representing the standard gravity on the equator and at the poles of the coordinate spheroid passing through the point in question (if it is not the base spheroid such a spheroid is not an equipotential surface). In the applications involving the base spheroid the rigorous Somigliana formula is quite suitable. However, since in general for each point in space the corresponding γ_e and γ_p would have to be computed first, the present approach giving γ_n in (3.30a) in conjunction with (3.28b) appears to be more practical. This assertion would hold all the more if the nonrotating

field were considered instead (such a case all the formulas of the present approach would be simplified upon replacing the explicit symbols $\tilde{\omega}^2$ by zeros).

Having obtained δ_2 , the desired derivatives can further be refined so as to refer to an $\tilde{i}$ system which characterizes the actual gravity field. This system, which could be termed as a system of the local vertical, differs from the i" system by two rotations, each corresponding to one component of the deflection of the vertical at P. In general, the second covariant derivatives in any two coordinate systems are connected by

$$\{\tilde{F}_{ij}\} = \{\partial x''^r/\partial\tilde{x}^i\}^T\{F''_{rs}\}\{\partial x''^s/\partial\tilde{x}^j\} ;$$

the indices are unimportant here since we are dealing with matrix expressions. If the two systems are Cartesian -- and thus the Christoffel symbols vanish -- one can write

$$\{\partial^2F/\partial\tilde{x}^i\partial\tilde{x}^j\} = C^T\{\partial^2F/\partial x''^r\partial x''^s\}C , \tag{3.32}$$

$$C^T = \{\partial\tilde{x}^i/\partial x''^r\} , \qquad \{d\tilde{x}^i\} = C^T\{dx''^r\} .$$

In our case C^T represents the following rotation matrix:

$$C^T = R_2(\eta)R_1(-\xi) \simeq \begin{bmatrix} 1 & 0 & -\eta \\ 0 & 1 & \xi \\ \eta & \xi & 1 \end{bmatrix} , \tag{3.33}$$

where ξ , η are the north and east components of the deflection of the vertical at P. If (3.33) is utilized in (3.32) and the previous conventions are adhered to ($d\tilde{x}^i$ written as $ds_{(\tilde{i})}$, F written as F'), it follows that

$$\left.\begin{aligned}
\partial^2F'/\partial s_{(\tilde{1})}\partial s_{(\tilde{1})} &\simeq \partial^2F'/\partial s_{(1'')}\partial s_{(1'')} - 2\eta\, \partial^2F'/\partial s_{(1'')}\partial s_{(3'')}\,, \\
\partial^2F'/\partial s_{(\tilde{1})}\partial s_{(\tilde{2})} &\simeq \partial^2F'/\partial s_{(1'')}\partial s_{(2'')} \\
&\quad - \xi\, \partial^2F'/\partial s_{(1'')}\partial s_{(3'')} - \eta\, \partial^2F'/\partial s_{(2'')}\partial s_{(3'')}\,, \\
\partial^2F'/\partial s_{(\tilde{1})}\partial s_{(\tilde{3})} &\simeq \partial^2F'/\partial s_{(1'')}\partial s_{(3'')} + \xi\, \partial^2F'/\partial s_{(1'')}\partial s_{(2'')} \\
&\quad - \eta[\partial^2F'/\partial s_{(3'')}\partial s_{(3'')} - \partial^2F'/\partial s_{(1'')}\partial s_{(1'')}]\,, \\
\partial^2F'/\partial s_{(\tilde{2})}\partial s_{(\tilde{2})} &\simeq \partial^2F'/\partial s_{(2'')}\partial s_{(2'')} - 2\xi\, \partial^2F'/\partial s_{(2'')}\partial s_{(3'')}\,, \\
\partial^2F'/\partial s_{(\tilde{2})}\partial s_{(\tilde{3})} &\simeq \partial^2F'/\partial s_{(2'')}\partial s_{(3'')} - \xi[\partial^2F'/\partial s_{(3'')}\partial s_{(3'')} \\
&\quad - \partial^2F'/\partial s_{(2'')}\partial s_{(2'')}] + \eta\, \partial^2F'/\partial s_{(1'')}\partial s_{(2'')}\,, \\
\partial^2F'/\partial s_{(\tilde{3})}\partial s_{(\tilde{3})} &\simeq \partial^2F'/\partial s_{(3'')}\partial s_{(3'')} + 2\xi\, \partial^2F'/\partial s_{(2'')}\partial s_{(3'')} \\
&\quad + 2\eta\, \partial^2F'/\partial s_{(1'')}\partial s_{(3'')}\,.
\end{aligned}\right\} \quad (3.34)$$

These relationships will be used also later when dealing with spherical coordinates, in which case the primes associated with F will be dropped.

3.3 Transformation of the Results from Spheroidal to Spherical Coordinates

The expressions in (3.8) and (3.9) being tensor invariants yield the same values in any coordinates, i.e.,

$$\partial^2 F/\partial s_{(\bar{i})}\partial s_{(\bar{j})} = F_{rs}\, \ell^r_{(\bar{i})}\ell^s_{(\bar{j})} = F'_{rs}\, \ell'^{\underline{r}}_{(i)}\ell'^{\underline{s}}_{(j)} \ . \tag{3.35}$$

In spheroidal coordinates the last relation resulted in (3.24) featuring the partial derivatives $\partial^2 F/\partial\omega^2$, ... , $\partial F/\partial\alpha$. It is now required that the second-order derivatives (3.35) be written in terms of $\partial^2 F/\partial\lambda^2$, ... , $\partial F/\partial r$. However, this task is to be accomplished without resorting to a development in spherical coordinates which is the subject of the next section. This amounts to avoiding the formulation of the Christoffel symbols (Γ^t_{rs}) in spherical coordinates -- or in some other coordinates if we wish to generalize this approach -- and taking instead advantage of Γ'^t_{rs} already found. The price to pay is the need for certain differential relationships between the two systems.

The straightforward approach adopted in this derivation proceeds from

$$F'_{rs} = \partial^2 F/\partial x'^r \partial x'^s - \Gamma'^t_{rs} F'_t \ , \tag{3.36}$$

where

$$F'_t = (\partial x^k/\partial x'^t)F_k \ ; \qquad F'_t \equiv \partial F/\partial x'^t, \qquad F_k \equiv \partial F/\partial x^k \ . \tag{3.37}$$

The first member on the right-hand side of (3.36) is developed as

$$\partial^2 F/\partial x'^r \partial x'^s = \partial F'_r/\partial x'^s = \partial[(\partial x^k/\partial x'^r)F_k]/\partial x'^s$$
$$= (\partial x^p/\partial x'^r)(\partial x^q/\partial x'^s)\partial^2 F/\partial x^p \partial x^q$$
$$+ F_k \partial(\partial x^k/\partial x'^r)/\partial x'^s ,$$

where the presence of the second term stems from the fact that in general coordinates a second derivative is not a tensor. If this expression as well as (3.37) are substituted in (3.36) and if the new equation is contracted with $\ell'^r_{(\bar{i})}\ell'^s_{(\bar{j})}$ as indicated in (3.35), one obtains

$$\partial^2 F/\partial s_{(\bar{i})}\partial s_{(\bar{j})} = (\partial^2 F/\partial x^r \partial x^s)\ell^r_{(\bar{i})}\ell^s_{(\bar{j})} + [\partial(\partial x^k/\partial x'^r)/\partial x'^s$$
$$- \Gamma'^t_{rs}\partial x^k/\partial x'^t]\ell'^r_{(\bar{i})}\ell'^s_{(\bar{j})}\partial F/\partial x^k , \tag{3.38}$$

where use has been made of the general transformation

$$\ell^m = (\partial x^m/\partial x'^n)\ell'^n . \tag{3.39}$$

Equation (3.38) is the desired formula in which all the derivatives involve only the spherical coordinates, yet the Christoffel symbols in these coordinates are absent.

As a matter of interest we may equate (3.38) with the middle member of (3.35) developed according to (3.22). It then follows that the second term on the right-hand side of (3.38) must be equal to $-\Gamma^k_{rs}\ell^r_{(\bar{i})}\ell^s_{(\bar{j})}F_k$ for any $\ell^r_{(\bar{i})}$, $\ell^s_{(\bar{j})}$ and F. Thus it must also hold that

$$\Gamma^k_{pq} = [\Gamma'^t_{rs}\partial x^k/\partial x'^t - \partial(\partial x^k/\partial x'^r)/\partial x'^s](\partial x'^r/\partial x^p)(\partial x'^s/\partial x^q). \tag{3.40}$$

The presence of the second term within the brackets in (3.40) is due to the Christoffel symbols not being tensors. When the Christoffel symbols on the left-hand side of (3.40) were computed in this manner, the agreement with those derived directly in spherical coordinates was perfect. This confirms the formula (3.38) of which (3.40) is a by-product.

An important step in the present development is the formation of the matrix $\{\partial x^k/\partial x'^r\}$ which, in (3.38), serves to obtain $\ell^r_{(\bar{i})}$, $\ell^s_{(\bar{j})}$ from their counterparts in spheroidal coordinates as is shown in (3.39). Furthermore, the elements of this matrix have to be differentiated with respect to x'^s. In addition to the formulas (3.11) - (3.16), some of the more important relationships needed in these tasks are:

$$\sin\delta_1 = \sin^2\alpha\sin\phi\cos\bar{\phi} = (\nu/r)\sin^2\alpha\sin\phi\cos\phi \ , \tag{3.41a}$$

$$\cos\delta_1 = a^2/(\nu r) \ , \tag{3.41b}$$

$$\sin u = (\nu/a)\cos\alpha\sin\phi \ , \tag{3.41c}$$

$$\cos u = (\nu/a)\cos\phi \ , \tag{3.41d}$$

$$\nu = a(1 - \sin^2\alpha\cos^2 u)^{\frac{1}{2}}/\cos\alpha = a/(1 - \sin^2\alpha\sin^2\phi)^{\frac{1}{2}} \ , \tag{3.41e}$$

$$1 - \sin^2\alpha\sin^2\phi = \cos^2\alpha + \sin^2\alpha\cos^2\phi = a^2/\nu^2 = (r/\nu)\cos\delta_1 \ . \tag{3.41f}$$

After some manipulation we deduce

$$\{\partial x^k/\partial x'^r\} \equiv \begin{bmatrix} \partial\lambda/\partial\omega & \partial\lambda/\partial u & \partial\lambda/\partial\alpha \\ \partial\bar{\phi}/\partial\omega & \partial\bar{\phi}/\partial u & \partial\bar{\phi}/\partial\alpha \\ \partial r/\partial\omega & \partial r/\partial u & \partial r/\partial\alpha \end{bmatrix} = \begin{bmatrix} 1 & 0 & 0 \\ 0 & (\nu/r)\cos\alpha\cos\delta_1 & -(\nu/r)\mathrm{cotg}\alpha\sin\delta_1 \\ 0 & -\nu\cos\alpha\sin\delta_1 & -\nu\mathrm{cotg}\alpha\cos\delta_1 \end{bmatrix}. \tag{3.42}$$

Since this matrix can be decomposed into a product of three matrices of which two are diagonal and one is a rotation matrix, $\{\partial x'^p/\partial x^q\}$ can be formed without any matrix inversions. However, the latter transformation matrix is not needed in this presentation.

By applying (3.39) and (3.42), the vectors appearing in (3.19) can now be expressed in spherical coordinates as

$$\left.\begin{aligned} \ell^r_{(\bar{1})} &= \{1/(r\cos\bar{\phi})\ ,\ 0\ ,\ 0\}\ , \\ \ell^r_{(\bar{2})} &= \{0\ ,\ \cos(\delta_1+\tau)/r\ ,\ -\sin(\delta_1+\tau)\}\ , \\ \ell^r_{(\bar{3})} &= \{0\ ,\ \sin(\delta_1+\tau)/r\ ,\ \cos(\delta_1+\tau)\}\ . \end{aligned}\right\} \tag{3.43}$$

In order to differentiate the elements of (3.42) with respect to x'^s the following auxiliary relations are derived:

$$\partial\phi/\partial\omega = 0, \quad \partial\phi/\partial u = r\cos\delta_1/(\nu\cos\alpha), \quad \partial\phi/\partial\alpha = r\sin\delta_1/(\nu\sin\alpha\cos\alpha);$$

$$\partial\nu/\partial\omega = 0, \quad \partial\nu/\partial u = r\sin\delta_1/\cos\alpha, \quad \partial\nu/\partial\alpha = \nu\mathrm{tg}\alpha - r\cos\delta_1/(\sin\alpha\cos\alpha);$$

$$\partial\delta_1/\partial\omega = 0, \quad \partial\delta_1/\partial u = r\cos\delta_1/(\nu\cos\alpha) - (\nu/r)\cos\alpha\cos\delta_1\ ,$$

$$\partial\delta_1/\partial\alpha = r\sin\delta_1/(\nu\sin\alpha\cos\alpha) + (\nu/r)\mathrm{cotg}\alpha\sin\delta_1\ .$$

After some manipulation, $\partial(\partial x^k/\partial x'^r)/\partial x'^s$ is expressed in the following (symmetric) pairs "(r,s)":

(1,1) ... $\partial\{1,0,0\}/\partial\omega = \{0,0,0\}$,

(1,2) ... $\{0,0,0\}$,

(1,3) ... $\{0,0,0\}$,

(2,2) ... $\{0,\ (\nu^2\cos^2\alpha/r^2)\sin 2\delta_1\ ,\ -r+(\nu^2\cos^2\alpha/r)\cos^2\delta_1\}$,

(2,3) ... $\{0,\ -1/\sin\alpha+(\nu^2/r^2)\cos\alpha\,\mathrm{cotg}\alpha\cos 2\delta_1\ ,$
$-(\nu^2/r)\cos\alpha\,\mathrm{cotg}\alpha\sin\delta_1\cos\delta_1\}$,

(3,3) ... $\{0,\ (\nu/r)\mathrm{cotg}^2\alpha\sin\delta_1-(\nu^2/r^2)\mathrm{cotg}^2\alpha\sin 2\delta_1\ ,$
$r/\sin^2\alpha+\nu\,\mathrm{cotg}^2\alpha\cos\delta_1+(\nu^2/r)\mathrm{cotg}^2\alpha\sin^2\delta_1\}$.

The next step involves the formation of $\Gamma'^t_{rs}\partial x^k/\partial x'^t$, all the elements being already known. The straightforward algebra produces the following results listed again according to the pairs "(r,s)":

(1,1) ... $\{0,\ \sin\bar{\phi}\cos\bar{\phi},\ -r\cos^2\bar{\phi}\}$,

(1,2) ... $\{-\cos\alpha\,\mathrm{tg}\phi,\ 0,\ 0\}$,

(1,3) ... $\{-\mathrm{cotg}\alpha,\ 0,\ 0\}$,

(2,2) ... $\{0,\ 0,\ -r\}$,

(2,3) ... $\{0,\ -1/\sin\alpha,\ 0\}$,

(3,3) ... $\{0,\ (\nu/r)\mathrm{cotg}^2\alpha\sin\delta_1,\ r/\sin^2\alpha+\nu\,\mathrm{cotg}^2\alpha\cos\delta_1\}$.

This, together with the preceding results, leads to the expressions for $[\partial(\partial x^k/\partial x'^r)/\partial x'^s - \Gamma'^t_{rs}\partial x^k/\partial x'^t]$ listed below again according to the pairs "(r,s)":

$$\left.\begin{array}{ll}
(1,1) \ldots & \{0,\ -\sin\bar{\phi}\cos\bar{\phi},\ r\cos^2\bar{\phi}\}\ , \\
(1,2) \ldots & \{\cos\alpha\,\mathrm{tg}\phi,\ 0,\ 0\}\ , \\
(1,3) \ldots & \{\mathrm{cotg}\alpha,\ 0,\ 0\}\ , \\
(2,2) \ldots & \{0,\ (\nu^2\cos^2\alpha/r^2)\sin 2\delta_1,\ (\nu^2\cos^2\alpha/r)\cos^2\delta_1\}\ , \\
(2,3) \ldots & \{0,\ (\nu^2/r^2)\cos\alpha\,\mathrm{cotg}\alpha\cos 2\delta_1,\ -(\nu^2/r)\cos\alpha\,\mathrm{cotg}\alpha\sin\delta_1\cos\delta_1\}, \\
(3,3) \ldots & \{0,\ -(\nu^2/r^2)\mathrm{cotg}^2\alpha\sin 2\delta_1,\ (\nu^2/r)\mathrm{cotg}^2\alpha\sin^2\delta_1\}\ .
\end{array}\right\} \quad (3.44)$$

The results (3.44) are to be contracted with $\ell'^r_{(\bar{i})}\ell'^s_{(\bar{j})}$ appearing in (3.19). The thus obtained expressions are now listed according to the (symmetric) pairs "$(\bar{i},\bar{j})$":

$$\left.\begin{array}{ll}
(1,1) \ldots & \{0,\ -\mathrm{tg}\bar{\phi}/r^2,\ 1/r\}\ , \\
(1,2) \ldots & \{\sin(\bar{\phi}+\delta_1+\tau)/(r^2\cos^2\bar{\phi}),\ 0,\ 0\}\ , \\
(1,3) \ldots & \{-\cos(\bar{\phi}+\delta_1+\tau)/(r^2\cos^2\bar{\phi}),\ 0,\ 0\}, \\
(2,2) \ldots & \{0,\ \sin 2(\delta_1+\tau)/r^2,\ \cos^2(\delta_1+\tau)/r\}\ , \\
(2,3) \ldots & \{0,\ -\cos 2(\delta_1+\tau)/r^2,\ \tfrac{1}{2}\sin 2(\delta_1+\tau)/r\}\ , \\
(3,3) \ldots & \{0,\ -\sin 2(\delta_1+\tau)/r^2,\ \sin^2(\delta_1+\tau)/r\}\ .
\end{array}\right\} \quad (3.45)$$

In the second and third expressions of (3.45), ϕ has been replaced by $\bar{\phi}+\delta_1$.

Finally, the second partial derivatives in the first term on the right-hand side of (3.38) are contracted with $\ell^r_{(\bar{i})}\ell^s_{(\bar{j})}$ appearing in (3.43) and the elements of (3.45) are contracted with $F_k \equiv \partial F/\partial x^k$. Thus the desired second-order derivatives of F expressed in spherical coordinates are:

$$
\left.
\begin{aligned}
\partial^2F/\partial s_{(\bar{1})}\partial s_{(\bar{1})} &= [1/(r^2\cos^2\bar{\phi})]\,\partial^2F/\partial\lambda^2 - (\mathrm{tg}\bar{\phi}/r^2)\partial F/\partial\bar{\phi} + (1/r)\partial F/\partial r, \\
\partial^2F/\partial s_{(\bar{1})}\partial s_{(\bar{2})} &= [\cos(\delta_1+\tau)/(r^2\cos\bar{\phi})]\,\partial^2F/\partial\lambda\partial\bar{\phi} \\
&\quad - [\sin(\delta_1+\tau)/(r\cos\bar{\phi})]\,\partial^2F/\partial\lambda\partial r \\
&\quad + [\sin(\bar{\phi}+\delta_1+\tau)/(r^2\cos^2\bar{\phi})]\,\partial F/\partial\lambda\ , \\
\partial^2F/\partial s_{(\bar{1})}\partial s_{(\bar{3})} &= [\sin(\delta_1+\tau)/(r^2\cos\bar{\phi})]\,\partial^2F/\partial\lambda\partial\bar{\phi} \\
&\quad + [\cos(\delta_1+\tau)/(r\cos\bar{\phi})]\,\partial^2F/\partial\lambda\partial r \\
&\quad + [\cos(\bar{\phi}+\delta_1+\tau)/(r^2\cos^2\bar{\phi})]\,\partial F/\partial\lambda\ , \\
\partial^2F/\partial s_{(\bar{2})}\partial s_{(\bar{2})} &= [\cos^2(\delta_1+\tau)/r^2]\,\partial^2F/\partial\bar{\phi}^2 - [\sin 2(\delta_1+\tau)/r]\,\partial^2F/\partial\bar{\phi}\partial r \\
&\quad + \sin^2(\delta_1+\tau)\partial^2F/\partial r^2 + [\sin 2(\delta_1+\tau)/r^2]\,\partial F/\partial\bar{\phi} \\
&\quad + [\cos^2(\delta_1+\tau)/r]\,\partial F/\partial r\ , \\
\partial^2F/\partial s_{(\bar{2})}\partial s_{(\bar{3})} &= [\tfrac{1}{2}\sin 2(\delta_1+\tau)/r^2]\,\partial^2F/\partial\bar{\phi}^2 + [\cos 2(\delta_1+\tau)/r]\,\partial^2F/\partial\bar{\phi}\partial r \\
&\quad - \tfrac{1}{2}\sin 2(\delta_1+\tau)\partial^2F/\partial r^2 - [\cos 2(\delta_1+\tau)/r^2]\,\partial F/\partial\bar{\phi} \\
&\quad + \tfrac{1}{2}[\sin 2(\delta_1+\tau)/r]\,\partial F/\partial r\ ,
\end{aligned}
\right\} \quad (3.46)
$$

$$\left.\begin{aligned}\partial^2F/\partial s_{(\bar{3})}\partial s_{(\bar{3})} = {} & [\sin^2(\delta_1+\tau)/r^2]\partial^2F/\partial\bar{\phi}^2 + [\sin 2(\delta_1+\tau)/r]\partial^2F/\partial\bar{\phi}\partial r \\ & + \cos^2(\delta_1+\tau)\partial^2F/\partial r^2 - [\sin 2(\delta_1+\tau)/r^2]\partial F/\partial\bar{\phi} \\ & + [\sin^2(\delta_1+\tau)/r]\partial F/\partial r\ .\end{aligned}\right\}$$

As in the preceding section, if τ is set to δ_2 , 0 , or $-\delta_1$ the desired derivatives are obtained for the triads i" , i' , or i , respectively. These results could again be refined upon transformation from the triad i" to the triad $\tilde{i}$ in the manner of equation (3.34) in which the symbol F' would now be replaced by F.

3.4 Separate Derivations in Spherical Coordinates

The well-known formula for the metric in spherical coordinates $\{\lambda,\bar{\phi},r\}$ reads

$$ds^2 = r^2\cos^2\bar{\phi}\, d\lambda^2 + r^2 d\bar{\phi}^2 + dr^2 ,$$

yielding the metric tensor and the associated metric tensor:

$$\{g_{rs}\} = \text{diag.}\,\{r^2\cos^2\bar{\phi},\ r^2,\ 1\} , \tag{3.47a}$$

$$\{g^{rs}\} = \text{diag.}\,\{1/(r^2\cos^2\bar{\phi}),\ 1/r^2,\ 1\} . \tag{3.47b}$$

In agreement with the procedure which lead to (3.18), we now have along the coordinate lines:

$$\left.\begin{aligned} \ell^r_{(1)} &= \{1/(r\cos\bar{\phi}),\ 0,\ 0\} , \\ \ell^r_{(2)} &= \{0,\ 1/r,\ 0\} , \\ \ell^r_{(3)} &= \{0,\ 0,\ 1\} . \end{aligned}\right\} \tag{3.48}$$

In order to represent the triad $\bar{i}$, the above triad i has to be rotated around the first axis by the angle $-(\delta_1+\tau)$ as can be gathered from Figure 3.1. We thus have

$$
\left.
\begin{aligned}
\ell^r_{(\bar{1})} &= \ell^r_{(1)} = \{1/(r\cos\bar{\phi}),\ 0\ ,\ 0\}\ , \\
\ell^r_{(\bar{2})} &= \cos(\delta_1+\tau)\ell^r_{(2)} - \sin(\delta_1+\tau)\ell^r_{(3)} = \{0\ ,\ \cos(\delta_1+\tau)/r, \\
&\qquad\qquad\qquad\qquad\qquad\qquad - \sin(\delta_1+\tau)\}\ , \\
\ell^r_{(\bar{3})} &= \sin(\delta_1+\tau)\ell^r_{(2)} + \cos(\delta_1+\tau)\ell^r_{(3)} = \{0\ ,\ \sin(\delta_1+\tau)/r\ , \\
&\qquad\qquad\qquad\qquad\qquad\qquad \cos(\delta_1+\tau)\}\ ,
\end{aligned}
\right\} \quad (3.49)
$$

which agrees with (3.43).

Upon inserting the expressions (3.47) into (3.20), the following nonzero Christoffel symbols are readily obtained:

$$
\left.
\begin{aligned}
\Gamma^1_{12} &= -\mathrm{tg}\bar{\phi}\ , \\
\Gamma^1_{13} &= 1/r\ ; \\
\Gamma^2_{11} &= \sin\bar{\phi}\cos\bar{\phi}\ , \\
\Gamma^2_{23} &= 1/r\ ; \\
\Gamma^3_{11} &= -r\cos^2\bar{\phi}\ , \\
\Gamma^3_{22} &= -r\ .
\end{aligned}
\right\} \quad (3.50)
$$

The application of (3.22) yields immediately the second covariant derivatives:

$$\left.\begin{aligned}
F_{11} &= \partial^2F/\partial\lambda^2 - \sin\bar\phi\cos\bar\phi\ \partial F/\partial\bar\phi + r\cos^2\bar\phi\ \partial F/\partial r\ ,\\
F_{12} &= \partial^2F/\partial\lambda\partial\bar\phi + \mathrm{tg}\bar\phi\ \partial F/\partial\lambda\ ,\\
F_{13} &= \partial^2F/\partial\lambda\partial r - (1/r)\partial F/\partial\lambda\ ,\\
F_{22} &= \partial^2F/\partial\bar\phi^2 + r\ \partial F/\partial r\ ,\\
F_{23} &= \partial^2F/\partial\bar\phi\partial r - (1/r)\partial F/\partial\bar\phi\ ,\\
F_{33} &= \partial^2F/\partial r^2\ .
\end{aligned}\right\} \qquad (3.51)$$

With the aid of (3.49) and (3.51) the desired second-order derivatives $\partial^2F/\partial s_{(\bar i)}\partial s_{(\bar j)}$ can be computed according to (3.9). Upon carrying out the indicated operations the results (3.46) are obtained. The link between the two coordinate systems established in the preceding section has thus confirmed much of the development in either coordinate system.

By setting τ to δ_2 , 0 , or $-\delta_1$ the desired derivatives are obtained for the triads i" , i' , or i , respectively, as stated earlier. In order to evaluate the present methodology, the case $\tau = -\delta_1$ is of interest. Accordingly, from (3.46) we deduce

$$\left.\begin{aligned}
\partial^2F/\partial s_{(1)}\partial s_{(1)} &= [1/(r^2\cos^2\bar\phi)]\,\partial^2F/\partial\lambda^2\\
&\quad - (\mathrm{tg}\bar\phi/r^2)\partial F/\partial\bar\phi + (1/r)\partial F/\partial r\ ,\\
\partial^2F/\partial s_{(1)}\partial s_{(2)} &= [1/(r^2\cos\bar\phi)]\,\partial^2F/\partial\lambda\partial\bar\phi\\
&\quad + [\sin\bar\phi/(r^2\cos^2\bar\phi)]\,\partial F/\partial\lambda\ ,
\end{aligned}\right|$$

$$
\left.
\begin{aligned}
\partial^2 F/\partial s_{(1)}\partial s_{(3)} &= \left[1/(r\cos\bar{\phi})\right]\partial^2 F/\partial\lambda\partial r - \left[1/(r^2\cos\bar{\phi})\right]\partial F/\partial\lambda\ , \\
\partial^2 F/\partial s_{(2)}\partial s_{(2)} &= (1/r^2)\partial^2 F/\partial\bar{\phi}^2 + (1/r)\partial F/\partial r\ , \\
\partial^2 F/\partial s_{(2)}\partial s_{(3)} &= (1/r)\partial^2 F/\partial\bar{\phi}\partial r - (1/r^2)\partial F/\partial\bar{\phi}, \\
\partial^2 F/\partial s_{(3)}\partial s_{(3)} &= \partial^2 F/\partial r^2\ .
\end{aligned}
\right\} \quad (3.52)
$$

Clearly, this outcome could be obtained also directly upon using (3.48) and (3.51). In this case, only the steps corresponding to (3.47), (3.48), (3.50) and (3.51) would have been involved while (3.49) and the more general results (3.46) would have been by-passed.

The process leading to (3.52) would have required considerably more space if the tensor approach to this problem had been avoided, whether for pedagogical or other reasons. This can be appreciated upon consulting the development in [Tscherning, 1976], where our formulas (3.52) were obtained, in the present order, in equations numbered as (53), (55), (57), (52), (56) and (54); our notations $ds_{(1)}$, $ds_{(2)}$, $ds_{(3)}$ correspond respectively to dy , dx , dz in this reference. The methodology used therein was not based on tensor analysis but made use of the ordinary differentiation and interrelationships between the local Cartesian coordinate system, the earth-fixed Cartesian coordinate system and the polar coordinate system. Such a paper is certainly useful, especially from the pedagogical point of view, since it addresses itself to large audiences and exposes the treated subject in great depth. On the other hand, in [Tscherning, 1976] the derivations leading to our formula (3.52) required eight pages (pages 73 through 80), even though only the simplest case corresponding to the triad i was treated. We might thus conclude that although the

methodology of Hotine [1969] requires prior knowledge of certain elements of tensor analysis, this disadvantage (if it is indeed a disadvantage) is more than offset by the ease and rapidity with which many general, as well as specialized, formulas in geodesy may be derived.

The well-known formula giving the Laplacian of F in spherical coordinates is readily obtained as the trace of the matrix composed of the elements presented in (3.46) for any choice of τ; the easiest choice is, of course, that of $\tau = -\delta_1$ corresponding to (3.52). In every case we obtain

$$\Delta F = [1/(r^2\cos^2\bar{\phi})]\,\partial^2F/\partial\lambda^2 + (1/r^2)\partial^2F/\partial\bar{\phi}^2 + \partial^2F/\partial r^2$$
$$- (\mathrm{tg}\bar{\phi}/r^2)\partial F/\partial\bar{\phi} + (2/r)\partial F/\partial r \ . \qquad (3.53)$$

As has already been pointed out in the closing statement of the preceding section, the results (3.46), specialized for the triad i" , can be further refined upon transformation to the triad $\tilde{i}$; it is immediately verified (see 3.34) that ΔF remains unchanged.

A practical question left unanswered so far concerns the determination of the angle δ_2 needed in specializing the results (3.46) for the triad i" . In fact, the angle needed in this task is the total angle

$$\delta = \delta_1 + \delta_2 \ , \qquad (3.54)$$

where δ_1 is known from (3.16). In order to determine δ we proceed as in Section 2 where δ_2 alone was sought. The vector U_r will now be projected onto the triad (3.48), the projections being respectively

$$\left.\begin{aligned} \partial U/\partial s_{(1)} &= U_r \ell^r_{(1)} = 0 \ , \\ \partial U/\partial s_{(2)} &= U_r \ell^r_{(2)} = (1/r)\partial U/\partial \bar{\phi} \ , \\ \partial U/\partial s_{(3)} &= U_r \ell^r_{(3)} = \partial U/\partial r \ . \end{aligned}\right\} \tag{3.55}$$

Similar to (3.29) we have

$$\mathrm{tg}\delta = (-\partial U/\partial s_{(2)})/(-\partial U/\partial s_{(3)}) \ , \tag{3.56}$$

which is in general positive whether in a rotating or a nonrotating field (at the poles and on the equator it is zero). The radial (positive inward) and the meridian (positive north) components of γ at P are now denoted as $\hat{\gamma}_n$, $\hat{\gamma}_m$; we have

$$\hat{\gamma}_n = -\partial U/\partial s_{(3)} \ , \tag{3.57a}$$

$$\hat{\gamma}_m = \partial U/\partial s_{(2)} \ , \tag{3.57b}$$

$$\gamma = (\hat{\gamma}_n^2 + \hat{\gamma}_m^2)^{\frac{1}{2}} \ , \tag{3.57c}$$

and from (3.56),

$$\mathrm{tg}\delta = -\hat{\gamma}_m/\hat{\gamma}_n \ . \tag{3.58}$$

In expressing (3.55) explicitly, use can be made of the spherical harmonic expansion of U which reads (see e.g. [Blaha, 1977], page 79)

$$U = (GM/r)[1 + (a_o/r)^2 C^*_{20} P_2(\sin\bar{\phi}) + (a_o/r)^4 C^*_{40} P_4(\sin\bar{\phi}) + \ldots]$$
$$+ \tfrac{1}{2}\tilde{\omega}^2 r^2 \cos^2\bar{\phi} \ , \tag{3.59}$$

where C^*_{20} , C^*_{40} , ... , are the spherical harmonic coefficients in the standard field, linked to iGA_{20} in (3.27b) as follows:

$$C^*_{(2n-2),0} = (-1)^n[-(2n+1) + (2n-2)\ Q\ e_o^{2n-2}] \ / \ [(2n-1)(2n+1)] \ ,$$

$$Q = iGA_{20}(ae)/GM \ .$$

In analogy to Section 2, if one wishes to consider a nonrotating field the terms containing $\tilde{\omega}^2$ explicitly should be dropped. From (3.59) we express

$$\partial U/\partial\bar{\phi} = (GM/r)\,[(a_o/r)^2 C^*_{20} dP_2(\sin\bar{\phi})/d\bar{\phi} + (a_o/r)^4 C^*_{40} dP_4(\sin\bar{\phi})/d\bar{\phi} + \ldots] - \tilde{\omega}^2 r^2 \sin\bar{\phi}\cos\bar{\phi} \ , \tag{3.60}$$

$$\partial U/\partial r = -(GM/r^2)\,[1 + 3(a_o/r)^2 C^*_{20} P_2(\sin\bar{\phi}) + 5(a_o/r)^4 C^*_{40} P_4(\sin\bar{\phi}) + \ldots] + \tilde{\omega}^2 r \cos^2\bar{\phi} \ ; \tag{3.61}$$

the terms containing the coefficients beyond C^*_{40} and certainly those beyond C^*_{60} are usually neglected. For reference purposes we list:

$$\left.\begin{aligned}
&P_2(\sin\bar{\phi}) = \tfrac{1}{2}(3\sin^2\bar{\phi} - 1) \ , \\
&P_4(\sin\bar{\phi}) = (1/8)(35\sin^4\bar{\phi} - 30\sin^2\bar{\phi} + 3) \ ; \\
&dP_2(\sin\bar{\phi})/d\bar{\phi} = 3\sin\bar{\phi}\cos\bar{\phi} \ , \\
&dP_4(\sin\bar{\phi})/d\bar{\phi} = (5/2)(7\sin^2\bar{\phi} - 3)\sin\bar{\phi}\cos\bar{\phi} \ ; \\
&d^2P_2(\sin\bar{\phi})/d\bar{\phi}^2 = 3(-2\sin^2\bar{\phi} + 1) \ , \\
&d^2P_4(\sin\bar{\phi})/d\bar{\phi}^2 = \tfrac{1}{2}(-140\sin^4\bar{\phi} + 135\sin^2\bar{\phi} - 15) \ .
\end{aligned}\right\} \tag{3.62}$$

The inclusion of C^*_{60} would follow along the same lines.

3.5 Practical Applicability of the Results

In this section the function F is treated in spherical coordinates and is first specialized to U (standard potential) and then to T (disturbing potential). Also, the more usual geodetic conventions corresponding to (3.3) are adopted. First we consider

$$F \equiv U \ ,$$

$$\tau \equiv \delta_2 \quad \text{(the triad } \bar{i} \text{ is replaced by the triad i")} \ ;$$

taking into account the property $\partial U/\partial\lambda = 0$ and the convention (3.54), the results (3.46) read

$$\left.\begin{aligned}
U_{x''x''} &= (\cos^2\delta/r^2)\partial^2U/\partial\bar{\phi}^2 - (\sin 2\delta/r)\partial^2U/\partial\bar{\phi}\partial r \\
&\quad + \sin^2\delta\ \partial^2U/\partial r^2 + (\sin 2\delta/r^2)\partial U/\partial\bar{\phi} + (\cos^2\delta/r)\partial U/\partial r \ , \\
U_{x''y''} &= 0 \ , \\
U_{x''z''} &= (\tfrac{1}{2}\sin 2\delta/r^2)\partial^2U/\partial\bar{\phi}^2 + (\cos 2\delta/r)\partial^2U/\partial\bar{\phi}\partial r \\
&\quad - \tfrac{1}{2}\sin 2\delta\ \partial^2U/\partial r^2 - (\cos 2\delta/r^2)\partial U/\partial\bar{\phi} + \tfrac{1}{2}(\sin 2\delta/r)\partial U/\partial r \ , \\
U_{y''y''} &= -(\mathrm{tg}\bar{\phi}/r^2)\partial U/\partial\bar{\phi} + (1/r)\partial U/\partial r \ , \\
U_{y''z''} &= 0 \ , \\
U_{z''z''} &= (\sin^2\delta/r^2)\ \partial^2U/\partial\bar{\phi}^2 + (\sin 2\delta/r)\partial^2U/\partial\bar{\phi}\partial r \\
&\quad + \cos^2\delta\ \partial^2U/\partial r^2 - (\sin 2\delta/r^2)\partial U/\partial\bar{\phi} + (\sin^2\delta/r)\partial U/\partial r \ .
\end{aligned}\right\} \quad (3.63)$$

Equation (3.53) applies now in the form

$$\Delta U = U_{x''x''} + U_{y''y''} + U_{z''z''} = (1/r^2)\partial^2 U/\partial\bar{\phi}^2 + \partial^2 U/\partial r^2 - (tg\bar{\phi}/r^2)\partial U/\partial\bar{\phi} + (2/r)\partial U/\partial r \ . \tag{3.64}$$

The first partial derivatives needed in (3.63), (3.64) have been presented in (3.60) - (3.62). The second partial derivatives follow as

$$\left.\begin{aligned}
\partial^2 U/\partial\bar{\phi}^2 &= (GM/r)\left[(a_o/r)^2 C^*_{20} d^2P_2(\sin\bar{\phi})/d\bar{\phi}^2 + (a_o/r)^4 C^*_{40} d^2P_4(\sin\bar{\phi})/d\bar{\phi}^2 + \ldots\right] - \tilde{\omega}^2 r^2(\cos^2\bar{\phi} - \sin^2\bar{\phi}) \ , \\
\partial^2 U/\partial\bar{\phi}\partial r &= -(GM/r^2)\left[3(a_o/r)^2 C^*_{20} dP(\sin\bar{\phi})/d\bar{\phi} + 5(a_o/r)^4 C^*_{40} dP_4(\sin\bar{\phi})/d\bar{\phi} + \ldots\right] - 2\tilde{\omega}^2 r \sin\bar{\phi}\cos\bar{\phi} \ , \\
\partial^2 U/\partial r^2 &= 2(GM/r^3)\left[1 + 6(a_o/r)^2 C^*_{20} P_2(\sin\bar{\phi}) + 15(a_o/r)^4 C^*_{40} P_4(\sin\bar{\phi}) + \ldots\right] + \tilde{\omega}^2\cos^2\bar{\phi} \ ,
\end{aligned}\right\} \tag{3.65}$$

in which the formulas (3.62) apply again. If these explicit partial derivatives of U are used in (3.64), the coefficients of C^*_{20} , C^*_{40} , ... , are seen to be zero and the Laplacian is confirmed to be

$$\Delta U = 2\tilde{\omega}^2 \ . \tag{3.66}$$

If a nonrotating field is considered the Laplacian becomes zero and U becomes a harmonic function (as is T or the gravitational part of W).

If we wish to obtain the second-order derivatives of U in the triad $\tilde{i}$ rather than in the triad i'', the expressions in (3.34) are specialized (U is written for F', etc.) and combined with (3.63) to give

$$
\left.
\begin{aligned}
U_{\tilde{x}\tilde{x}} &\simeq U_{x''x''} - 2\xi\, U_{x''z''} = [(\cos^2\delta - \xi \sin 2\delta)/r^2]\partial^2 U/\partial\bar{\phi}^2 \\
&\quad - [(\sin 2\delta + 2\xi\cos 2\delta)/r]\, \partial^2 U/\partial\bar{\phi}\partial r \\
&\quad + (\sin^2\delta + \xi\sin 2\delta)\partial^2 U/\partial r^2 + [(\sin 2\delta + 2\xi\cos 2\delta)/r^2]\partial U/\partial\bar{\phi} \\
&\quad + [(\cos^2\delta - \xi\sin 2\delta)/r]\partial U/\partial r\ , \\[2ex]
U_{\tilde{x}\tilde{y}} &\simeq -\eta U_{x''z''} = -\eta[\tfrac{1}{2}(\sin 2\delta/r^2)\partial^2 U/\partial\bar{\phi}^2 + (\cos 2\delta/r)\partial^2 U/\partial\bar{\phi}\partial r \\
&\quad - \tfrac{1}{2}\sin 2\delta\ \partial^2 U/\partial r^2 - (\cos 2\delta/r^2)\partial U/\partial\bar{\phi} + \tfrac{1}{2}(\sin 2\delta/r)\partial U/\partial r]\ , \\[2ex]
U_{\tilde{x}\tilde{z}} &\simeq U_{x''z''} - \xi(U_{z''z''} - U_{x''x''}) = [(\tfrac{1}{2}\sin 2\delta + \xi\cos 2\delta)/r^2]\partial^2 U/\partial\bar{\phi}^2 \\
&\quad + [(\cos 2\delta - 2\xi\sin 2\delta)/r\,]\partial^2 U/\partial\bar{\phi}\partial r - (\tfrac{1}{2}\sin 2\delta + \xi\cos 2\delta)\partial^2 U/\partial r^2 \\
&\quad - [(\cos 2\delta - 2\xi\sin 2\delta)/r^2]\partial U/\partial\bar{\phi} + [(\tfrac{1}{2}\sin 2\delta + \xi\cos 2\delta)/r]\partial U/\partial r\ , \\[2ex]
U_{\tilde{y}\tilde{y}} &\simeq U_{y''y''} = -(\mathrm{tg}\phi/r^2)\partial U/\partial\bar{\phi} + (1/r)\partial U/\partial r\ , \\[2ex]
U_{\tilde{y}\tilde{z}} &\simeq -\eta(U_{z''z''} - U_{y''y''}) = -\eta\{(\sin^2\delta/r^2)\partial^2 U/\partial\bar{\phi}^2 + (\sin 2\delta/r)\partial^2 U/\partial\bar{\phi}\partial r \\
&\quad + \cos^2\delta\ \partial^2 U/\partial r^2 + [(\mathrm{tg}\bar{\phi} - \sin 2\delta)/r^2]\partial U/\partial\bar{\phi} - (\cos^2\delta/r)\partial U/\partial r\}\ , \\[2ex]
U_{\tilde{z}\tilde{z}} &\simeq U_{z''z''} + 2\xi\, U_{x''z''} = [(\sin^2\delta + \xi\sin 2\delta)/r^2]\partial^2 U/\partial\bar{\phi}^2 \\
&\quad + [(\sin 2\delta + 2\xi\cos 2\delta)/r]\ \partial^2 U/\partial\bar{\phi}\partial r + (\cos^2\delta - \xi\sin 2\delta)\partial^2 U/\partial r^2 \\
&\quad - [(\sin 2\delta + 2\xi\cos 2\delta)/r^2]\partial U/\partial\bar{\phi} + [(\sin^2\delta + \xi\sin 2\delta)/r]\partial U/\partial r\ .
\end{aligned}
\right\} \tag{3.67}
$$

For practical applications, the relation

$$W = U + T$$

leads to $W_{\tilde{z}\tilde{z}} = U_{\tilde{z}\tilde{z}} + T_{\tilde{z}\tilde{z}}$, etc., where $W_{\tilde{z}\tilde{z}}$, etc., may be directly observed. The observations could be considered at the ground level or at higher levels (aircraft altitude, satellite altitude) and distinction could be made between the rotating and nonrotating fields. From the observations $W_{\tilde{z}\tilde{z}}$, etc., and from their counterparts $U_{\tilde{z}\tilde{z}}$, etc., the values $T_{\tilde{z}\tilde{z}}$, etc., can be derived and modeled by spherical harmonics, point masses and other means. For example, lower degree and order spherical harmonic coefficients may be considered fixed and higher degree and order coefficients may be solved for in a least squares adjustment; or instead of solving for these coefficients, local parameters such as point mass magnitudes can be adjusted. In the most rigorous case, the values to be modeled are

$$\left.\begin{aligned}
T_{\tilde{x}\tilde{x}} &= W_{\tilde{x}\tilde{x}} - U_{\tilde{x}\tilde{x}} , \\
T_{\tilde{x}\tilde{y}} &= W_{\tilde{x}\tilde{y}} - U_{\tilde{x}\tilde{y}} , \\
T_{\tilde{x}\tilde{z}} &= W_{\tilde{x}\tilde{z}} - U_{\tilde{x}\tilde{z}} , \\
T_{\tilde{y}\tilde{y}} &= W_{\tilde{y}\tilde{y}} - U_{\tilde{y}\tilde{y}} , \\
T_{\tilde{y}\tilde{z}} &= W_{\tilde{y}\tilde{z}} - U_{\tilde{y}\tilde{z}} , \\
T_{\tilde{z}\tilde{z}} &= W_{\tilde{z}\tilde{z}} - U_{\tilde{z}\tilde{z}} .
\end{aligned}\right\} \qquad (3.68)$$

Since I_{zz} , etc., are relatively small quantities, the triad i involved in their formulation can be replaced by the triad i" , i' , or even i ; the case i' can be viewed as a spheroidal approximation and the case i , as a spherical approximation. On the other hand, the spherical approximation with regard to $U_{\tilde{z}\tilde{z}}$, etc., would in general result in prohibitive errors. If a simplification is to take place in this respect, we assume that it will result in $U_{z''z''}$, etc., replacing $U_{\tilde{z}\tilde{z}}$, etc. Below are listed the practical counterparts of (3.68). With regard to T, the triad i identifying the spherical approximation (in parentheses) and the triad i" are considered:

$$\left.\begin{aligned}
&(T_{xx}\simeq)\ T_{x''x''} \simeq W_{\tilde{x}\tilde{x}} - U_{x''x''} ,\\
&(T_{xy}\simeq)\ T_{x''y''} \simeq W_{\tilde{x}\tilde{y}} ,\\
&(T_{xz}\simeq)\ T_{x''z''} \simeq W_{\tilde{x}\tilde{z}} - U_{x''z''} ,\\
&(T_{yy}\simeq)\ T_{y''y''} \simeq W_{\tilde{y}\tilde{y}} - U_{y''y''} ,\\
&(T_{yz}\simeq)\ T_{y''z''} \simeq W_{\tilde{y}\tilde{z}} ,\\
&(T_{zz}\simeq)\ T_{z''z''} \simeq W_{\tilde{z}\tilde{z}} - U_{z''z''} ;
\end{aligned}\right\} \qquad (3.69)$$

the values $U_{z''z''}$, etc., have been presented in (3.63) and the values T_{zz} , $T_{z''z''}$, etc., will be developed shortly. It can be shown that errors caused by simplifications in the horizontal gradients of standard gravity ($U_{\tilde{x}\tilde{z}}$, $U_{\tilde{y}\tilde{z}}$) and in the vertical gradient of standard gravity ($U_{\tilde{z}\tilde{z}}$) reach approximately the following values:

$U_{\tilde{x}\tilde{z}}$ ... -0.011 E per 1" in ξ ,

$U_{\tilde{y}\tilde{z}}$ ... -0.011 E per 1" in η ,

$U_{\tilde{z}\tilde{z}}$ ... 0.000024 sin $2\bar{\phi}$ E per 1" in ξ .

The error in $U_{\tilde{z}\tilde{z}}$ is completely negligible under any circumstances since even if ξ were 60" it would only reach 0.001 E (the measurements are often considered good to ±0.05 E, where E ≡ Eötvös = 0.1 mgal/km).

In order to develop the second-order derivatives of T in (3.69), we specialize (3.46):

$$F \equiv T \quad ,$$

$$\tau \equiv \delta_2 \; .$$

The expressions for $T_{z''z''}$, etc., can be obtained by simply transcribing (3.46) with T replacing F , δ replacing $(\delta_1+\tau)$ and dx, etc., replacing $ds_{(2)}$, etc.; there is no need to list the results again with these minor notational changes. When T is developed in spherical harmonics, such results could be made computationally more economical by eliminating $\partial^2T/\partial\bar{\phi}^2$ which involves the evaluation of $d^2P_{nm}(\sin\bar{\phi})/d\bar{\phi}^2$, where $P_{nm}(\sin\bar{\phi})$ are the associated Legendre functions in argument $\sin\bar{\phi}$. By contrast, when U was considered, the corresponding two or at most three second partial derivatives with respect to $\bar{\phi}$ were exceedingly simple to evaluate in terms of even powers of $\sin\bar{\phi}$ (see equation 3.62). In the present situation, $\partial^2T/\partial\bar{\phi}^2$ can be eliminated upon using

$$\Delta T = 0, \tag{3.70}$$

where the Laplacian of T is given in (3.53) with T replacing F , hence

$$(1/r^2)\partial^2 T/\partial\phi^2 = -\left[1/(r^2\cos^2\phi)\right]\partial^2 T/\partial\lambda^2 - \partial^2 T/\partial r^2 + (tg\bar{\phi}/r^2)\partial T/\partial\bar{\phi} - (2/r)\partial T/\partial r \ . \tag{3.71}$$

With the substitution (3.71) the transcription of (3.46) yields upon incorporating the above-mentioned notational changes:

$$\left.\begin{aligned}
T_{x''x''} &= -\left[\cos^2\delta/(r^2\cos^2\bar{\phi})\right]\partial^2 T/\partial\lambda^2 - (\sin 2\delta/r)\partial^2 T/\partial\bar{\phi}\partial r \\
&\quad - \cos 2\delta\ \partial^2 T/\partial r^2 + \left[(tg\bar{\phi}\cos^2\delta + \sin 2\delta)/r^2\right]\partial T/\partial\bar{\phi} \\
&\quad - (\cos^2\delta/r)\partial T/\partial r \ , \\
T_{x''y''} &= \left[\cos\delta/(r^2\cos\bar{\phi})\right]\partial^2 T/\partial\lambda\partial\bar{\phi} - \left[\sin\delta/(r\cos\bar{\phi})\right]\partial^2 T/\partial\lambda\partial r \\
&\quad + \left[\sin(\bar{\phi}+\delta)/(r^2\cos^2\bar{\phi})\right]\partial T/\partial\lambda \ , \\
T_{x''z''} &= -\tfrac{1}{2}\left[\sin 2\delta/(r^2\cos^2\bar{\phi})\right]\partial^2 T/\partial\lambda^2 + (\cos 2\delta/r)\partial^2 T/\partial\bar{\phi}\partial r \\
&\quad - \sin 2\delta\ \partial^2 T/\partial r^2 - \left[(\cos 2\delta - \tfrac{1}{2}\sin 2\delta\ tg\bar{\phi})/r^2\right]\partial T/\partial\bar{\phi} \\
&\quad - \tfrac{1}{2}(\sin 2\delta/r)\partial T/\partial r \ , \\
T_{y''y''} &= \left[1/(r^2\cos^2\bar{\phi})\right]\partial^2 T/\partial\lambda^2 - (tg\bar{\phi}/r^2)\partial T/\partial\bar{\phi} + (1/r)\partial T/\partial r \ , \\
T_{y''z''} &= \left[\sin\delta/(r^2\cos\bar{\phi})\right]\partial^2 T/\partial\lambda\partial\bar{\phi} + \left[\cos\delta/(r\cos\bar{\phi})\right]\partial^2 T/\partial\lambda\partial r \\
&\quad - \left[\cos(\bar{\phi}+\delta)/(r^2\cos^2\bar{\phi})\right]\partial T/\partial\lambda \ , \\
T_{z''z''} &= -\left[\sin^2\delta/(r^2\cos^2\bar{\phi})\right]\partial^2 T/\partial\lambda^2 + (\sin 2\delta/r)\partial^2 T/\partial\bar{\phi}\partial r \\
&\quad + \cos 2\delta\ \partial^2 T/\partial r^2 - \left[(\sin 2\delta - \sin^2\delta tg\bar{\phi})/r^2\right]\partial T/\partial\bar{\phi} \\
&\quad - (\sin^2\delta/r)\partial T/\partial r \ .
\end{aligned}\right\} \tag{3.72}$$

Some of the algebra is verified immediately by confirming (3.70).

The specialization of (3.46) with $\tau \equiv -\delta_1$ already resulted in (3.52). If also (3.71) is utilized (3.52) can be transcribed as

$$\left.\begin{aligned}
T_{xx} &= -[1/(r^2\cos^2\bar{\phi})]\,\partial^2T/\partial\lambda^2 - \partial^2T/\partial r^2 + (tg\bar{\phi}/r^2)\partial T/\partial\bar{\phi} \\
&\quad - (1/r)\partial T/\partial r\ , \\
T_{xy} &= [1/(r^2\cos\bar{\phi})]\,\partial^2T/\partial\lambda\partial\bar{\phi} + [tg\bar{\phi}/(r^2\cos\bar{\phi})]\,\partial T/\partial\lambda\ , \\
T_{xz} &= (1/r)\partial^2T/\partial\bar{\phi}\partial r - (1/r^2)\partial T/\partial\bar{\phi}\ , \\
T_{yy} &= [1/(r^2\cos^2\bar{\phi})]\,\partial^2T/\partial\lambda^2 - (tg\bar{\phi}/r^2)\partial T/\partial\bar{\phi} + (1/r)\partial T/\partial r\ , \\
T_{yz} &= [1/(r\ \cos\bar{\phi})]\,\partial^2T/\partial\lambda\partial r - [1/(r^2\cos\bar{\phi})]\,\partial T/\partial\lambda\ , \\
T_{zz} &= \partial^2T/\partial r^2\ .
\end{aligned}\right\} \qquad (3.73)$$

However, in this case only T_{xx} originally contained $\partial^2T/\partial\bar{\phi}^2$; this original form is

$$T_{xx} = (1/r^2)\partial^2T/\partial\bar{\phi}^2 + (1/r)\partial T/\partial r\ . \qquad (3.73')$$

Before discussing the usefulness of (3.73') and some of the circumstances leading to the choice of the triad i over the triad i" or vice versa, we present yet another set of formulas which may be said to characterize an intermediate precision. This set is essentially (3.72) where the second and higher powers of δ are neglected in the series expansion of trigonometric functions. We thus obtain (with 3.71 already incorporated) from either (3.72) or (3.73):

$$
\left.
\begin{aligned}
T_{x''x''} &\simeq T_{xx} - 2\delta T_{xz} = -[1/(r^2\cos^2\bar{\phi})]\,\partial^2T/\partial\lambda^2 - 2(\delta/r)\,\partial^2T/\partial\bar{\phi}\partial r \\
&\quad - \partial^2T/\partial r^2 + [(\mathrm{tg}\bar{\phi} + 2\delta)/r^2]\,\partial T/\partial\bar{\phi} - (1/r)\,\partial T/\partial r\ , \\
T_{x''y''} &\simeq T_{xy} - \delta T_{yz} = [1/(r^2\cos\bar{\phi})]\,\partial^2T/\partial\lambda\partial\bar{\phi} - [\delta/(r\cos\bar{\phi})]\,\partial^2T/\partial\lambda\partial r \\
&\quad + [(\sin\phi + \delta\cos\bar{\phi})/(r^2\cos^2\bar{\phi})]\,\partial T/\partial\lambda\ , \\
T_{x''z''} &\simeq T_{xz} + \delta(T_{xx} - T_{zz}) = -[\delta/(r^2\cos^2\bar{\phi})]\,\partial^2T/\partial\lambda^2 + (1/r)\,\partial^2T/\partial\bar{\phi}\partial r \\
&\quad - 2\delta\ \partial^2T/\partial r^2 - [(1 - \delta\,\mathrm{tg}\bar{\phi})/r^2]\,\partial T/\partial\bar{\phi} - (\delta/r)\,\partial T/\partial r\ , \\
T_{y''y''} &= T_{yy} = [1/(r^2\cos^2\bar{\phi})]\,\partial^2T/\partial\lambda^2 - (\mathrm{tg}\bar{\phi}/r^2)\,\partial T/\partial\bar{\phi} + (1/r)\,\partial T/\partial r\ , \\
T_{y''z''} &\simeq T_{yz} + \delta T_{xy} = [\delta/(r^2\cos\bar{\phi})]\,\partial^2T/\partial\lambda\partial\bar{\phi} + [1/(r\cos\bar{\phi})]\,\partial^2T/\partial\lambda\partial r \\
&\quad - [(\cos\bar{\phi} - \delta\sin\bar{\phi})/(r^2\cos^2\bar{\phi})]\,\partial T/\partial\lambda\ , \\
T_{z''z''} &\simeq T_{zz} + 2\delta T_{xz} = 2(\delta/r)\,\partial^2T/\partial\bar{\phi}\partial r + \partial^2T/\partial r^2 - 2(\delta/r^2)\,\partial T/\partial\bar{\phi}\ .
\end{aligned}
\right\}
\tag{3.74}
$$

The angle δ called for in (3.72) or (3.74) is usually known beforehand since it is needed for computing the second-order derivatives of U in (3.63). If this angle were not readily available (e.g. if the second-order derivatives of T were supplied directly and would not have to be determined from the second-order derivatives of W), it could be approximated by $\delta_1 = \phi - \bar{\phi}$ and we would then be in the presence of the spheroidal approximation mentioned earlier. In this case one would quite logically use (3.74) over (3.72), since the errors caused by the spheroidal approximation would be in general much larger than the errors in (3.74) caused by the simplification of the formulas in (3.72).

It has been suggested that the quantities to be modeled (second-order derivatives of T) could be described by more than one set of parameters, for example by a given set of spherical harmonic coefficients and a set of local parameters such as point mass magnitudes. The first set could be considered known and thus only the second set (e.g. point mass magnitudes) could be subject to adjustment. This second set would be required to accommodate, in a least squares adjustment, the "residual second-order derivatives" of T obtained by subtracting the "computed second-order derivatives" of T from the original ones. The "computed" quantities, obtained via fixed spherical harmonic coefficients, could be evaluated as in (3.72); the partial derivatives $\partial^2 T/\partial\lambda^2$, etc., will be listed below. The "computed" quantities can be easily obtained without introducing any errors, thus (3.72) is indeed suitable for this purpose. The formulas (3.74) of intermediate precision would be almost equally suitable. It is conceivable that for many practical applications even the formulas (3.73) could be acceptable. On the other hand, when dealing with the "residual second-order derivatives" the formulas (3.73) are believed to be sufficient in most circumstances and could be used with great advantage. For example, in the case of a point mass model important mathematical simplications will occur if these "residual" quantities are described by (3.73) provided they can be considered distributed on or near a sphere and the point masses are chosen to lie on another (concentric) sphere of a smaller radius. It may thus be necessary to introduce further simplifications in the formulas (3.73) in order to make them computationally viable for an actual adjustment process. One notices that in the case of point masses or other local parameters there is no reason to avoid the expression $\partial^2 T/\partial\bar{\phi}^2$ and it may be more advantageous to use (3.73') in lieu of its counterpart in (3.73).

For reference purposes, the partial derivatives of T with respect to the spherical coordinates are now listed for T expanded in terms of spherical harmonics. As explained earlier, $\partial^2 T/\partial\bar{\phi}^2$ is not among them. The familiar expression for the disturbing potential is (see e.g. [Blaha, 1977], page 80)

$$T = (GM/r) \sum_{n=2}^{N} (a_o/r)^n \, \Delta S(n) \ , \tag{3.75}$$

where

$$\Delta S(n) = \sum_{m=0}^{n} (\Delta C_{nm} \cos m\lambda + \Delta S_{nm} \sin m\lambda) P_{nm}(\sin\bar{\phi}) \ , \tag{3.76}$$

N = degree and order of the truncation ,

$\Delta C_{20} = C_{20} - C^*_{20}$,

$\Delta C_{40} = C_{40} - C^*_{40}$, etc.,

the other ΔC_{nm} , ΔS_{nm} being C_{nm} , S_{nm} , the spherical harmonic potential coefficients themselves (in practice this could apply already for C_{60}). We then have

$$\left.\begin{aligned}
\partial T/\partial\lambda &= (GM/r) \sum_{n=2}^{N} (a_o/r)^n \, \Delta S'(n) \ , \\
\partial T/\partial\bar{\phi} &= (GM/r) \sum_{n=2}^{N} (a_o/r)^n \, \Delta\bar{S}(n) \ , \\
\partial T/\partial r &= -(GM/r^2) \sum_{n=2}^{N} (n+1)(a_o/r)^n \, \Delta S(n) \ , \\
\partial^2 T/\partial\lambda^2 &= (GM/r) \sum_{n=2}^{N} (a_o/r)^n \, \Delta S''(n) \ ,
\end{aligned}\right|$$

$$\left.\begin{aligned}
\partial^2 T/\partial\lambda\partial\bar{\phi} &= (GM/r) \sum_{n=2}^{N} (a_0/r)^n \, \Delta\bar{S}'(n) \, , \\
\partial^2 T/\partial\lambda\partial r &= -(GM/r^2) \sum_{n=2}^{N} (n+1)(a_0/r)^n \, \Delta S'(n) \, , \\
\partial^2 T/\partial\bar{\phi}\partial r &= -(GM/r^2) \sum_{n=2}^{N} (n+1)(a_0/r)^n \, \Delta\bar{S}(n) \, , \\
\partial^2 T/\partial r^2 &= (GM/r^3) \sum_{n=2}^{N} (n+1)(n+2)(a_0/r)^n \, \Delta S(n) \, ,
\end{aligned}\right\} \quad (3.77)$$

where the following four notations have been introduced:

$$\Delta S'(n) = \sum_{m=0}^{n} m(-\Delta C_{nm} \sin m\lambda + \Delta S_{nm} \cos m\lambda) P_{nm}(\sin\bar{\phi}) \, , \quad (3.78a)$$

$$\Delta S''(n) = -\sum_{m=0}^{n} m^2(\Delta C_{nm} \cos m\lambda + \Delta S_{nm} \sin m\lambda) P_{nm}(\sin\bar{\phi}) \, , \quad (3.78b)$$

$$\Delta\bar{S}(n) = \sum_{m=0}^{n} (\Delta C_{nm} \cos m\lambda + \Delta S_{nm} \sin m\lambda) dP_{nm}(\sin\bar{\phi})/d\bar{\phi} \, , \quad (3.78c)$$

$$\Delta\bar{S}'(n) = \sum_{m=0}^{n} m(-\Delta C_{nm} \sin m\lambda + \Delta S_{nm} \cos m\lambda) dP_{nm}(\sin\bar{\phi})/d\bar{\phi} \, . \quad (3.78d)$$

3.6 Summary and Conclusion

One vertical and two horizontal gradients of gravity are among the quantities which can routinely be measured and used in specific geodetic applications. They represent three out of six distinct second-order derivatives of the potential in a local Cartesian coordinate system as revealed by various sensors. These six quantities describe the curvature properties of the gravity field. If their knowledge is to contribute to a better description of the earth's gravity field, they should be properly related to the model parameters of the field, such as a set of spherical harmonic potential coefficients and/or a set of chosen localized parameters, etc. However, before these second-order derivatives can be related to a set of parameters, they have to be expressed in terms of the partial derivatives of the potential with respect to the coordinates of a chosen coordinate system. In this chapter, the coordinate systems used are the spheroidal coordinate system $\{\delta,u,\alpha\}$ and the spherical coordinate system $\{\lambda,\bar{\phi},r\}$.

The model parameters themselves are brought into the picture only in the closing paragraph of Section 3.5 where they are limited to a set of spherical harmonic potential coefficients. For the most part, this chapter has been concerned with the second-order derivatives of a general scalar function of position (F) with respect to the length elements along a family of local Cartesian axes, expressed in terms of the partial derivatives of F with respect to the coordinates of the two systems just mentioned. The function F is most likely to represent W (actual potential), U (standard potential), T (disturbing potential), or a coordinate itself (α, r, etc.).

The desired second-order derivatives of F are expressed in spheroidal coordinates in Section 3.2 and in spherical coordinates in Section 3.4. A link between the two formulations is established in Section 3.3 where all the results in spherical coordinates are obtained also indirectly through a transformation from the spheroidal system. In addition to possible applications of similar links, a by-product of such a demonstration is the verification of the results obtained in either system by direct methods.

A benefit which surfaced during the development in spherical coordinates is that the demonstrations can be significantly shortened and brought sharply into focus if the approach pioneered by Marussi [1951] and elaborated by Hotine [1969] is followed and advantage is taken of tensor analysis. It thus comes as no surprise that this study, in which such a methodology has been followed, is intended as a tribute to Professor Marussi and to the late Martin Hotine for their contributions to theoretical geodesy.

The general formulas giving the second-order derivatives of F are made useful for practical applications in Section 3.5, upon decomposing W into U and T. At least some of the second-order derivatives of W are considered as observed quantities and F is first specialized to represent U. In this way the second-order derivatives of $T = W-U$ are obtained and may in turn be considered as observations to be modeled by a chosen set of parameters. For this purpose the new "observations" are expressed in terms of the partial derivatives of T with respect to the coordinates, accomplished by specializing F to represent T. The above practical procedure is developed

in detail in spherical coordinates. If the computation of $\partial^2 T/\partial\bar{\phi}^2$ is more complicated than that of the other partial derivatives -- as would be the case with the spherical harmonic expansion -- this computation can be avoided by taking advantage of the property $\Delta T = 0$. A typical set of second-order derivatives of T with the property $\Delta T = 0$ incorporated (and $\partial^2 T/\partial\bar{\phi}^2$ absent) can be found in (3.72). If there is no need to avoid the formulation of $\partial^2 T/\partial\bar{\phi}^2$, the desired second-order derivatives can be readily transcribed from equations (3.46).

The possibility of considering a whole family of local Cartesian coordinate systems has lead to the second-order derivatives of T in the following two basic forms. The first form (associated with the Cartesian triad called i") is essentially rigorous and is expressed in the above-mentioned equations (3.72) or, eventually, (3.46). The second form (associated with the Cartesian triad called i) corresponds to the spherical approximation and is expressed in equations (3.73) where $\Delta T = 0$ has been incorporated; if there is no need to avoid the formulation of $\partial^2 T/\partial\bar{\phi}^2$, the first relation in (3.73) can be replaced by (3.73'). Another form of intermediate precision (with $\Delta T = 0$ incorporated) may be found in (3.74).

The formulas in this chapter have been developed for all six second-order derivatives of W, U, T, or a more general function, although only one vertical and/or two horizontal gradients of gravity may be routinely measured. One notices that if the observed quantities were given directly as the second-order derivatives of T (instead of W), the approach and all the formulas would remain unchanged except that the steps associated with U would be skipped.

The versatility in possible applications of the presented formulas becomes further apparent upon the realization that they have been derived for a general point in space and can thus be used for measurements made at the ground level as well as at higher altitudes, such as aircraft or satellite altitudes.

Although the formulas giving the desired second-order derivatives are to be applied most often in a rotating field, they can be easily specialized for a nonrotating field as could be required for certain satellite applications. This specialization consists in replacing $\tilde{\omega}$(angular velocity of the earth's rotation) by zero wherever it appears in the formulas explicitly, and the same modification also takes place in connection with the orientation of the triad i".

4. ADJUSTMENT MODELS FOR FIVE INVESTIGATED OBSERVATIONAL MODES

4.1 Mathematical Background

In a simultaneous adjustment of spherical harmonic (S.H.) potential coefficients and point mass (P.M.) magnitudes as parameters, an observation equation would read as follows:

$$V = L^a - L^b = F(X_1^a, X_2^a) - L^b \tag{4.1a}$$

$$= F(X_1^a, 0) + A_2 X_2 - L^b \tag{4.1b}$$

$$= F(X_1^o, 0) + A_1 X_1 + A_2 X_2 - L^b \ , \tag{4.1c}$$

where V is the residual, L^a and L^b are the adjusted and measured values of the observable, the subscripts "1" and "2" refer to the S.H. and P.M. parameters, and the superscripts "a", "o" attributed to "X" indicate the adjusted and initial values of the parameters. Furthermore, "F" denotes the general model describing the observable, "A_i" denotes the row matrix of partial derivatives of F with respect to the appropriate parameters (sets "1" and "2" above), and

$$X_1 = X_1^a - X_1^o \ ,$$

$$X_2 = X_2^a \ , \quad X_2^o = 0 \ ;$$

the last relation indicates that the model is linear in the P.M. parameters.

Equation (4.1b) is written as

$$V = A_2X_2 + [F(X_1^a,0) - L^b] , \tag{4.2}$$

where

$$F(X_1^a,0) = F(X_1^o,0) + A_1X_1 ;$$

the expression in brackets of (4.2) becomes the constant term in the observation equation in the cases where the set X_1^a is given (fixed) and only X_2 is subject to adjustment. In either case, the expressions to be developed include $F(X_1^o,0)$ and

$$\Delta F_1 = A_1X_1 ,$$

$$\Delta F_2 = A_2X_2 .$$

In practice it is useful to proceed in two consecutive adjustments of the same observations. First, one minimizes, in the least-squares (L.S.) sense, the expressions in the brackets of (4.2) as if the observation equations were of the type

$$V_1 = A_1X_1 + [F(X_1^o,0) - L^b] , \tag{4.3a}$$

and then one forms

$$V = A_2X_2 + V_1 , \tag{4.3b}$$

as if V_1 represented the minus observed values in a linear model where X_2 are the parameters. The equations (4.3a) and (4.3b) considered together are identical in form to (4.1c). However, the adjustment itself is performed in

two steps rather than simultaneously as suggested by (4.1c). Splitting the adjustment in this way is possible in some cases without introducing any approximations; for example, with the S.H. coefficients as parameters and with an almost perfect distribution of observations (such as geoid undulations) over the entire globe, two or more subsets of these parameters can be solved for consecutively with no loss in accuracy, owing to the familiar orthogonality relations (see e.g. Section 8.1 of [Blaha,1977]). This is not the case when both the S.H. and P.M. parameters are present, and the adopted procedure of consecutive adjustments is only an approximation to a simultaneous solution. However, due to perhaps insurmountable computer requirements accompanying such a simultaneous solution, the consecutive adjustment algorithm offers a viable alternative allowing for a great reduction in the number of parameters solved for in any individual adjustment. The first, global (S.H.) adjustment leads to a higher-order surface (it could be called a "S.H. geoid"). This surface then serves as a reference surface in separate local (P.M.) adjustments in the areas covered by a dense net of observations consisting typically of satellite altimeter data. The number of point masses and their location including their depth below the earth's surface are stipulated beforehand. The model equations for both ΔF_1 and ΔF_2 are based on the expressions for the disturbing potential (T).

After a L.S. solution, predictions of various quantities investigated in this chapter may be of interest. They are given by any of the right-hand sides in equations (4.1), but with the quantity "L^b" absent. The corresponding variances are obtained as follows:

$$\sigma_1^2 = A_1 \Sigma_{S.H.} A_1^T ,$$

$$\sigma_2^2 = A_2 \Sigma_{P.M.} A_2^T ,$$

$$\sigma^2 = \sigma_1^2 + \sigma_2^2 ,$$

where the variance-covariance matrix Σ for the parameters (S.H. or P.M.) is obtained as the inverse of the normal equation matrix in the pertinent adjustment. The simple addition of variances yielding the total variance in the last equation above stems from the approximation allowing for an independent treatment of the two kinds of parameters by the adjustment algorithm.

The expressions for the fundamental quantity, T , will now be recapitulated. The S.H. formulation appeared in (3.75) essentially as

$$T = (kM/r) \sum_{n=2}^{N} (a/r)^n \Delta S(n) , \tag{4.4}$$

where the symbol a has replaced a_0 , the symbol k (the gravitational constant) has replaced G , and $\Delta S(n)$ has been given in (3.76). The P.M. formulation at point i can be adopted from (5.9) of [Blaha,1979], giving

$$T_i = \sum_j (1/\ell_{ij})(kM)_j , \tag{4.5}$$

where

ℓ_{ij} = distance between the i-th (observation) point and the j-th point mass,

$(kM)_j$ = j-th scaled point mass magnitude.

In the spherical approximation, R represents the earth's mean radius (6371 km) and G is the average value of gravity (980 gals) on the earth's surface; the point masses are assumed to be at the depth d below the sphere of radius R, so that

$$\ell_{ij} = (R^2 + R_1^2 - 2F_{ij})^{\frac{1}{2}} , \tag{4.6a}$$

$$R_1 = R - d , \tag{4.6b}$$

$$F_{ij} = R\, R_1 \cos \psi_{ij} , \tag{4.6c}$$

$$\cos \psi_{ij} = \sin\phi_i \sin\phi_j + \cos\phi_i \cos\phi_j \cos(\lambda_i - \lambda_j) , \tag{4.6d}$$

where ψ_{ij} is the spherical distance between the points i,j with the coordinates (ϕ_i,λ_i) and (ϕ_j,λ_j), respectively.

We now develop, in a straightforward fashion, several expressions where the differentiation is performed with respect to ϕ_i, λ_i and r_i (r_i is the radial distance from the geocenter to point i, numerically $r_i = R$):

$$\partial(1/\ell_{ij})/\partial\phi_i = (1/\ell_{ij}^3)\partial F_{ij}/\partial\phi_i$$

$$= (1/\ell_{ij}^3)\, RR_1 \; [\cos\phi_i \sin\phi_j - \sin\phi_i \cos\phi_j \cos(\lambda_i - \lambda_j)],$$

etc., which lead to

$$\partial T_i/\partial\phi_i = \sum_j [\partial(1/\ell_{ij})/\partial\phi_i](kM)_j \tag{4.7a}$$

$$= RR_1 \sum_j (1/\ell_{ij}^3)[\cos\phi_i \sin\phi_j - \sin\phi_i \cos\phi_j \cos(\lambda_i - \lambda_j)](kM)_j ,$$

$$\partial T_i/\partial\lambda_i = -RR_1 \cos\phi_i \sum_j (1/\ell_{ij}^3) \cos\phi_j \sin(\lambda_i - \lambda_j)(kM)_j \ , \tag{4.7b}$$

$$\partial T_i/\partial r_i = -\sum_j (1/\ell_{ij}^3)(R - R_1 \cos\psi_{ij})(kM)_j \ , \tag{4.7c}$$

$$\partial^2 T_i/\partial\phi_i^2 = RR_1 \sum_j (1/\ell_{ij}^3)\{(3RR_1/\ell_{ij}^2)$$
$$\cdot[\cos\phi_i \sin\phi_j - \sin\phi_i \cos\phi_j \cos(\lambda_i - \lambda_j)]^2 - \cos\psi_{ij}\}(kM)_j \ , \tag{4.7d}$$

$$\partial^2 T_i/\partial\lambda_i^2 = RR_1 \sum_j (1/\ell_{ij}^3)\{(3RR_1/\ell_{ij}^2)$$
$$\cdot[\cos\phi_i \cos\phi_j \sin(\lambda_i - \lambda_j)]^2 - \cos\phi_i \cos\phi_j \cos(\lambda_i - \lambda_j)\}(kM)_j \ , \tag{4.7e}$$

$$\partial^2 T_i/\partial r_i^2 = \sum_j (1/\ell_{ij}^3)[3(R - R_1 \cos\psi_{ij})^2/\ell_{ij}^2 - 1](kM)_j \ , \tag{4.7f}$$

$$\partial^2 T_i/\partial\phi_i\partial\lambda_i = -RR_1 \sum_j (1/\ell_{ij}^3)\{(3RR_1/\ell_{ij}^2)\cos\phi_i \cos\phi_j \sin(\lambda_i - \lambda_j)$$
$$\cdot[\cos\phi_i \sin\phi_j - \sin\phi_i \cos\phi_j \cos(\lambda_i - \lambda_j)]$$
$$- \sin\phi_i \cos\phi_j \sin(\lambda_i - \lambda_j)\}(kM)_j \ , \tag{4.7g}$$

$$\partial^2 T_i/\partial\phi_i\partial r_i = -R_1 \sum_j (1/\ell_{ij}^3)[\cos\phi_i \sin\phi_j - \sin\phi_i \cos\phi_j \cos(\lambda_i - \lambda_j)]$$
$$\cdot[3R(R - R_1 \cos\psi_{ij})/\ell_{ij}^2 - 1](kM)_j \ , \tag{4.7h}$$

$$\partial^2 T_i/\partial\lambda_i\partial r_i = R_1 \cos\phi_i \sum_j (1/\ell_{ij}^3)\cos\phi_j \sin(\lambda_i - \lambda_j)$$
$$\cdot[3R(R - R_1 \cos\psi_{ij})/\ell_{ij}^2 - 1](kM)_j \ . \tag{4.7i}$$

The mixed second derivatives can be verified upon reversing the order of differentiation. Furthermore, the Laplace condition should be fulfilled by construction. This is verified as follows. Upon applying (3.73') at point i we have

$$T_{xx} = (1/R)\ \partial T_i/\partial r_i + (1/R^2)\ \partial^2 T_i/\partial \phi_i^2 \tag{4.8}$$

$$= \sum_j (1/\ell_{ij}^3)\{(3R_1^2/\ell_{ij}^2)[\cos\phi_i \sin\phi_j - \sin\phi_i \cos\phi_j \cos(\lambda_i - \lambda_j)]^2 - 1\}(kM)_j;$$

and from T_{yy} and T_{zz} in (3.73) we deduce

$$T_{yy} = \sum_j (1/\ell_{ij}^3)\ [(3R_1^2/\ell_{ij}^2)\cos^2\phi_j \sin^2(\lambda_i - \lambda_j) - 1](kM)_j\ , \tag{4.9}$$

$$T_{zz} = \sum_j (1/\ell_{ij}^3)\ [3(R - R_1 \cos\psi_{ij})^2/\ell_{ij}^2 - 1](kM)_j\ , \tag{4.10}$$

(4.10) being essentially (4.7f). From (4.8) - (4.10), straightforward algebra yields

$$T_{xx} + T_{yy} + T_{zz} = 0 \tag{4.11}$$

as it should. For reference purposes, from (3.73) we also have

$$T_{xy} = -3R_1^2 \sum_j (1/\ell_{ij}^5)\cos\phi_j \sin(\lambda_i - \lambda_j)$$
$$\cdot[\cos\phi_i \sin\phi_j - \sin\phi_i \cos\phi_j \cos(\lambda_i - \lambda_j)](kM)_j\ , \tag{4.12}$$

which, however, will not be used in the balance of this report.

In the following sections, five observational modes will be investigated: geoid undulations, gravity anomalies, deflections (north and east) of the vertical, horizontal gradients (north and east) of gravity disturbance, and vertical gradients of gravity disturbance. In a first step for each mode, the S.H. formulation for $F(X_1^0,0)$ and $\Delta F_1 = A_1 X_1$ with the row matrix A_1 given explicitly will be presented; this part will not contain the familiar spherical approximation. In a subsequent step, the P.M. formulation for $\Delta F_2 = A_2 X_2$ with A_2 given explicitly will be considered in spherical approximation. Also included will be the practical discussion pertaining to the cut-off distance, i.e., to the size of a spherical cap centered at the observation point beyond which the P.M. parameters are ignored during the formation of an observation equation.

4.2 Geoid Undulations

For the most part this model has been already treated in [Blaha, 1977] and [Blaha,1979], referred to in this chapter as [B1] and [B2], respectively.

S.H. part. Upon the customary assumption $W_o \equiv U_o$, stating that the potential of the geoid equals the potential of the geocentric reference ellipsoid and is not subject to adjustment, we have from Section 2.1 of [B2]:

$$N = \tilde{N}(1+\tilde{c}) , \tag{4.13}$$

where

$$\tilde{N} = r_o \sum_{n=2}^{N} (a/r')^n \, \Delta S(n) , \tag{4.14}$$

with

$$r_o = kM/W_o ,$$

$$r' = a/\left[1+e^2 \sin^2\bar{\phi}/(1-e^2)\right]^{\frac{1}{2}} ,$$

r' being the radial distance from the geocenter to the ellipsoid at the point where N is being sought, a and e being the semi-major axis and the eccentricity of this ellipsoid, respectively, and $\bar{\phi}$ being the geocentric latitude of the ellipsoidal point in question; and where

$$\tilde{c} = c_1 \sin^2\bar{\phi} + c_2 , \tag{4.15}$$

with

$$c_1 = -3.0033\, C_{20} - 0.005169 \simeq -0.00192 ,$$

$$c_2 = 1.0011\, C_{20} + 0.005169 \simeq 0.00408.$$

The expression (4.13) corresponds to $F(X_1^0,0)$ upon the recognition that the initial values of the S.H. parameters enter into the definition of $\Delta S(n)$. A similar statement will be applicable in the following sections, and it need not be repeated.

If the geoid undulations are part of a satellite altimetry model, the model equation becomes

$$H = R - r + (\text{correction})$$

as described in Section 2.4 of [B1], where H is the distance from the satellite to the (S.H.) geoid, R is the radial distance from the geocenter to the satellite, and

$$r \approx r' + N , \tag{4.16}$$

$$(\text{correction}) \simeq 4.9\text{m} \sin^2 2\bar{\phi} \ldots \text{ per } 1000\,\text{km of H} .$$

The parameters X_1 are the corrections to the initial values of the S.H. potential coefficients C_{no}, C_{nm}, S_{nm} (referred to as C's and S's), and the row matrix A_1 is composed of the partial derivatives of N with respect to these coefficients. Most often the value $\tilde{c}$ in (4.13) could be ignored during the differentiation, the greatest possible relative error thus introduced being 0.4%; in this case we have

$$\partial N/\partial C_{no} \simeq r_o(a/r')^n P_n(\sin\phi) ,$$

$$\partial N/\partial C_{nm} \simeq r_o(a/r')^n \cos m\lambda \, P_{nm}(\sin\bar{\phi}) ,$$

$$\partial N/\partial S_{nm} \simeq r_o(a/r')^n \sin m\lambda \, P_{nm}(\sin\bar{\phi}) .$$

For more accuracy these partial derivatives can be multiplied by $(1+\tilde{c})$. In order to eliminate the remaining error, $\tilde{N}(1.0011 - 3.0033 \sin^2\bar{\phi})$ can be added to $\partial N/\partial C_{20}$.

If used as a part of the satellite altimetry model, the above partial derivatives are combined with those pertaining to the state vector parameters as demonstrated in Sections 2.4 or 4.1 of [B1]. In the latter section, the partial derivatives $\partial N/\partial C_{nm}$, etc., are replaced by the equivalent expressions for $\partial r/\partial C_{nm}$, etc.

<u>P.M. part</u>. As in Section 5.2 of [B2], the part ΔF_2 attributed to the point masses is

$$N_i = (1/G) \sum_j (1/\ell_{ij})(kM)_j , \tag{4.17}$$

which can be evaluated with the aid of equations (4.6). The row matrix A_2 can be formed directly from (4.17) with the $(kM)_j$'s absent and with the j's determining the ordering of the elements. Since all the investigated observational modes are linear insofar as the P.M. parameters are concerned, the formation of A_2 is thus settled once and for all.

An important decision to be made when formulating the P.M. adjustment model in practice regards the cut-off distance. In addressing

this task, only one point mass $(kM)_j$ is considered and the position of the observation point i on the earth's surface (here a sphere of radius R) is varied relative to this point mass. According to [B2], the depth of the point masses is taken as a 1.6-multiple of their horizontal separation (as projected on the earth's surface). In particular, if the separation in degrees of arc is $s^0 = 2^0$, then

$$s \simeq 222.4 \text{ km} ,$$

$$d = 1.6s \simeq 350.0 \text{ km} ,$$

$$R_1 = 6021 \text{ km} .$$

We now specialize (4.17) for $j = 1$, giving

$$N_i = (1/\ell_{ij})(kM)_j/G , \tag{4.17'}$$

where the one point mass present, $(kM)_j$, is chosen to be a 10^{-6}-part of the earth's kM ($kM \simeq 3.986 \times 10^{14}$ m^3/sec^2). Next the position of the observation point i is varied and the corresponding value N_i computed. This variation can proceed by s^0 (with intermediate values of interest included), which makes it possible to see at how many s-intervals away from the observation point the P.M. parameters will still significantly affect the modeled value (and vice versa) and should therefore be included in the observation equation or in the prediction formulas. In theory one could include all of the P.M. parameters in every observation equation, but this would often result in prohibitive computer run-time requirements. The specialization illustrated in (4.17') is typical for the present cut-off analysis and will be used

for all the other investigated modes as well (the values of s, d and R_1 will be unchanged from the above). Therefore, little additional explanation will be needed.

The procedure just described leads to the values below which could serve to plot a curve of geoid undulations (N_i) generated by the given value $(kM)_j$ for various angles ψ_{ij} (in degrees):

0^0 ... 116 m	6^0 ... 55.2 m
2^0 ... 98.9 m	8^0 ... 43.6 m
4^0 ... 73.1 m	10^0 ... 35.8 m

The undulation curve decreases asymptotically. At the distance 4s (corresponding to 8^0 above) the effect of the P.M. has diminished to about 37.6% of the maximum effect exercised by a P.M. directly underneath the observation point. Compelled by practical considerations -- mainly by the fact that the curve decreases rather slowly beyond 4s -- we can adopt this distance as the cut-off distance with regard to both observations and predictions.

this task, only one point mass $(kM)_j$ is considered and the position of the observation point i on the earth's surface (here a sphere of radius R) is varied relative to this point mass. According to [B2], the depth of the point masses is taken as a 1.6-multiple of their horizontal separation (as projected on the earth's surface). In particular, if the separation in degrees of arc is $s^0 = 2^0$, then

$$s \simeq 222.4 \text{ km},$$

$$d = 1.6s \simeq 350.0 \text{ km},$$

$$R_1 = 6021 \text{ km}.$$

We now specialize (4.17) for $j = 1$, giving

$$N_i = (1/\ell_{ij})(kM)_j/G, \tag{4.17'}$$

where the one point mass present, $(kM)_j$, is chosen to be a 10^{-6}-part of the earth's kM ($kM \simeq 3.986 \times 10^{14}$ m^3/sec^2). Next the position of the observation point i is varied and the corresponding value N_i computed. This variation can proceed by s^0 (with intermediate values of interest included), which makes it possible to see at how many s-intervals away from the observation point the P.M. parameters will still significantly affect the modeled value (and vice versa) and should therefore be included in the observation equation or in the prediction formulas. In theory one could include all of the P.M. parameters in every observation equation, but this would often result in prohibitive computer run-time requirements. The specialization illustrated in (4.17') is typical for the present cut-off analysis and will be used

4.3 Gravity Anomalies

As in the previous section, much of the development in [B1] and [B2] will now be briefly recapitulated and complemented by the cut-off considerations.

S.H. part. A satisfactory yet simple model has been analyzed in Chapter 5 of [B1]. From (5.24a) of this reference we write

$$\Delta g = C \sum_{n=2}^{N} (n-1)(a/r)^n \, \Delta S(n) , \tag{4.18}$$

where

$$C = kM/r^2$$

with r obtained as in (4.16).

According to equations (5.27) of [B1], A_1 is composed of the elements

$$\partial\Delta g/\partial C_{no} = C(n-1)(a/r)^n \, P_n(\sin\bar{\phi}) ,$$

$$\partial\Delta g/\partial C_{nm} = C(n-1)(a/r)^n \cos m\lambda \, P_{nm}(\sin\bar{\phi}) ,$$

$$\partial\Delta g/\partial S_{nm} = C(n-1)(a/r)^n \sin m\lambda \, P_{nm}(\sin\bar{\phi}).$$

The gravity anomaly model as well as the above partial derivatives have been refined in Chapter 4 of [B2]. Exceptionally, such a model could be used for maximum accuracy, but there is no need to rewrite all the pertinent formulas.

P.M. part. According to (5.10) of [B2], we have

$$\Delta g_i = (1/R) \sum_j (1/\ell_{ij}) [(R^2 - F_{ij})/\ell_{ij}^2 - 2](kM)_j \ , \tag{4.19}$$

which, as in the case of geoid undulations, can be evaluated by means of equations (4.6).

The results pertaining to the cut-off distance are presented as follows:

0^0 ... 290 mgal	6^0 ... 21.2 mgal
2^0 ... 172 mgal	10^0 ... 1.0 mgal
4^0 ... 62.0 mgal	20^0 ... -3.0 mgal

Clearly, the cut-off distance could be chosen as 2s (here 4^0) where the effect of the P.M. has diminished to about 21.4% of the maximum effect exercised by a P.M. underneath the observation point. The 3s-cap (here 6^0) would be more than sufficient, the corresponding effect shrinking to a mere 7.3%.

4.4 Deflections of the Vertical

A component of the deflection of the vertical (ε) in any azimuth is given (see e.g. [Heiskanen and Moritz,1967], page 112) as

$$\varepsilon = -dN/ds \ .$$

In the north-south direction we have

$$\xi = -dN/ds_1 \ ,$$

and in the east-west direction,

$$\eta = -dN/ds_2 \ ,$$

where ds_1 and ds_2 are positive with increasing latitude and longitude, respectively, and dN is the change in geoid undulation along the appropriate directions. From the geometry of a spheroid it follows that

$$ds_1 = \rho \, d\phi \simeq r' \, d\bar{\phi} \, (1 - 2e^2 \cos 2\bar{\phi}) \ ,$$

$$ds_2 = \nu \cos\phi \, d\lambda = r' \cos\bar{\phi} \, d\lambda \ ,$$

where ρ and ν are the radii of curvature in the meridian and in the prime vertical, respectively. It thus follows that

$$\xi \simeq -(1/r')(1 + 2e^2 \cos 2\bar{\phi}) \, \partial N/\partial\bar{\phi} \ , \tag{4.20}$$

$$\eta = -[1/(r' \cos\bar{\phi})] \, \partial N/\partial\lambda \ , \tag{4.21}$$

the last expression not to be used for the poles. In the spherical approximation r' would be replaced by R and e would be replaced by zero, and the formula (2-204) of the above reference would be recovered.

S.H. part. From (4.14) it follows that

$$(1/r')\partial\tilde{N}/\partial\bar{\phi} = (r_o/r') \sum_{n=2}^{N} (a/r')^n \, \Delta\bar{S}(n) \ ,$$

where $\Delta\bar{S}(n)$ has been defined in (3.78c). Formulas (4.13) and (4.20) thus result in

$$\xi \simeq -(r_o/r')(1+\tilde{c})(1+2e^2 \cos 2\bar{\phi}) \sum_{n=2}^{N} (a/r')^n \, \Delta\bar{S}(n) \ ; \qquad (4.22)$$

in spherical approximation this would reduce to

$$\xi \simeq - \sum_{n=2}^{N} \Delta\bar{S}(n) \ .$$

Similarly, (4.13), (4.14) and (4.21) yield

$$\eta = -(1/\cos\bar{\phi})(r_o/r')(1+\tilde{c}) \sum_{n=2}^{N} (a/r')^n \, \Delta S'(n) \ , \qquad (4.23)$$

where $S'(n)$ has been defined in (3.78a). In spherical approximation one would write

$$\eta \simeq -(1/\cos\bar{\phi}) \sum_{n=2}^{N} \Delta S'(n) \ .$$

When forming the elements of A_1 for ξ, it follows from (4.22) that

$$\partial\xi/\partial C_{no} = -t\,t'(a/r')^n\, dP_n(\sin\bar{\phi})/d\bar{\phi} ,$$

$$\partial\xi/\partial C_{nm} = -t\,t'(a/r')^n \cos m\lambda\, dP_{nm}(\sin\bar{\phi})/d\bar{\phi} ,$$

$$\partial\xi/\partial S_{nm} = -t\,t'(a/r')^n \sin m\lambda\, dP_{nm}(\sin\bar{\phi})/d\bar{\phi} ,$$

where

$$t = (r_o/r')(1+\tilde{c}) ,$$

$$t' = (1+2e^2 \cos 2\bar{\phi}) .$$

Similarly, from (4.23) we obtain

$$\partial\eta/\partial C_{no} = 0,$$

$$\partial\eta/\partial C_{nm} = (t/\cos\bar{\phi})(a/r')^n\, m \sin m\lambda\, P_{nm}(\sin\bar{\phi}) ,$$

$$\partial\eta/\partial S_{nm} = -(t/\cos\bar{\phi})(a/r')^n\, m \cos m\lambda\, P_{nm}(\sin\bar{\phi}) .$$

In spherical approximation all of t, t' and $(a/r')^n$ would be replaced by unity.

<u>P.M. part</u>. From (4.20) and (4.21) we write in spherical approximation:

$$\xi_i = -[1/(GR)]\, \partial T_i/\partial\phi_i ,$$

$$\eta_i = -[1/(GR \cos\phi_i)]\, \partial T_i/\partial\lambda_i ,$$

where we have used

$$N_i = (1/G)\, T_i .$$

Thus, upon utilizing (4.7a) and (4.7b) one obtains

$$\xi_i = -(R_1/G) \sum_j (1/\ell_{ij}^3)$$
$$\cdot[\cos\phi_i \sin\phi_j - \sin\phi_i \cos\phi_j \cos(\lambda_i - \lambda_j)](kM)_j \ , \qquad (4.24)$$

$$\eta_i = (R_1/G) \sum_j (1/\ell_{ij}^3) \cos\phi_j \sin(\lambda_i - \lambda_j)(kM)_j \ . \qquad (4.25)$$

With regard to the cut-off decision, either (4.24) or (4.25) is applied in conjunction with the given point mass as usual. It is useful to carry out this analysis in a "canonical form" where the P.M. latitude is chosen to be zero and where the position of the observation point varies either in the northerly direction (in conjunction with ξ_i) or in the easterly direction (in conjunction with η_i). The same results are obtained for either quantity as will become clear by inspection. They are listed as

0^0	... 0.0"	6^0	... 13.2"
1^0	... 18.0"	8^0	... 8.7"
2^0	... 25.4"	10^0	... 6.0"
2.3^0	... 25.7"	12^0	... 4.4"
4^0	... 20.5"	20^0	... 1.7"

At a point above the P.M. the thus generated deflection is zero (a result highly plausible). The deflection values rise sharply until slightly more than 1s (here 2^0) and then fall off quite rapidly; the curve joining such values approaches zero asymptotically. The P.M. has the most significant

effect for distances between 0 and 3s (here 6^0). At the distance 5s (here 10^0), which can be adopted as a cut-off distance, this effect has diminished to only about 23% of the maximum effect around 1s. The cut-off distance of 4s corresponding to about 34% of the maximum effect could also be adopted.

4.5 Horizontal Gradients of Gravity Disturbance

The gradients (horizontal and vertical) of gravity can easily be reduced to the gradients of gravity disturbance as outlined in the previous chapter. Thus W_{zx}, etc., can be transformed to T_{zx}, etc., where $T_{zx} = W_{zx} - U_{zx}$, etc. Another possibility is to obtain T_{zx}, etc., directly from a gradiometer as indicated in [Moritz,1975]. Although working with $T_{z''x''}$, etc., would be more rigorous, the errors introduced by replacing the triad i" by the triad i are deemed negligible for the present purpose. In any event, replacing the formulas (3.73) by (3.72), if needed, is an easy matter. When dealing with the gradients of gravity disturbance in the form T_{zx}, etc., we are in fact using a "spherical approximation" but only insofar as the formulas for the gradients are concerned; the value of r in the S.H. part is not replaced by R or by another constant but is computed as in (4.16), with a height above the earth's surface eventually added in case of aerial or satellite observations. In the P.M. part, r will be replaced by R as usual.

S.H. part. From the 3rd and 5th relations in (3.73) in combination with the appropriate expressions of (3.77), we deduce for the horizontal gradients of gravity disturbance in the north- and east- directions, respectively:

$$T_{zx} = -\bar{C} \sum_{n=2}^{N} (n+2)(a/r)^n \, \Delta\bar{S}(n) , \tag{4.26}$$

$$T_{zy} = -(\bar{C}/\cos\bar{\phi}) \sum_{n=2}^{N} (n+2)(a/r)^n \, \Delta S'(n) , \tag{4.27}$$

where

$$\bar{C} = kM/r^3 ,$$

and where $\Delta\bar{S}(n)$ and $\Delta S'(n)$ have been defined in equations (3.78).

The row matrix A_1 pertaining to the "north" gradient is seen from (4.26) to be composed of the elements

$$\partial T_{zx}/\partial C_{no} = -\bar{C}(n+2)(a/r)^n \, dP_n(\sin\bar{\phi})/d\bar{\phi} ,$$

$$\partial T_{zx}/\partial C_{nm} = -\bar{C}(n+2)(a/r)^n \cos m\lambda \, dP_{nm}(\sin\bar{\phi})/d\bar{\phi} ,$$

$$\partial T_{zx}/\partial S_{nm} = -\bar{C}(n+2)(a/r)^n \sin m\lambda \, dP_{nm}(\sin\bar{\phi})/d\bar{\phi} .$$

Similarly, with regard to the "east" gradient we have from (4.27):

$$\partial T_{zy}/\partial C_{no} = 0 ,$$

$$\partial T_{zy}/\partial C_{nm} = (\bar{C}/\cos\bar{\phi})(n+2)(a/r)^n \, m \sin m\lambda \, P_{nm}(\sin\bar{\phi}) ,$$

$$\partial T_{zy}/\partial S_{nm} = -(\bar{C}/\cos\bar{\phi})(n+2)(a/r)^n \, m \cos m\lambda \, P_{nm}(\sin\bar{\phi}) .$$

<u>P.M. part</u>. Upon replacing r by R in the 3rd and 5th relation in (3.73) we write for the observation point i in the P.M. model:

$$T_{zx} = (1/R)\partial^2 T_i/\partial\phi_i\partial r_i - (1/R^2)\partial T_i/\partial\phi_i ,$$

$$T_{zy} = [1/(R\cos\phi_i)]\partial^2 T_i/\partial\lambda_i\partial r_i - [1/R^2 \cos\phi_i)]\partial T_i/\partial\lambda_i .$$

With the use of the appropriate expressions from (4.7) this becomes

$$T_{zx} = -3R_1 \sum_j (1/\ell_{ij}^5)(R - R_1 \cos\psi_{ij})$$

$$\cdot [\cos\phi_i \sin\phi_j - \sin\phi_i \cos\phi_j \cos(\lambda_i - \lambda_j)](kM)_j \ , \tag{4.28}$$

$$T_{zy} = 3R_1 \sum_j (1/\ell_{ij}^5)(R - R_1 \cos\psi_{ij}) \cos\phi_j \sin(\lambda_i - \lambda_j)(kM)_j \ . \tag{4.29}$$

It can be noticed that the parts beyond $(R - R_1 \cos\psi_{ij})$ in these equations agree with the corresponding parts in (4.24), (4.25).

Similar to the analysis carried out for the deflections of the vertical, the results obtained for T_{zx} and T_{zy} in the "canonical form" are again indentical. Listed below are a few values in E (Eötvös, 0.1 mgal/km or 10^{-9} sec^{-2}) obtained by this procedure:

0^0	... 0.00 E	6^0	... 1.33 E
1^0	... 6.68 E	8^0	... 0.58 E
1.8^0	... 7.75 E	10^0	... 0.29 E
2^0	... 7.54 E	12^0	... 0.17 E
4^0	... 3.44 E	20^0	... 0.04 E

A curve constructed from these values would be steeper than its counterpart for the deflections of the vertical. Again, the gradient generated above the P.M. is zero. The P.M. has the most significant effect between 0 and 2s (here 4^0). The cut-off decision could be made in favor of 3s (here 6^0) where this effect has diminished to about 17% of the maximum effect around 1s.

4.6 Vertical Gradients of Gravity Disturbance

S.H. part. From the last relation in (3.73) and from the last expression of (3.77) we obtain the vertical gradient of gravity disturbance as

$$T_{zz} = \bar{C} \sum_{n=2}^{N} (n+1)(n+2)(a/r)^n \, \Delta S(n) \ , \tag{4.30}$$

where $\Delta S(n)$ has been defined in (3.76).

Accordingly, A_1 contains the elements

$$\partial T_{zz}/\partial C_{no} = \bar{C}(n+1)(n+2)(a/r)^n \, P_n(\sin\bar{\phi}) \ ,$$

$$\partial T_{zz}/\partial C_{nm} = \bar{C}(n+1)(n+2)(a/r)^n \cos m\lambda \, P_{nm}(\sin\bar{\phi}) \ ,$$

$$\partial T_{zz}/\partial S_{nm} = \bar{C}(n+1)(n+2)(a/r)^n \sin m\lambda \, P_{nm}(\sin\bar{\phi}) \ .$$

P.M. part. In spherical approximation, the last relation of (3.73) is written for the observation point i in the P.M. model as

$$T_{zz} = \partial^2 T_i/\partial r_i^2 \ ,$$

which, according to (4.7f), is

$$T_{zz} = \sum_j (1/\ell_{ij}^{\,3}) \left[3(R - R_1 \cos\psi_{ij})^2/\ell_{ij}^{\,2} - 1\right](kM)_j \ . \tag{4.31}$$

The procedure involving the "canonical form" and one point mass results in

0^0 ... 18.59 E	6^0 ... -0.19 E
2^0 ... 6.97 E	8^0 ... -0.21 E
4^0 ... 0.67 E	10^0 ... -0.15 E

The vertical gradient curve is thus seen to be steeper than its counterpart for the horizontal gradients. The maximum effect corresponds now to $\psi_{ij} = 0$. The cut-off distance of 2s (here 4^0) is more than adequate, the effect of the P.M. at that distance being about 3.6% of the maximum effect (at 1s this effect would correspond to 37.5%).

AD-A089 072 NOVA UNIV OCEAN SCIENCE CENTER DANIA FL F/G 8/5
EXTENDED APPLICABILITY OF THE SPHERICAL-HARMONIC AND POINT-MASS--ETC(U)
FEB 80 G BLAHA F19628-78-C-0013
UNCLASSIFIED SCIENTIFIC-2 AFGL-TR-80-0180 NL

2 OF 2
AD A
089072

END
DATE
FILMED
10-80
DTIC

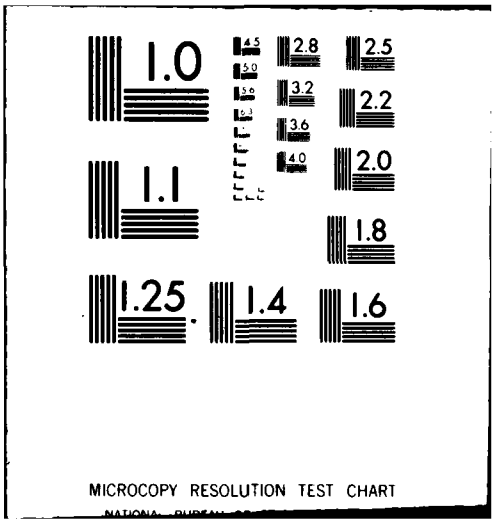
1.0
2.8
2.5
3.2
2.2
3.6
4.0
2.0
1.1
1.8
1.25
1.4
1.6
MICROCOPY RESOLUTION TEST CHART

5. SPECIFIC CONSIDERATIONS RELATED TO SEA SURFACE TOPOGRAPHY

5.1 Outline

The sea surface topography represents a dynamic surface whose slight changes in shape are imputable to astronomical forces in combination with other effects (oscillations in water basins, shallow water effects, meteorological effects, etc.). The astronomical forces are at the basis of tidal changes in the sea surface. The attraction of the moon represents the most important aspect of these forces. By comparison, the effect of the sun amounts to only about 46% of the effect of the moon, both effects having similar characteristics.

If the moon's orbit were in the plane of the earth's equator, there would be two high tides and two low tides in a lunar day (approximately 24 hours and 50 minutes, or 1.035 solar day), and the tides would be semi-diurnal. If the plane of the ecliptic coincided with the plane of the earth's equator, the sun would produce similar effects except for the magnitude and the period of the tidal cycle (a solar day has 24 hours). The varying declinations of the moon and the sun produce additional effects that are essentially diurnal. Irregularities of the moon's orbit around the earth and in the earth's orbit around the sun (varying distance and varying velocity) require additional considerations as explained e.g. in Chapter 2 of [Macmillan, 1966].

Further complications are due to the departure of the earth's structure from an idealized model which would give rise to the "equilibrium tide". Assumptions associated with the equilibrium tide include a completely rigid earth covered over its entire surface by deep water, absence of friction in the water envelope, absence of meteorological and other disturbances, etc.

In reality, tidal changes include two important effects expressed by Love's numbers; these effects are the ocean floor deformation and an additional tide induced by such a deformation. If included in the tidal model, they would result in modifying the amplitude of the equilibrium tide to a limited extent. However, this consideration is not always of paramount importance in applications of satellite altimetry. In particular, when one proceeds to adjust satellite altimetry in a localized area this amplitude may also be subject to adjustment and the inclusion of a factor due to the above two effects would simply lead to the replacing of one unknown parameter by another (the altimeter does not offer means for separate solution of Love's numbers). Accordingly, only the equilibrium tide will be considered in this discussion.

In the satellite altimetry mathematical model the ocean surface is considered as equipotential. At a given moment the equilibrium model results in an equipotential surface (under the assumption of an idealized spherical earth it is a spheroid). Time averaging applied to this surface also results in an equipotential surface (a different spheroid). Accordingly, if the altimeter could, over a sufficiently long time span, sense the latter (average equipotential) surface, the two models would indeed

be compatible. However, this is not the case because of several effects not accounted for including water friction, continent boundaries, currents, meteorological factors, etc. Consequently, the surface sensed over a given time span exhibits slopes in different areas with respect to an equipotential surface. If an adjustment does not allow for the inclusion of such slopes, the parameters describing the equipotential surface may be slightly deformed so as to accommodate, in a least-squares sense, the measured surface. It is thus desirable to provide for additional parameters describing the sea surface slopes, at least in the areas where the slopes are suspected or known to exist. If the time history of such slopes is of interest (assuming that the slopes are changing) the adjustment may be repeated at suitable time intervals provided sufficient altimeter data are available. A simple model will be developed shortly that allows for the inclusion of new parameters in an adjustment, accommodating the slopes (including a vertical separation) between the measured surface and the equipotential surface in predetermined areas.

However, prior to this task we shall direct some attention to the problem of a reference surface for heights, which we shall call the fixed, or static, geoid. In [Bomford, 1975], page 247, it is suggested that "the geoid (and the datum of height) is an equipotential surface of the earth's attraction and centrifugal force only, not including the sun and moon...". It is also stated that "for its datum surface for height, every country or group of countries select mean sea-level at a defined tide gauge...". However, even if the best possible mean (in time) sea level were selected at given points, it could not represent globally a

consistent datum for heights, i.e., the static geoid. This can be visualized as follows. Suppose that the static geoid is a perfect sphere with a known center and of the same volume as a mean sea surface covering the whole globe, assuming the equilibrium model. Due to the moon's and sun's attractive forces, the mean sea surface is a spheroid. If one wishes to define the static geoid (a sphere in this context) passing through a given tide gauge on the equator, one is faced with the problem that this sphere is larger than that representing the static geoid passing through a given tide gauge at a higher latitude. Thus, in order to define a unique global datum for heights, a suitable correction should be applied to the mean sea level as a function of latitude. This problem is discussed in the following section where the moon's effect is considered first and the moon-earth distance is assumed constant, equal to the mean distance. The sun's effect is incorporated along similar lines.

5.2 Considerations Related to Static Geoid

In this section the equipotential surface without the influence of astronomical forces is assumed to be a sphere. This would be equivalent to considering the earth a point mass or a homogeneous nonrotating sphere, or simply to retaining only the leading term in the expansion of the earth's potential in spherical harmonics, etc. In determining the changes in the potential due to the moon and/or sun such approximation is acceptable. The static geoid is thus considered to be a sphere and the main task consists in determining its radius (R) or, equivalently, its relation to the mean sea surface. The assumption of the equilibrium tide is used throughout.

In considering the moon's effect in this model, the total potential at a point (P) on the static geoid is determined as the sum of the potential generated by the earth's mass concentrated at its center, of the potential due to the moon's mass (concentrated at the moon's center) and of the potential generated by the monthly rotation of P around the barycenter of the earth-moon system. A new equipotential surface passing through P is computed (see [Bomford, 1975], pp. 271, 272) through its "tidal undulation", N, with respect to the sphere of radius R. In this process, the volume enclosed by the two surfaces is constrained to be the same, i.e., the mean value of N over the sphere is constrained to zero. This is plausible since the volume of the water envelope as well as the volume of the solid earth beneath it do not change -- no mass is added or subtracted. Upon considering the moon's orbit as circular and adopting

the average earth-moon distance for this purpose, the tidal undulation N for any time and place is

$$N = k(\cos 2z + 1/3) , \tag{5.1}$$

where z is the angle between the directions toward P and toward the moon measured at the earth's center; it is approximately equal to the zenith distance of the moon at P (the angle under which the earth's radius is seen from the center of the moon is neglected). The angle z is computed as a function of geographic location (of P) and of time. The above approximation of circular orbit yields

$$k = k_1 = 0.267\,\mathrm{m} . \tag{5.2a}$$

In case of the sun (5.1) would hold again, but with

$$k = k_2 = 0.123\,\mathrm{m} , \tag{5.2b}$$

which indicates that the tidal amplitude associated with the sun is about 46% of that associated with the moon. If an overbar denotes the mean over a unit sphere, it is confirmed that $\overline{N} = 0$ because at a given moment $\overline{\cos 2z} = -1/3$.

It will be shown shortly that the surface determined by (5.1) is a prolate spheroid (ellipsoid of revolution) with its long axis pointing toward the moon. This situation is schematically illustrated in Figure 5.1 where the "z" corresponding to P_1 , P_2 and P' could be denoted as z_1 , z_2 and z' , respectively; in particular, $z_1 = 0$, $z_2 = 90^0$ and

$$z' = 54.7^{\circ} . \tag{5.3}$$

(There are four such values of z' corresponding to $N = 0$, symmetric about the axes x,y.) Associated with (5.2a), we have

$$N_1 = 0.356\,\mathrm{m}, \qquad N_2 = -0.178\,\mathrm{m}, \tag{5.4}$$

while for (5.2b) these undulations would be 0.164 m and -0.082 m, respectively; if both the moon and sun were in line with the earth (i.e., at conjunction or opposition) the corresponding values would be added algebraically and the tidal undulations would reach 0.52 m and -0.26 m, respectively. If, in this case, the x axis in Figure 5.1 depicted the earth's equator, the tidal range on the equator would reach about 0.78 m (i.e., 0.52 m + 0.26 m); this order of magnitude is in agreement with the realistic tidal range in open ocean.

In order to show that the curve representing "spheroid" in Figure 5.1 is indeed an ellipse -- or very nearly so -- we adopt from the figure and from (5.1):

$$a = R + (4/3)k , \qquad b = R - (2/3)k ;$$

upon attributing to the point Q the coordinates $x = (R+N) \cos z$ and $y = (R+N) \sin z$ with N given in (5.1), after some manipulation we obtain

$$x^2/a^2 + y^2/b^2 = 1 + \tau ,$$

where

$$\tau \sim 0.25 \times 10^{-13} ,$$

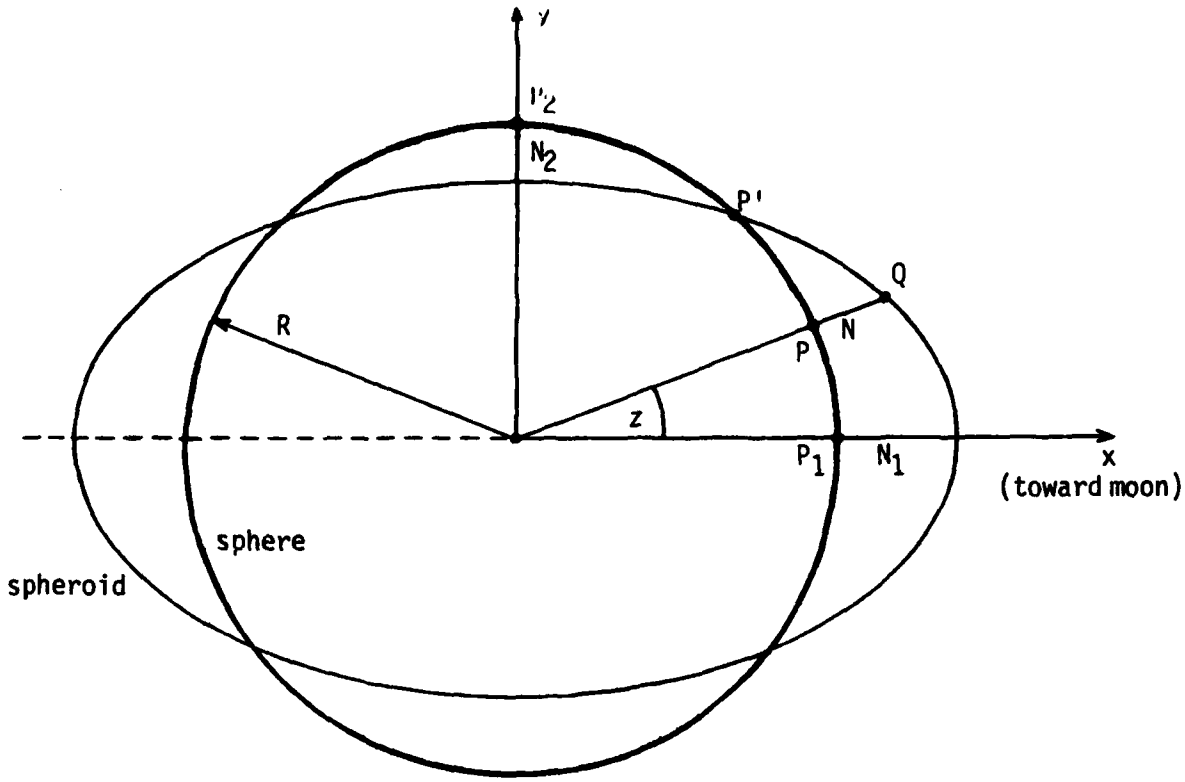

Figure 5.1
Schematic representation of the static geoid and equilibrium tide

which indicates that to any reasonable approximation the curve in question is an ellipse.

In order to acquire a good idea about the separation between the two surfaces depicted in Figure 5.1, we compute an "RMS separation" as follows:

$$N^2 = k^2\left[\cos^2 2z + (2/3)\cos 2z + 1/9\right] ,$$

$$\overline{\cos^2 2z} = (4\pi)^{-1} \int_{z=0}^{\pi} \int_{u=0}^{2\pi} \cos^2 2z \sin z \, dz \, du .$$

The last expression eventually yields 14/30; with $\overline{\cos 2z}$ given earlier, we find

$$(\overline{N^2})^{\frac{1}{2}} = 0.596\,k\,.$$

Repeating also a previous result, we have for the effect of the moon:

$$\overline{N} = 0\,, \tag{5.5a}$$

$$(\overline{N^2})^{\frac{1}{2}} = 0.16\,m\,. \tag{5.5b}$$

If the effect of both the moon and sun at conjunction or opposition are considered, the value in (5.5b) is replaced by 0.23 m.

The main point of the present discussion is the consideration of mean values over a given time interval. The (approximate) zenith distance z is changing with time due to the earth's rotation and the moon's orbit, and it can be expressed from the following standand formula of spherical astronomy relating the horizon and hour angle systems (see e.g. [Mueller, 1969], p. 38):

$$\left.\begin{aligned} \sin z \cos A &= \sin\delta \cos\phi - \cos\delta \cos h \sin\phi \\ \sin z \sin A &= -\cos\delta \sin h \\ \cos z &= \sin\delta \sin\phi + \cos\delta \cos h \cos\phi\,, \end{aligned}\right\} \tag{5.6}$$

where A is the azimuth of the celestial body (here the moon), h and δ are its hour angle and declination, respectively, and ϕ is the (geocentric) latitude of the observer. From (5.6) it readily follows that

$$\cos 2z = -\cos 2\phi + \sin 2\phi \sin 2\delta \cos h + \cos 2\phi \cos^2\delta + \cos 2\phi \cos^2\delta \cos^2 h - \cos^2\delta \sin^2 h \ . \tag{5.7}$$

With regard to h, great simplifications will take place if the averaging is carried out over an integer number of lunar days (i.e., over an integer number of 2π).

The time-averaging process for δ is facilitated by assuming that the plane of the moon's orbit coincides with the ecliptic which makes an $\varepsilon = 23.5^0$ angle with the equator. In reality, the plane of the moon's orbit is inclined by about 5^0 with respect to the ecliptic and thus intersects the plane of the equator at angles ranging from a minimum of 18.5^0 to a maximum of 28.5^0. However, it will be shown that this approximation results in an error in tidal undulation of less than 2 cm in the worst case. Consequently, the formula giving the declination of the moon can be transcribed in our context from the formula below, giving the declination of the sun. In particular, the relationship between the right ascension and ecliptic systems yields for $\beta = 0$ (the ecliptic latitude of the sun):

$$\sin\delta = \sin\lambda \sin\varepsilon \ , \tag{5.8}$$

where λ is the sun's ecliptic longitude measured counterclockwise from the vernal equinox (point of intersection between the plane of the ecliptic and that of the equator). This follows from equation (3.11) of [Mueller, 1969]. We only have to remember that when adopting this equation for the moon, λ covers the interval 2π in a sideral month (27.32 days). When averaging, it

will be advantageous to integrate, with respect to λ, over an integer number of π corresponding to an integer number of 13.66 days. If the variations in ε were significant, the integration could probably be extended only over 13.66 days which would correspond to π in λ and to about $13 \times 2\pi$ in h (more precisely, to $13.2 \times 2\pi$ in h). However, since ε has been fixed in our model, the integration can be extended over any number of 13.66 days which will, of course, include a very large number of 1.035 days (the larger this number the lesser the averaging error if this number is not a perfect integer). This device also allows for a simple mathematical combination of the moon's and sun's effects not only because the "ε" are identical but also because in the case of the sun the integration over merely π in λ involves the time interval of half a year (which is an order of magnitude greater than 13.66 days). The useful outcome of this argument is that our simplified -- although sufficiently accurate -- model allows for a simultaneous time-averaging over an integer number of 2π in h and an integer number of π in λ for both the moon's and sun's effects.

When averaging (5.7) over the above intervals, the second term on the right-hand side vanishes because of cos h. We then substitute (5.8) in (5.7) and deduce:

$$(n\pi)^{-1} \int_{\lambda_1}^{\lambda_1+n\pi} (1 - \sin^2\varepsilon \, \sin^2\lambda)d\lambda = 1 - \tfrac{1}{2}\sin^2\varepsilon \ ,$$

$$(2m\pi)^{-1} \int_{h_1}^{h_1+2m\pi} \begin{Bmatrix} \cos^2 h \\ \sin^2 h \end{Bmatrix} dh = \tfrac{1}{2} \ ,$$

yielding

$$\langle\cos 2z\rangle = -\cos 2\phi + (1 - \tfrac{1}{2}\sin^2\varepsilon)\left[(3/2)\cos 2\phi - \tfrac{1}{2}\right] ,$$

where $\langle\ \rangle$ indicates a time average. After little manipulation, from (5.1) we obtain

$$\langle N\rangle = \tfrac{1}{2}k(\cos 2\phi - 1/3)\left[1 - (3/2)\sin^2\varepsilon\right] , \qquad (5.9)$$

where k may represent k_1 (for the moon), k_2 (for the sun), or $k_1 + k_2$ (for both). In order to illustrate the error due to fixing ε in the model involving the moon, we take k from (5.2a) and consider $\phi = \pm\tfrac{1}{2}\pi$ resulting in the largest magnitude of $\langle N\rangle$. The following values $\langle N\rangle$ are obtained for chosen ε's:

$18.5^0 \ldots -15.1$ cm , $23.5^0 \ldots -13.6$ cm , $28.5^0 \ldots -11.7$ cm.

Thus the worst error associated with $\varepsilon = 23.5^0$ is 1.9 cm; for $\phi = 0$ this error would be 0.9 cm. The acceptability of our model has thus been established.

The relation (5.9) can also be presented as

$$\langle N\rangle = (3/8)k(\cos 2\phi - 1/3)(\cos 2\varepsilon + 1/3) . \qquad (5.10)$$

This formula indicates that if ε were 54.7^0 (as z' in equation 5.3) the time average of N would be identically zero and the mean sea surface would coincide with the static geoid. If the x-axis in Figure 5.1 represented the equator, the "ecliptic" would pass through the point P'. As a matter of interest we confirm that the average of $\langle N\rangle$ taken over the sphere is

zero, due to $\overline{\cos 2\phi} = 1/3$; since in (5.5a) we had $\overline{N} = 0$ at any given mement, it thus follows that

$$\overline{\langle N \rangle} = \langle \overline{N} \rangle = 0$$

as it should (the order of integration does not matter).

Upon taking $\varepsilon = 23.5^0$ in (5.10), we have

$$\langle N \rangle = \tilde{k}(\cos 2\phi - 1/3) , \tag{5.11a}$$

$$\tilde{k} = 0.381\, k ; \tag{5.11b}$$

if k represents k_1 , k_2 , or $k_1 + k_2$, the values of $\tilde{k}$ are 0.102 m, 0.047 m, or 0.149 m, respectively. In terms of the polar distance $\theta(\theta = \frac{1}{2}\pi - \phi)$, equation (5.11a) is rewritten as

$$\langle N \rangle = (-\tilde{k})(\cos 2\theta + 1/3) .$$

Thus the mean sea surface in our model is a geocentric ellipsoid of revolution whose minor axis passes through the poles. This is seen immediately from the analogy with the formula (5.1) and Figure 5.1; the x-axis and the angle z are now replaced by the polar axis and the angle θ, and the negative value of $(-\tilde{k})$ indicates that this axis is the minor axis of an ellipse.

Upon including the effect of both the moon and the sun, the formulas (5.11) giving the separation between the static geoid and the mean sea surface under the assumption of equilibrium tide is

$$\langle N \rangle = 0.15 \times (\cos 2\phi - 1/3) \text{ meter} . \tag{5.12}$$

From (5.12) the largest separation is found for the poles where it reaches -20 cm. For the equator we have $\langle N \rangle = 10$ cm. This or a similar type of "correction" is significant if a consistent relationship between the two surfaces is needed to within a decimeter precision.

5.3 Considerations Related to Sea Surface Slopes

It has been mentioned that in various areas the sea surface may depart from an equipotential surface. In a global adjustment of satellite altimetry the latter is described by spherical harmonic potential coefficients (C's and S's) truncated at a predetermined degree and order; for example, the model may be complete through the degree and order (14,14), etc. If, in a given area, the sea surface is believed to intersect an equipotential surface along a line of known direction, a parameter describing an average slope of the sea surface with respect to the equipotential surface can be added to the adjustable C's and S's.

There may be as many new parameters of this type as there are areas suspect to exhibit sea surface slopes. One such area can be, for example, the Equatorial Pacific Ocean where an east-west slope may be indicated. The line of intersection, henceforth called "zero line", is in this case chosen to run north-south, typically through the middle of the area of interest (the area can be delimited by the geographic coordinates of its four corners and every observation point is checked whether it falls within the boundaries).

However, an additional parameter may be included in an adjustment, representing a vertical shift of the sea surface. This has the effect of allowing the zero line to translate, parallel to itself, to the right or left from its stipulated position. Accordingly, two sea slope parameters (one for the slope as such, one for the shift) per region of interest may be introduced in a global adjustment.

The slope parameters have characteristics of an average with regard to both the surface and the time. The first property follows from the fact that one slope parameter applies for a whole area and indicates a general trend of the sea surface from one end of the area to the other. And the second property can be ascribed to altimeter data being usually collected over extended periods of time (e.g., several months) so that many periodic (e.g., tides) or random fluctuations are smoothed out by the adjustment.

If a time variation of a given sea slope is of interest, the same kind of adjustment may be repeated with data sets having a comparable spacial distribution as well as time span, but collected at different time epochs. In order to bring the sea slope parameters into focus during such a process, the C's and S's could be fixed (eliminated from the adjustment) or weighted at the values which would be the same during all such adjustments.

A localized adjustment has been performed in the past with point mass magnitudes as parameters, based on the residuals obtained in a global adjustment (via C's and S's). The localized adjustment can contain the sea slope parameters as well, but there is likely to be only one "area of interest", i.e., the total area of the point mass adjustment. In other respects the sea slope parameters can be treated in a similar way as described above. Thus the localized adjustment may contain only two additional parameters, provided the slope and the (vertical) shift of the sea surface are indeed sought in that area.

We now return to the global adjustment and illustrate how the sea slope parameters could be useful and how they could be handled. It has already been suggested that they may contribute to a "better" adjustment. In particular, they could prevent the C's and S's from being contaminated by long-wavelength distortions represented by actual sea slopes if these are significant. Furthermore, the residuals will have in general smaller magnitude when these parameters are included since the adjusted surface will fit better the observed surface in a physically meaningful manner. As a by-product,knowledge about sea surface slopes can serve, in its own right, in specific applications.

An example of two areas with separate sea slope parameters is illustrated in Figure 5.2. An added complication is that the zero line is not straight which accounts for an auxiliary area wedged between the other two. In this particular area the zero line reduces to a point (Q). The sea slope parameters in this area could be taken as the mean of the corresponding parameters in the neighboring areas. A simpler case would be represented by a straight zero line with the two areas separated by a straight line (perpendicular to the zero line). Eventually, there could be an intermediate area between the two in the form of a strip (not a wedge) where the values of the sea slope parameters would again be the appropriate means. The simplest case consists of individual disjoint areas or of only one area attributed sea slope parameters.

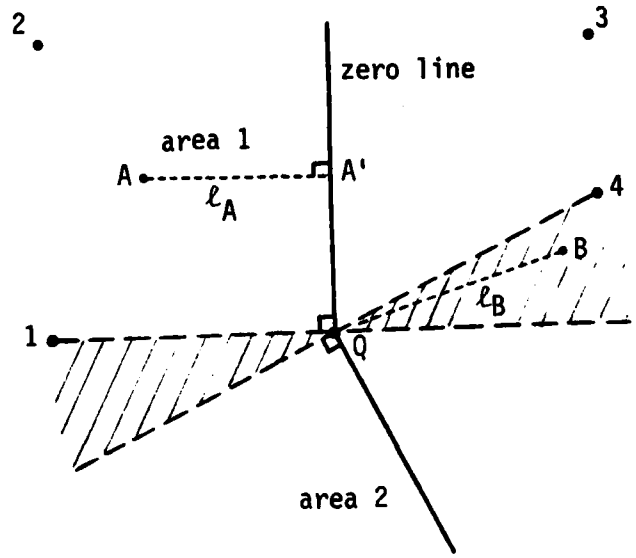

Figure 5.2
Illustration of two basic areas (1 and 2) and a bent zero line; the area 1 is delimited by the points 1, 2, 3, 4, Q

The adjusted global geoid described by the C's and S's will be smooth, but slight discontinuities in the residuals may be experienced at the edges of a sea slope area, especially far from the zero line, except where the area is delimited by continents. However, this represents no cause for concern since a subsequent local adjustment usually involves a region which is all within one such area, and even if there should be an exception to this statement the point mass parameters would provide for a smoothed local geoid.

If the sea slope areas present in an adjustment cover most of the world's oceans and if all the zero lines are chosen to have central locations, one would expect that

$$\sum_{i=1}^{\text{all areas}} (\text{area})_i \times (\text{shift parameter})_i \simeq 0 \ . \tag{5.13}$$

It is so because the sea surface topography is not likely to enclose different volume from that enclosed by an equipotential surface (fluctuations of the sea surface around an equipotential surface are believed to be small and to have random characteristics). In fact, equation (5.13) could be adopted as a constraint or, which amounts to the same thing in practice, as a heavily weighted observation equation.

Before forming an observation equation involving the two sea slope parameters ("t" for the slope itself, "q" for the shift) the distance between an observation point and the zero line has to be computed. This distance (ℓ_A in Figure 5.2) will have the sign associated with it in such a way that the distance is positive due west of the zero line. This means that for $t>0$, the sea surface slopes "up" due west of the zero line and "down" due east of this line; for $t<0$ the situation is reversed. Since, in the observation equation, the constant terms are expressed in meters the parameter q will have units m and the parameter t will have units mm/km (i.e., meter/megameter), provided the angular distance ℓ_A (in radians) is multiplied by R, the earth's radius, expressed in megameters ($R \simeq 6.371$ Mm). The value of ℓ_A is found with the aid of Figure 5.3. From the spherical triangle PAE we have

$$\sin p \sin\tau = \sin(\lambda_o - \lambda)\cos\phi \ , \tag{5.14a}$$

$$\sin p \cos\tau = \sin\phi \ , \tag{5.14b}$$

where the index "o" is associated with the zero line and the geographic coordinates (ϕ,λ) associated with the observation point (A) are not indexed. From AEA' we deduce

$$\sin \ell_A = \cos\alpha \sin p \cos\tau + \sin\alpha_o \sin p \sin\tau \ . \tag{5.14c}$$

When (5.14a) and (5.14b) are used in (5.14c), ℓ_A with the appropriate sign is given as

$$\ell_A = \arcsin\left[\cos\alpha_o \sin\phi + \sin\alpha_o \sin(\lambda_o - \lambda)\cos\phi\right] . \tag{5.15}$$

The values of $\cos\alpha_o$ and $\sin\alpha_o$ are computed once and for all in the region of interest (α_o is measured as indicated in Figure 5.3).

In case of the situation leading to ℓ_B of Figure 5.2, a simple application of the law of cosine yields

$$\cos \ell_B = \sin\phi \sin\phi_Q + \cos\phi \cos\phi_Q \cos(\lambda_Q - \lambda) \ ,$$

$$\operatorname{sign} \ell_B = \operatorname{sign}(\lambda_Q - \lambda) \ ,$$

where $\sin\phi_Q$ and $\cos\phi_Q$ are computed once and for all for the whole "wedge" region.

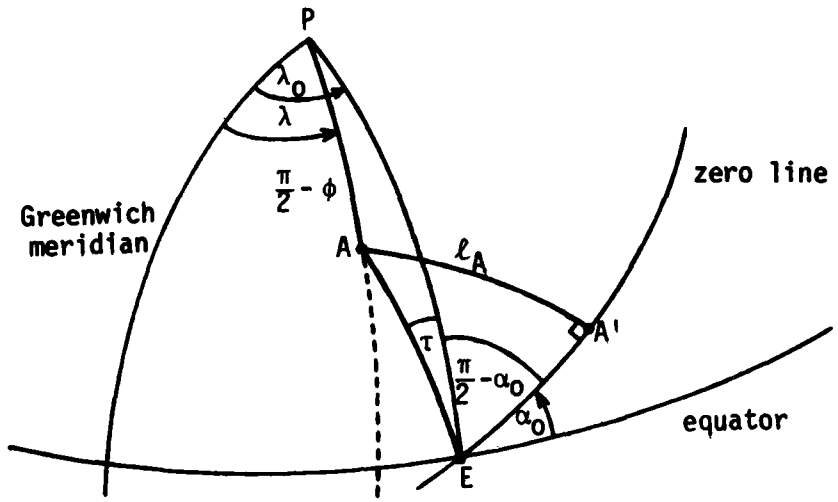

Figure 5.3
Spherical triangles depicting the zero line and an observation point (A)

In a matrix form, the "undulation" in one area due to the sea slope parameters is

$$\Delta N = \begin{bmatrix} 1 & \ell R \end{bmatrix} \begin{bmatrix} q \\ t \end{bmatrix},$$

where ℓ can be of the type ℓ_A or ℓ_B . In general, this can be written as

$$\Delta N = \begin{bmatrix} a & b \end{bmatrix} \begin{bmatrix} q \\ t \end{bmatrix}, \tag{5.16}$$

where

$$\left.\begin{array}{l} a = 1 \\ b = \ell R \end{array}\right\} \text{ in the area of interest} \tag{5.17a}$$

$$\left.\begin{array}{l} a = 0 \\ b = 0 \end{array}\right\} \text{ outside the area of interest.} \tag{5.17b}$$

If there are more than one area of interest, they are numbered 1,2,... The same applies for the coefficients a,b and for the parameters q,t so that we may have a_1 , b_1 ; a_2 , b_2 ; ... q_1 , t_1 ; q_2 , t_2 ; ... In forming the observation equation we keep in mind that the initial values of the parameters q,t and thus of ΔN are zero so that the constant term is unchanged from an earlier formulation without the sea surface slopes. The part corresponding to (5.16) simply augments the "terrestrial part" in the original equation of satellite altimetry as presented in Section 2.4 of [Blaha, 1977]. With the other symbols described -- and expressed in detail -- in this reference, we present schematically the augmented observation equation:

$$V = \left[\frac{\partial(R-r)}{\partial(X,Y,Z,\dot{X},\dot{Y},\dot{Z})}\right]\begin{bmatrix} dX \\ dY \\ dZ \\ d\dot{X} \\ d\dot{Y} \\ d\dot{Z} \end{bmatrix} - \left[\frac{\partial r}{\partial r_o}; \ldots \frac{\partial r}{\partial C_{n0}} \ldots; \ldots \frac{\partial r}{\partial C_{nm}} \ldots; \ldots \frac{\partial r}{\partial S_{nm}} \ldots ;\right. \tag{5.18}$$

$$
a_1\ b_1\ ;\ a_2\ b_2\ ;\ \ldots \Bigg]
\begin{bmatrix}
dr_o \\ \vdots \\ dC_{n0} \\ \vdots \\ dC_{nm} \\ \vdots \\ dS_{nm} \\ \vdots \\ q_1 \\ t_1 \\ q_2 \\ t_2 \\ \vdots
\end{bmatrix}
+ \left[(R^o - r^o + d) - H^b\right],
$$

where a_i , b_i are determined as in equations (5.17).

APPENDIX

COMPARISON OF THE NODE-POINT APPROACH AND THE POINT-MASS APPROACH

The present topic deals with the geoidal adjustment by means of node point parameters and point mass parameters. The node point approach has been treated in the papers [Hadgigeorge and Trotter, 1976], abbreviated as [HT], and [Eckhardt and Hadgigeorge, 1977], abbreviated as [EH]. The notion of covariance function computed via the spherical harmonic potential coefficients is used in both papers; however, the solution bandwidth in [HT] corresponds essentially to the degrees 3 through N and in [EH], to the degrees $\tilde{n}$ through N, where $\tilde{n}$ was chosen as 7. According to $\tilde{n}$, the reference surface can be either a spheroid ($\tilde{n} = 3$) or a higher order surface ($\tilde{n} = 7$,etc.); in general, the model is assumed to be known through the degree $\tilde{n} - 1$. The paper [HT] also contains the spheroidal multiquadric surface model in which the covariance function is replaced by the "kernel function".

The spacing of the nodes may be limited by the data distribution; in any event, it is reasonable to require that at least two observations in each direction should be present per node point. The node points are assumed to be fairly uniformly distributed through the region of interest, the nodal spacing being s^0 (degrees of arc). If the solution is carried out in terms of spherical harmonics, the harmonics up to and including the degree $N = 180^0/s^0$ could be adjusted provided the global distribution of data exists and, of course, a sufficiently large computer is available. The covariance function for geoid undulations corresponding to the bandwidth $\tilde{n}$ through N

is given as

$$D(\psi_{ij}) = \sum_{n=\tilde{n}}^{N} \sigma_n^2 \{N,N\} P_n(\cos \psi_{ij}) , \tag{A.1}$$

where $D(\psi_{ij})$ represents the covariance of the geoid undulation (denoted N -- not to be confused with "N" of the truncation) for two points, i and j, separated by the spherical distance ψ_{ij}, $\sigma_n^2 \{N,N\}$ is the degree variance (degree n) for geoid undulations, and $P_n(\cos \psi_{ij})$ are the Legendre functions in argument $\cos \psi_{ij}$. The cross-covariance function for gravity anomalies (Δg) and geoid undulations (N) can similarly be written as

$$H(\psi_{ij}) = \sum_{n=\tilde{n}}^{N} \sigma_n^2 \{\Delta g,N\} P_n(\cos \psi_{ij}) , \tag{A.2}$$

where $\sigma_n^2 \{\Delta g,N\}$ is the degree variance linking gravity anomalies and geoid undulations.

In the above papers the covariance function serves to express the geoid "undulation" (N_i) at a geoidal point i as a function of parameters c_j at selected nodes j, namely

$$N_i = \sum_j D(\psi_{ij})c_j , \tag{A.3}$$

where the summation is carried out, in theory, over all of the node points; the "undulation" is written in quotes to indicate that the value N_i may be referred to a spheroid (as is customary for geoid undulations) as well as to a higher order surface. The vector of parameters c_j is interpreted as

$$[c] = [M\{NN^T\}]^{-1}[N] . \tag{A.4}$$

where $[N]$ is the vector of geoid "undulations" at the node points and the matrix $[M\{NN^T\}]$ is composed of variances and covariances at these points computed from the (single) covariance function, such as (A.1) in the present case. This follows from the definition of covariance function, i.e., from

$$D(\psi_{ij}) \equiv M\{N_i N_j\} ,$$

where M indicates a mean value over a given domain (in the present context the domain for the covariance functions is the whole globe represented by a unit sphere; in the averaging process the "unwanted" harmonics are neglected). With the interpretation (A.4) the model expressed in (A.3) is the classical prediction model where the values N_i are predicted from the values N_j the "best" way, in the sense that the variances of the prediction computed through the same operator M are the smallest possible.

In the following step, the prediction model (A.3) is adopted as the mathematical model to be used in a least squares adjustment. The values N_i , whose number is much higher than that of N_j , are considered as observations and the quantities c_j are adjusted in the usual sense ($V^T PV = \text{minimum}$). In this process $D(\psi_{ij})$ simply represent the deterministic partial derivatives and c_j are the unknown parameters. These parameters can then be used to estimate other quantities, not only the geoid "undulations" at arbitrary points, but also gravity "anomalies" (the same meaning is attached to the quotes as previously), etc. The formula for predicting the "anomalies" is again based on a prediction model which, in this case, has the form

$$\Delta g_i = \sum_j H(\psi_{ij}) c_j . \qquad (A.5)$$

When considering the "kernel function" of Section 2.2 of [HT], one should keep in mind that only the geoid "undulations" can be estimated from the adjustment and that the main difference between that approach and the one with the covariance function consists in a different shape of the pertinent functions (kernel versus covariance function). Accordingly, only the covariance function approach will be considered in the upcoming comparison with the point mass approach.

The mathematical models relating the geoid "undulations" and gravity "anomalies" to the point masses can be obtained from (4.17) and (4.19) as

$$N_i = \sum_j (c/\ell_{ij})(PM)_j \ , \tag{A.6}$$

where $c = 40.68 \times 10^6\ m^2$, ℓ_{ij} is the separation between the i-th "undulation" point and the j-th point mass and $(PM)_j$ is the magnitude of the j-th point mass in units of 10^{-6} the earth's mass; and

$$\Delta g_i = \sum_j (ab)_{ij}(PM)_j \ , \tag{A.7}$$

where

$$a_{ij} = c'/\ell_{ij} \ ,$$

$$c' = 6.2565 \times 10^6\ \text{mgal m} \ ,$$

$$b_{ij} = Rb'_{ij}/\ell^2_{ij} - 2 \ ,$$

$$b'_{ij} = R - R_1 \cos \psi_{ij} \ ,$$

$$R = \text{earth's mean radius } (6.371 \times 10^6\ m) \ ,$$

R_1 R d ,

d = depth of point masses.

If properly scaled, the model (A.6) is comparable to the model (A.3) except for the form of the "covariance" functions; the quotes will be used to include the function c/ℓ_{ij} in (A.6) which has not been derived as a covariance function. The scaling of the adjustment models (A.3) and (A.6) would not affect the respective least squares solutions; however, the predictions (A.5) and (A.7) would be affected if the scale factors did not correspond to their counterparts in the original models (equations A.3 and A.6). In the sequel, the scaling of (A.5) and (A.7) will not correspond to that of (A.3) and (A.6) for practical reasons; however, the differences in scaling will be listed. In all the cases considered, the scaling will be such that the "covariance" functions in (A.3), (A.6) as well as in (A.5), (A.7) will have the value "100" for $\psi_{ij} = 0$. Thus, the shape of the functions may be easily compared upon first inspection. The units in any of the models present no cause for concern; the functions may be imagined scaled also in this respect so that the units are comparable.

The cases compared correspond to the spacing of node points in $s^0 = 6^0$ (equilateral) intervals which are considered to entail the degree and order truncation $N = 30$. The covariance functions for this N are then computed according to (A.1) and (A.2), for the cases $\tilde{n} = 3$ and $\tilde{n} = 7$. The horizontal separation of point masses is also 6^0 or $.667 \times 10^6$ m. For illustration purposes three different depths of the point masses have been selected:

$$d = 1.6\ s = 1.07 \times 10^6\ m\ , \tag{A.8a}$$

$$d = .52s = 0.35 \times 10^6\ m\ , \tag{A.8b}$$

$$d = .80s = 0.53 \times 10^6\ m\ . \tag{A.8c}$$

Originally, the ratio $d/s = 0.8$ as in (A.8c) has been suggested in [Blaha, 1977] under the assumption that the spacing s^0 of point masses should provide an adequate description of the geoid to within the degree and order $N = 180^0/s^0$. Later, in [Blaha, 1979], a one-decimeter precision of the adjusted geoid was contemplated; a recommendation was reached to the effect that the number of point masses should be doubled in each direction while their depth should remain unchanged. This would result in the angular separation of point masses $s^0 = \frac{1}{2}180^0/N$ and in the ratio $d/s = 1.6$. However, to make a meaningful comparison with the present node point approach, the original arrangement has been reverted to in (A.8c); in particular, $s^0 = 180^0/30 = 6^0$ has been adhered to as well as $d/s = 0.8$. If a more faithful representation of the geoid were required, the number of point masses as well as the number of node points would be doubled along each dimension. But in that case the comparisons would be completely analogous to those carried out presently.

The "covariance" functions corresponding to the adjustment models (A.3) and (A.6) are presented in Figure A.1. The cases denoted 1) and 2) represent the (scaled) covariance function of the node point approach; the curve 1) is the result of the choice $\tilde{n} = 3$ while the curve 2) is the result of the choice $\tilde{n} = 7$. For higher and higher order reference surface (i.e., for greater values of $\tilde{n}$) the covariance function becomes markedly steeper.

The cases 3), 4), 5) in the figure represent the "covariance" function of the point mass approach and they correspond to the depths of point masses selected in (A.8a), (A.8b) and (A.8c), respectively. The shallower the point masses, the steeper the "covariance" function. In either approach, when this function is steeper the local detail can be better represented provided the data are sufficient.

The "cross-covariance" functions corresponding to the prediction models (A.5) and (A.7) appear in Figure A.2 where the same five cases are presented. All the curves are now steeper than their counterparts in Figure A.1; this is natural since gravity anomalies represent a less smooth function than geoid undulations (the same holds true for "anomalies" versus "undulations"). As in Figure A.1, greater values of n and smaller values of d give rise to steeper functions. In both figures, ψ^0 is the angle ψ_{ij} in degrees. Below are listed the numerical scale factors used for the geoid "undulation" models (Figure A.1) and the gravity "anomaly" models (Figure A.2):

Case 1) Scale factor 6.042 (for N) and 3.397 (for Δg), ratio 0.5622,
Case 2) Scale factor 0.837 (for N) and 1.336 (for Δg), ratio 1.596;

Case 3) Scale factor 0.3811 (for N) and 0.2325 (for Δg), ratio 0.6101,
Case 5) Scale factor 0.7621 (for N) and 1.164 (for Δg), ratio 1.528,
Case 4) Scale factor 1.162 (for N) and 2.896 (for Δg), ratio 2.492.

The above numbering of cases 3, 5 and 4 corresponds to their degree of steepness. When the above scale factors are applied to the functions of the figures, original (unscaled) numerical values of the functions are recovered.

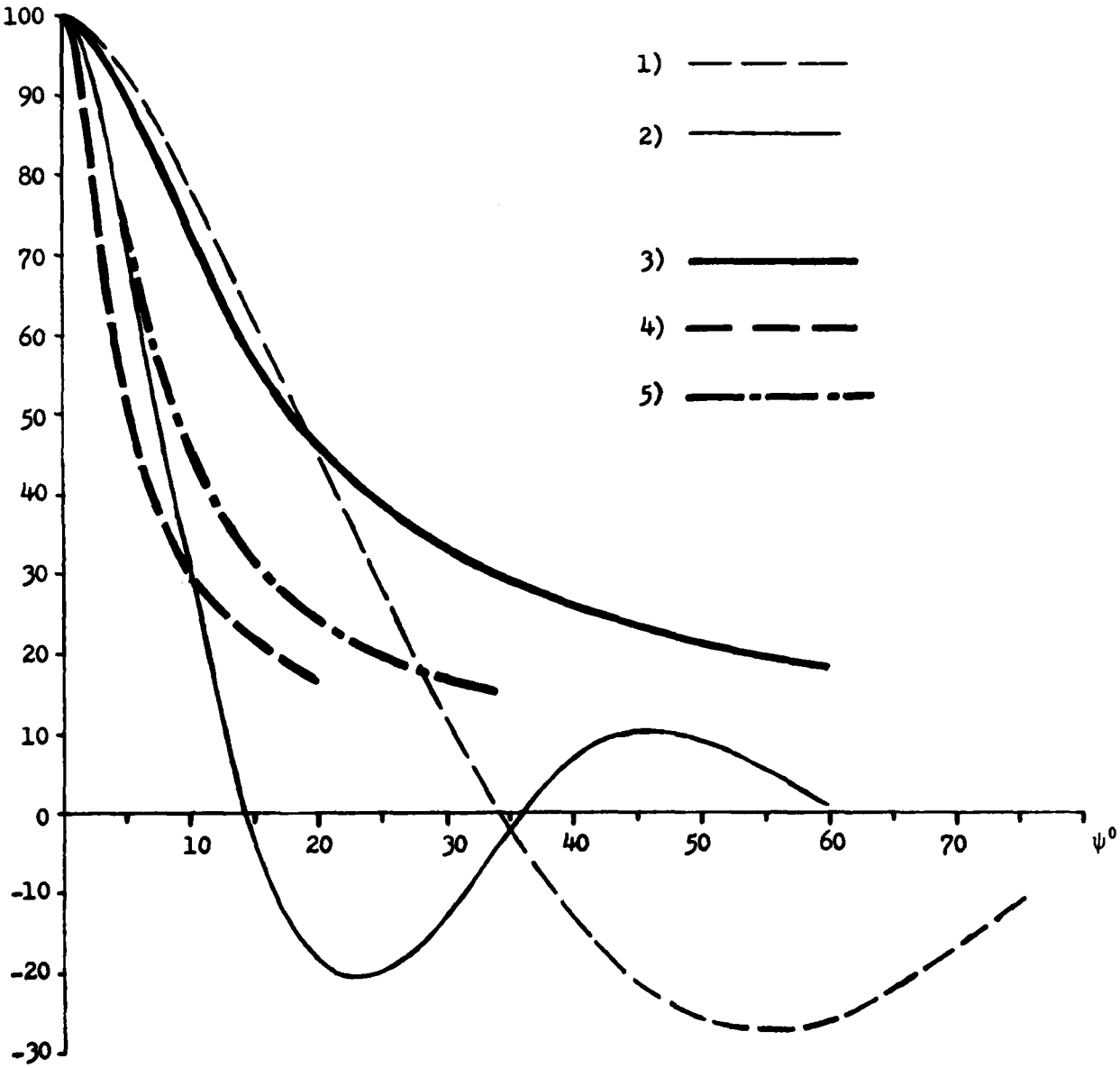

Figure A.1

Scaled covariance functions for N in the node-point approach and comparable functions in the point-mass approach

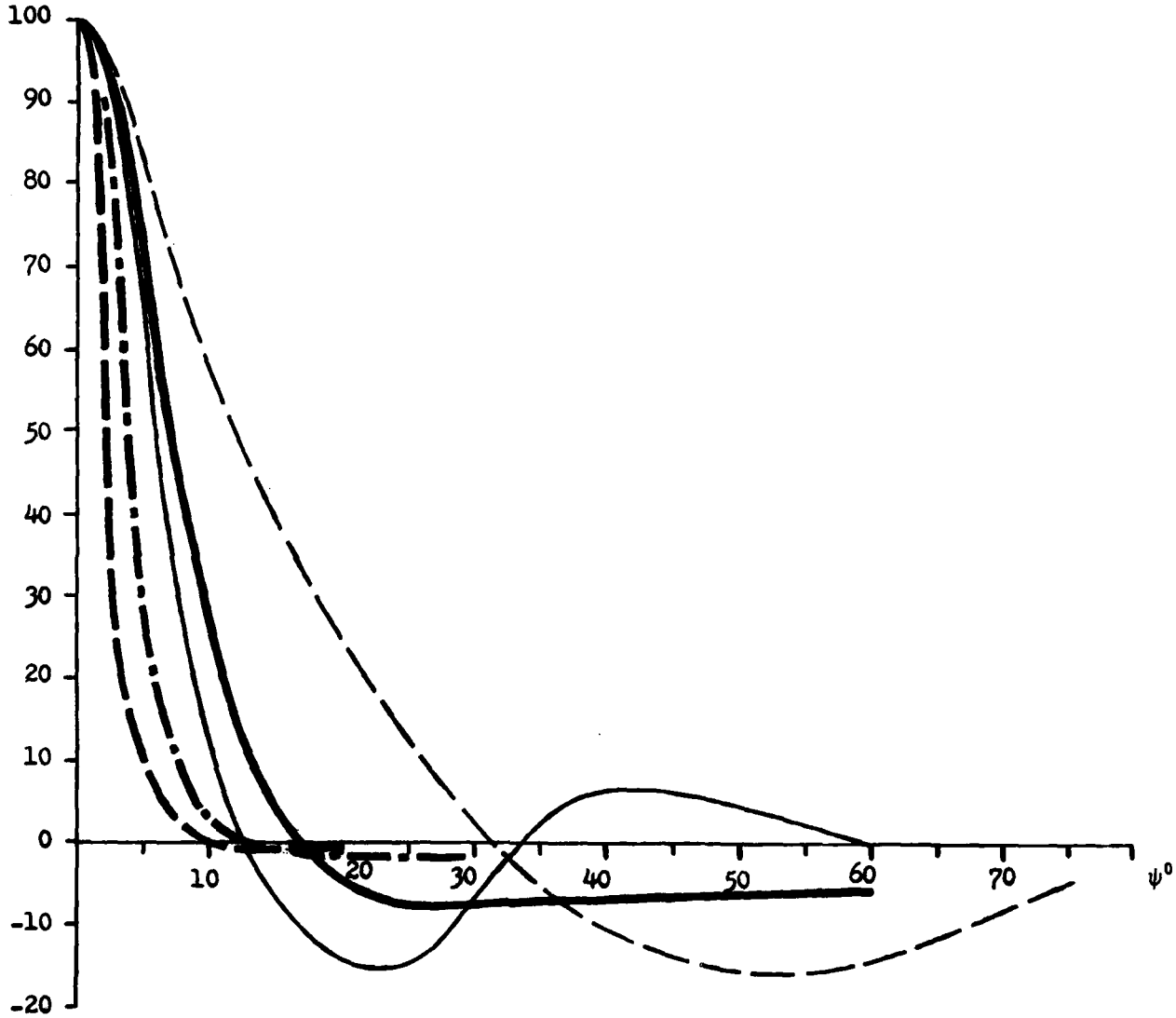

Figure A.2

Scaled cross-covariance functions for Δg,N in the node-point approach and comparable functions in the point-mass approach

The term "ratio" indicates the ratio of the two scale factors in each case (scale factor for Δg divided by the scale factor for N). In both approaches a steeper curve exhibits a higher "ratio".

Initially, the case 5) of the point mass approach was to be compared with the cases 1) and 2) of the node point approach corresponding respectively to the adjustments carried out in [HT] and [EH]. From the figures it appears that the case 5) is quite comparable with the case 2) where $\tilde{n} = 7$. For the sake of a better understanding of the point mass approach two additional cases have been included, one corresponding to deeper masses (case 3) and the other corresponding to shallower point masses (case 4).

These comparisons have indicated that the main difference between the node-point approach and the point-mass approach consists in somewhat different shapes of the "covariance" functions. In certain cases the disparity of the two approaches is not great; this is apparent for the cases 2) versus 5) where a fairly good agreement may be observed in the two figures, especially for smaller values of ψ^0. Here the covariance function constructed for the degrees $\tilde{n} = 7$ and $N = 30$ corresponds to the depth 0.53×10^6 m of the points masses distributed exactly as the node points. A remarkable agreement is noticed with respect to the values "ratio" for these two cases. This seems to indicate that not only the adjusted values (geoid "undulations") but also the predicted values (gravity "anomalies" in addition to predicted "undulations" at arbitrary locations) could agree fairly closely between the two adjustments. In other instances the difference between the two approaches may become significant, for example if shallower point masses are

not matched by a sufficiently high-order reference surface. Comparisons with other localized adjustment models would proceed along similar lines with emphasis on the corresponding "covariance" functions, the earlier-mentioned multiquadric model being a good example in this respect.

REFERENCES

Blaha, G., The Combination of Gravity and Satellite Altimetry Data for Determining the Geoid Surface. AFCRL Report No. 75-0347, Air Force Cambridge Research Laboratories, Hanscom AFB, Massachusetts, 1975.

Blaha, G., Refinements in the Combined Adjustment of Satellite Altimetry and Gravity Anomaly Data. AFGL Technical Report No. 77-0169, Air Force Geophysics Laboratory, Hanscom AFB, Massachusetts, 1977.

Blaha, G., Improved Determinations of the Earth's Gravity Field. AFGL Technical Report No. 79-0058, Air Force Geophysics Laboratory, Hanscom AFB,Massachusetts, 1979.

Blaha, G., "Second-Order Derivatives in a Local Frame Developed in Spheroidal and Spherical Coordinates". Bulletin Géodésique, Vol. 54, No. 1, Bureau Central de l'Association Internationale de Géodésie, Paris,France, 1980 (in press).

Bomford, G., Geodesy. 3rd edition, University Press, Oxford, reprinted with corrections, 1975.

Brown, D.C., Investigations of the Feasibility of a Short Arc Reduction of Satellite Altimetry for Determination of the Oceanic Geoid. AFCRL Report No. 73-0520, Air Force Cambridge Research Laboratories, Hanscom AFB, Massachusetts, 1973.

Eckhardt, D.H. and G. Hadgigeorge, "GEOS-3 Altimetry Reductions in the Australia - New Zealand Region". Paper presented at AFGL, Air Force Geophysics Laboratory, Hanscom AFB, Massachusetts, 1977.

Hadgigeorge, G. and J.E. Trotter, "Short Arc Reductions of GEOS-3 Altimetry Data". Paper presented at AFGL, Air Force Geophysics Laboratory, Hanscom AFB, Massachusetts, 1976.

Heiskanen, W.A. and H. Moritz, Physical Geodesy. W. H. Freeman and Co., San Francisco, 1967.

Hotine, M., Mathematical Geodesy. Monogr. Ser., Vol. 2, Environ. Sci. Serv. Admin., Washington, D.C., 1969.

Macmillan, D.H., Tides. American Elsevier Publishing Co., Inc., New York, 1966.

Marussi, A., Fondamenti di Geodesia Intrinseca. Published by the Italian Geodetic Commission, No. III 7, Milano, 1951.

Moritz, H., Combination of Aerial Gravimetry and Gradiometry. AFCRL Technical Report No. 75-0378, Air Force Cambridge Research Laboratories, Hanscom AFB, Massachusetts, 1975.

Mueller, I.I., Spherical and Practical Astronomy as Applied to Geodesy. Frederic Ungar Publishing Co., Inc., New York, 1969.

Needham, P.E., The Formation and Evaluation of Detailed Geopotential Models Based on Point Masses. Department of Geodetic Science, Report No. 149, The Ohio State University, Columbus, 1970.

Tscherning, C.C., "Computation of the Second-Order Derivatives of the Normal Potential Based on the Representation by a Legendre Series". Paper published in Manuscripta Geodaetica, Vol. 1 (pp 71-92), 1976.